IOWA STATE UNIVERSITY
Digital Repository

Retrospective Theses and Dissertations

Iowa State University Capstones, Theses and Dissertations

1999

Elemental speciation in biomolecules by LC-ICP-MS with magnetic sector and collision cell instruments

Jin Wang
Iowa State University

Follow this and additional works at: https://lib.dr.iastate.edu/rtd

 Part of the Analytical Chemistry Commons

Recommended Citation
Wang, Jin, "Elemental speciation in biomolecules by LC-ICP-MS with magnetic sector and collision cell instruments " (1999). *Retrospective Theses and Dissertations*. 12181.
https://lib.dr.iastate.edu/rtd/12181

This Dissertation is brought to you for free and open access by the Iowa State University Capstones, Theses and Dissertations at Iowa State University Digital Repository. It has been accepted for inclusion in Retrospective Theses and Dissertations by an authorized administrator of Iowa State University Digital Repository. For more information, please contact digirep@iastate.edu.

www.manaraa.com

INFORMATION TO USERS

This manuscript has been reproduced from the microfilm master. UMI films the text directly from the original or copy submitted. Thus, some thesis and dissertation copies are in typewriter face, while others may be from any type of computer printer.

The quality of this reproduction is dependent upon the quality of the copy submitted. Broken or indistinct print, colored or poor quality illustrations and photographs, print bleedthrough, substandard margins, and improper alignment can adversely affect reproduction.

In the unlikely event that the author did not send UMI a complete manuscript and there are missing pages, these will be noted. Also, if unauthorized copyright material had to be removed, a note will indicate the deletion.

Oversize materials (e.g., maps, drawings, charts) are reproduced by sectioning the original, beginning at the upper left-hand corner and continuing from left to right in equal sections with small overlaps. Each original is also photographed in one exposure and is included in reduced form at the back of the book.

Photographs included in the original manuscript have been reproduced xerographically in this copy. Higher quality 6" x 9" black and white photographic prints are available for any photographs or illustrations appearing in this copy for an additional charge. Contact UMI directly to order.

UMI®

Bell & Howell Information and Learning
300 North Zeeb Road, Ann Arbor, MI 48106-1346 USA
800-521-0600

NOTE TO USERS

This reproduction is the best copy available

UMI

Elemental speciation in biomolecules by LC-ICP-MS with magnetic sector and collision cell instruments

By

Jin Wang

A dissertation submitted to the graduate faculty
in partial fulfillment of the requirements for the degree of
DOCTOR OF PHILOSOPHY

Major: Analytical Chemistry
Major Professor: R. S. Houk

Iowa State University
Ames, Iowa
1999

UMI Number: 9940253

UMI Microform 9940253
Copyright 1999, by UMI Company. All rights reserved.

This microform edition is protected against unauthorized
copying under Title 17, United States Code.

UMI
300 North Zeeb Road
Ann Arbor, MI 48103

Graduate College

Iowa State University

This is to certify that the Doctoral dissertation of

Jin Wang

Has met the requirement of Iowa State University

Signature was redacted for privacy.

Major Professor

Signature was redacted for privacy.

For the Major Program

Signature was redacted for privacy.

For the Graduate College

TABLE OF CONTENTS

ABSTRACT

A methodology that can monitor and identify inorganic elements in biological and environmental systems was developed. Size exclusion chromatography (SEC) separates biomolecules, which are then nebulized by a microconcentric nebulizer. The resulting aerosol is desolved and introduced into either a high resolution ICP-MS device or a quadrupole device with a collision cell. Because of the high sensitivity and spectral resolution and high sample introduction efficiency, many unusual or difficult elements, such as Cr, Se, Cd and U, can be observed at ambient levels bound to proteins in human serum. These measurements are made in only a few minutes without preliminary isolation and preconcentration steps. Serum samples can be titrated with spikes of various elements to determine which proteins bind a given metal and oxidation state. Experiments concerning the effects of breaking disulfide linkages and denaturation on metal binding in proteins were also investigated. . Elemental distribution in liver extract was also obtained.

Binding of metal cations to DNA restriction fragments can be observed by similar procedures both for essential elements like Mn and Fe and toxic-ones like Cd and Pb. Reactions of metal species with DNA can also be studied, such as reduction of chromate and subsequent binding of the cation produced and reaction of the chemotherapeutic reagent cisplatin with DNA.

A collision cell ICP-MS can remove or reduce argon adduct interferences. The effects of some important parameters have been investigated on the enhancement of ion transmission and reduction of polyatomic interferences using a Platform ICP-hQMS. By examining the reaction rate of hydrogen, methane and xenon with argon adduct ions and related analyte

ions, it is clearly demonstrated that the analyte ion signals such as Fe^+ can be separated from the argon adduct interferences such as ArO^+. The results provide important information for developing the optimal collision conditions for the removal of polyatomic interferences and also for the further modification and development of this new analytical tool.

The applications of ICP-hQMS in the measurement of metal ions in urine and metals bound to proteins in human milk have been studied. The elemental distribution information in milk proteins is very important in identifying nutritional potential and ensuring toxicological risks.

CHAPTER 1: INTRODUCTION

Inductively coupled plasma mass spectrometry (ICP-MS) has become one of the most successful methods for elemental and isotopic analysis.[1,2] ICP-MS instruments are capable of routine analysis at part per trillion levels with absolute detection limits in part per quadrillion levels. Sensitivities in these instruments can be as high as 200 million counts per second per part per million with linear dynamic ranges up to eight orders of magnitude. And with standards for only a few elements, rapid semiquantitative analysis of over 70 elements in an individual sample can be performed.[3]

Since its very first days of ICP-MS,[4] ICP-MS has shown to be applicable to several areas of science. These include geochemistry,[5-7] the nuclear industry,[8-10] environmental chemistry,[11-13] clinical chemistry,[14,15] the semiconductor industry,[16-19] and forensic chemistry.[20,21]

In this introduction, the general attributes of ICP-MS will be outlined in terms of application in elemental speciation, instrumentation and sample introduction.

Elemental Speciation

In elemental speciation, one wants to identify and quantify various chemical species that together comprise the total elemental concentration in a sample, This is important because the toxicity and biological function of many trace or ultratrace elements depend greatly on their chemical forms and/or oxidation states. For example in the case of chromium: $Cr_2O_7^{-2}$ is toxic, whereas Cr^{+3} is essential at trace level. There are a lot of promising fields in elemental speciation: Environmental Risk Assessment; Ecotoxicology; Food Industry; Occupational Health/hygiene; Clinical Chemistry and Medicine and Industrial Analysis. A lot of analytical methods have been developed for a wide variety of important scientific applications, including the following: accurate assessment of actual risks to human health from toxic elements; facile identification and study of structure and binding of trace elements in proteins, DNA and other molecules of biological and geological interest; detailed studies of uptake, retention and excretion of trace metal ions; direct evaluation of the accuracy of various geochemical and soil chemical modes that predict elemental speciation based on

equilibrium calculation. Most analytical procedures can only determine the total amount of the elements, not their chemical forms. By coupling with chromatographic separations. ICP-MS detection provides unambiguous identification of the metal elements and most nonmetals associated with these chemical forms.[22]

ICP-MS has been successfully used as a detector in chromatographic separation after on-line coupling between various liquid chromatography techniques and ICP-MS. So far various separation schemes, including reversed phase (RP),[23] reversed-phase ion-pairing (RP-IP), [23] ion chromatography (IC),[24] size exclusion chromatography (SEC),[25] supercritical fluid chromatography (SFC),[25] gas chromatography (GC)[22] and capillary electrophoresis(CE)[26] have been coupled with ICP-MS. In particular, proteins and other biopolymers are separated by size exclusion chromatography, and ICP-MS identifies the elements in each protein fractions. Size exclusion chromatography is enjoying increasing popularity especially for the separation of metal-binding proteins. The risk of breaking up the original metal-protein bond during the sample preparation and chromatographic separation steps, insufficient detection of the elements in the eluting fraction, and contamination are the major obstacles in speciation analysis for metal-containing biomelecules. There is still substantial room for developing faster and better chromatographic separation, better detection limits, more sensitive, less interference-prone methods, and more general methods applicable to analysis of real world samples![27]

ICP-MS Instrumentation

The basic design of all ICP-mass spectrometers includes four main components: sample introduction, the ICP, the ion extraction and focusing optics, and the mass analyzer and detector. A brief description of the last three components follows.[28]

The ICP is an atmospheric pressure electrical discharge sustained in an atmosphere of an inert gas, typically argon (Ar). Radio-frequency (RF) energy is supplied to the plasma through a series of water-cooled copper loops known as the load coil. The RF power operates at one of two frequencies, 27.12 or 40.68 MHz, and at powers nominally between 650-1500 watts. The load coil surrounds a quartz torch, which consists of three concentric

tubes through which the argon gas is introduced to the plasma. The outermost tube supplies the largest flow of Ar. This outer gas flow must be sufficient to sustain the plasma and prevent overheating of the outer tube of the torch. The middle tube supplies what is known as the auxiliary gas which is typically used to control the position of the plasma inside the torch. An increase in auxiliary gas flow tends to push the entire plasma forward. The auxiliary gas flow also contributes to plasma stability. Sample is introduced to the plasma through the innermost tube by the nebulizer or aerosol gas flow. The aerosol gas delivers the sample aerosol to the plasma and contributes to the signal stability. This flow punches a hole, or "central channel" through the center of the plasma. A diagram of the ICP is shown in Fig 1. A plasma is defined as the high energy state of a gas in which all the atoms and molecules are ionized. The ICP is a partially ionized gas (typically Ar, which is less than 1%

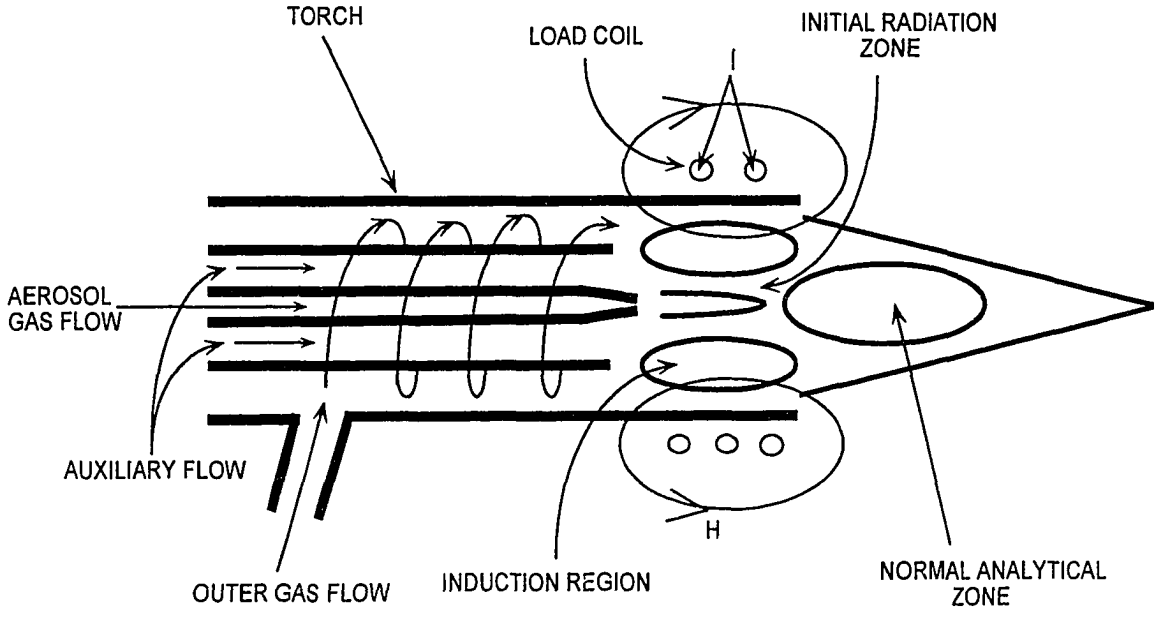

Fig 1. Diagram of the ICP (Ref. 29)

ionized in the plasma). In order to initiate the plasma, a gas stream is seeded with free electrons from a high voltage spark with a potential large enough to overcome the dielectric resistance of the gas. The load coil, once energized with kilowatt rf power, induces an electro-magnetic field within the torch. These fields inductively couple energy into the plasma by accelerating free electrons on the periphery of the plasma into the induction zone within the load coil. Energy is then transferred to other plasma species by collision. The plasma is maintained by transfer of the RF energy passed through the load coil into the induction region. The temperature in this region is believed to possibly reach 10 000 K. The center of the plasma or so called the central channel is heated by conductive, convective, and radiative transfer of energy from the induction region, and is probably between 5000 K and 7000 K.[3] In this manner the analyte, which flows only through the central channel, is not ionized directly, rather indirectly by the plasma.

As the analyte droplets pass through the central channel they undergo the following processes: desolvation, dissociation, atomization, ionization, and excitation. The ions produced are predominantly singly charged. Ions are produced at atmospheric pressure by the ICP, and mass spectrometers must operate under vacuum, thus necessitating a system of differential pumping. Typical ICP-mass spectrometers with a quadrupole mass filter have three stages of pumping to extract ions from the atmospheric pressure plasma into the low pressure (typically $10^{-5} - 10^{-6}$ torr). The first stage of pumping exists between the sampler and skimmer cones, and typically operates at ~ 1 torr. The second stage is the region between the skimmer cone and the differential pumping orifice which contains the extraction lens and other ion optics, and operates at about 10^{-4} torr. The third stage contains further ion optics, the mass analyzer, and the detector, and typically operates at around 10^{-6} torr.

The plasma is quasineutral, that is, the numbers of positive ions and electrons are approximately equal. Ions from the plasma are first extracted through the sampling cone, which is immersed in the plasma. As it passes through the sampler, the ion beam expands supersonically. The ion beam is further extracted through the skimmer cone, whose tip protrudes into the collision-free region of the supersonic expansion. As the particles enter the extraction lens, the lighter and more mobile electrons are eliminated, leaving an ion beam of

almost exclusively positive ions. A detailed review of the ion extraction process is provided elsewhere.[30] The surviving ions are focused into the remaining ion optics and into the mass analyzer. The ions that successfully traverse the mass analyzer are detected by one of a number of ion detection devices. Briefly, the detector produces a signal, which is directly proportional to the amount of ions impacting the detector per given time. This signal can then be further manipulated for data analysis.

In this dissertation several types of mass spectrometers have been employed for use with the ICP. Each employs a different method for the differentiation of ions for subsequent detection:

[1] Quadrupole mass filter (Q)

The quadrupole mass filter consists of four long metal rods with round or hyperbolic cross section which are arranged parallel to each other, and have RF and DC voltages applied to them. By varying these voltages, the rods acts as a mass filter, allowing only ions of a specific mass to charge ratio to pass through the center of the quadrupole at any given combination of applied voltages. Ions of other masses undergo unstable trajectories and collide with the rods. These voltages are ramped very rapidly so the quadrupole can scan the whole mass range (2-260 m/z) in 100 ms. As a result, spectra of intensity versus m/z can be obtained for all elements. Quadrupoles are limited effectively to unit resolution so ICP-QMS generally can't resolve polyatomic and isobaric interferences. The interference problem is still the most significant weakness of ICP-QMS.

[2] Double-Focusing Mass Spectrometers in ICPMS - one of the *general methods for overcoming spectroscopic interference requires double-focusing instrumentation.*

ICP-MS with a quadrupole mass filter suffers from a number of spectroscopic and nonspectroscopic interferences that have limited the analytical figures of merit. Many techniques have been considered to reduce interferences, but none of these can cope with the problem in general.[31] All are limited to some specific interferences or are applicable for some selected elements only. One of the general methods to overcome limitations from spectroscopic interferences is high mass resolution, which includes using double-focusing instruments that combine a magnetic and an electric sector field analyzer. This is in contrast

with the low-resolution instruments that manage with simpler and cheaper quadrupole analyzers. With respect to sensitivity and resolution significant enhancement can be achieved by using magnetic sector based high resolution analysers instead of quadrupoles. Finnigan MAT introducing a double focusing reverse geometry Nier Johnson High resolution ICP-MS (Fig. 2): A magnetic sector field focuses ions with diverging angles of motion from the entrance slit to the intermediate slit. The magnetic sector field disperses ions with respect to momentum (**mv**). The electric sector field (ESA) focuses the ions with diverging angles of motion from the beta slit on to the exit slit. It disperses with respect to kinetic energy ($\mathbf{mV^2/2}$). Together, with optimized field shapes, deflection angles and field strengths, the magnet (B) and ESA (E) focus both ion angles (first focusing) and ion energies (double focusing) while being dispersive for m/z. The resolution can be changed by adjusting the

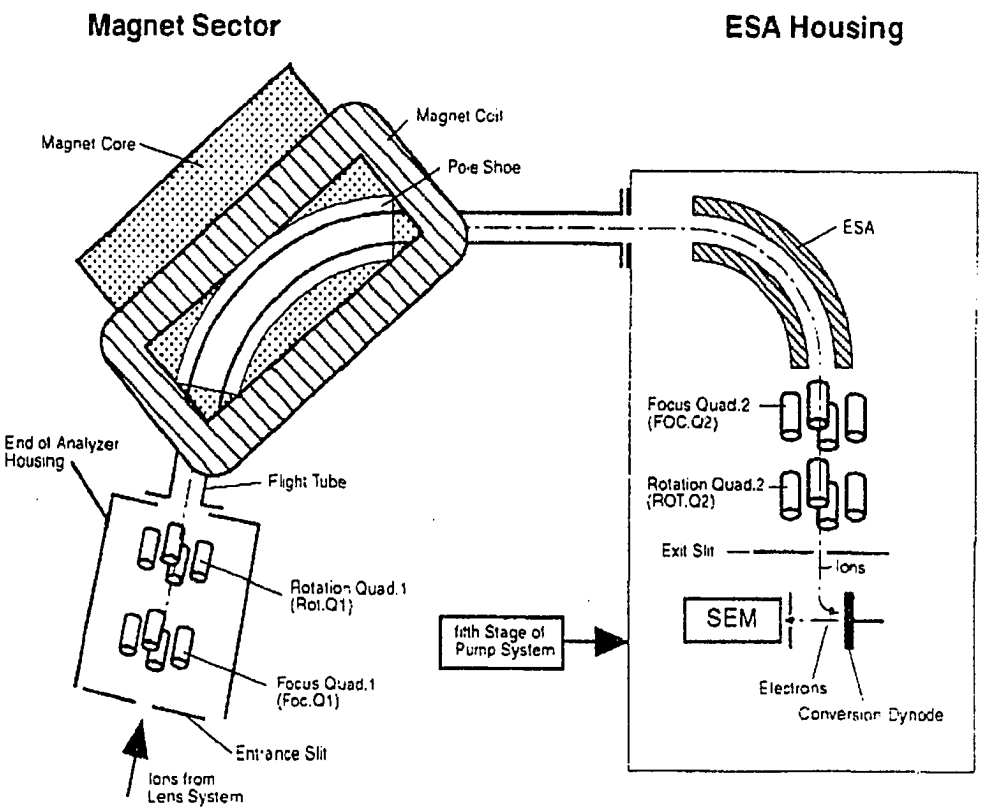

Fig. 2. Diagram of a typical double focusing reverse Nier Johnson geometry High resolution ICP-MS system (operating manual of ELEMENT)

width of exit slit. With magnetic sector instruments like the ELEMENT, mass resolution is constant over the whole mass range. This inherent feature differentiates the ELEEMNT from all ICP-MS based on quadrupole technology. With quadrupoles, mass resolution varies with mass. The ELEMENT can remove interferences by high resolution for unambiguous and accurate elemental analysis, provide high sensitivity and low dark noise for ultimate detection limit[32].

[3] Platform ICP with a collision cell, *solving the argon interference problem in ICP-MS.*[33]

The majority of spectral interferences in ICP-MS are the result of molecular species; combinations of matrix elements, for instance oxygen with argon (e.g. $^{40}Ar^{12}C^{+}$ on $^{52}Cr^{+}$, $^{40}Ar^{16}O^{+}$ on $^{56}Fe^{+}$ and $^{40}Ar_2^{+}$ on $^{80}Se^{+}$). These interferences produce an elevated background at the analyte mass that raises the achievable detection limits and make the analyte isotope unusable. The Platform ICP is the first commercial instrument to use a new technique (Fig. 3): ICP-hQMS incorporates a hexapole ion lens located behind the skimmer cone surrounded

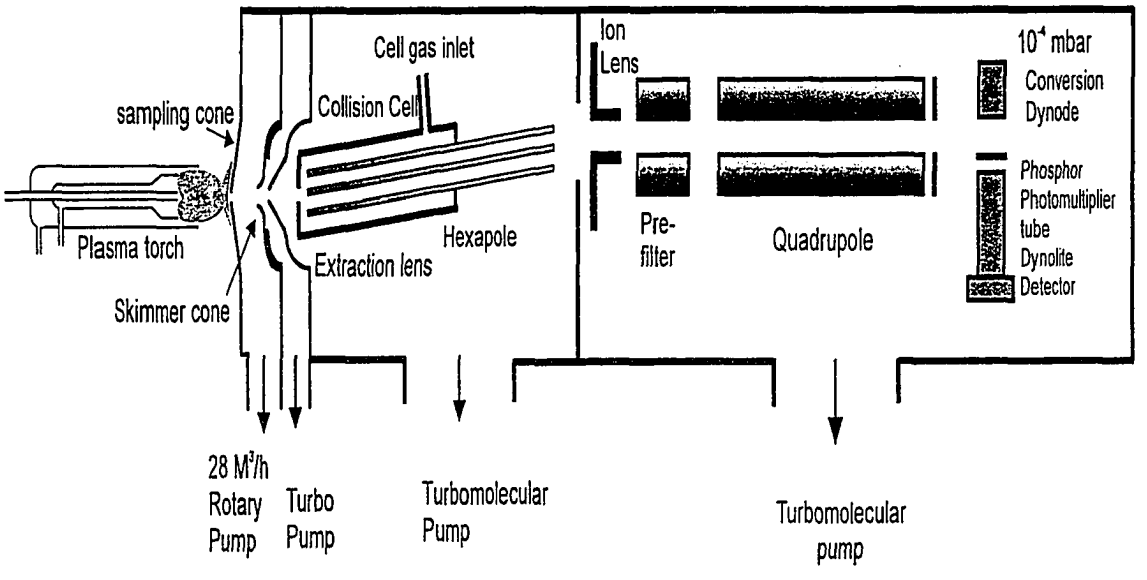

Fig.3. Diagram of a typical ICP-MS with a collision cell

by a gas cell. By adding small amounts of helium, the pressure inside the collision cell is increased, the collision among the helium and ions will break up molecular species before they enter the mass analyser, while the hexapole lens reduces the ion energy spread of the ions as they emerge from the skimmer. These ions assume the energy of the collision gas, and are directed down the hexapole by the RF field. In the Platform the ions are then accelerated to 1000 volts and then to the Dynolite™ detector. The result is a mass spectrum free from argon interferences, which makes it possible to determine previously difficult or impossible elements at ultratrace levels. Other kinds of trace levels of gas may also be introduced into the hexapole to react chemically with the ions generated in the plasma. Some interferences can be removed or reduced depending on the properties of these collision gases. For experiments such as iron, calcium or selenium, where ArO^+, Ar^+ and $Ar\text{-}Ar^+$ need to be removed, the addition of small amounts of hydrogen will remove or dramatically reduce these interferences. He is generally used for all the elements. All of these gases are controlled by computer controlled mass flow controllers. For routine multielement analysis, a mixture of helium and hydrogen is the best choice of collision gases.

Sample Introduction

Although samples can be introduced to the ICP in liquid, solid, or gaseous forms, aqueous solution is the most common by far.[3] To aid in its reduction to atomic ions in the ICP, the bulk liquid must first be reduced to small droplets. This is achieved through the use of a device known as a nebulizer. Nebulizers work basically by shattering the large liquid drops by vibration or gas flow into a fine mist of droplets, where they are swept by an argon stream through a spray chamber and then to the ICP. Several different kinds of nebulizers have been employed for use with ICP spectrometry, of which common ones include pneumatic and ultrasonic nebulizer.[34] In the spray chamber the larger droplets are removed by collision with the chamber walls, The spray chamber is usually cooled to a temperature can be precisely controlled which give a very stable ion signal. In addition, cooling the sample aerosol also removes some of the water from the sample, reducing the level of polyatomic oxide species formed, which in turn reduces the interference on certain analytes.

There are quite a lot of approaches on reducing the solvent loading into the plasma: conventional desolvation,[4] cryogenic desolvation,[35] membrane desolvation.[36]

Dissertation Organization

This dissertation is composed of five papers formatted for publication in five different journals. Each paper stands independent of the others as a completely manuscript with accompanying tables, figures and literature cited. A summary chapter follows the last paper.

References

1. Houk, R. S., *Acc. Chem. Res.*, 1994, **27**, 333.
2. Hieftje, G. M., and Norman, L. A., *Int. J. Mass Spectrom. Ion Processes*, 1992, **118/119**, 519.
3. Jarvis, K. E., Gray, A. L., and Houk, R. S., *Handbook of Inductively Coupled Plasma Mass Spectrometry*, Blackie & Son, Glasgow, 1992; Gustavsson A. "liquid Sample Introduction into Plasama" *In Inductively Coupled Plasma in Analytical Atomic Spectrometry* 2nd ed., Montaser A. and Golightly Eds. VCH, New York, 1992
4. Houk, R. S., Fassel, V. A., Flesch, D. D., Svec, H. J., Gray, A. L., and Taylor, C. E., *Anal Chem.*, 1980, **52**, 2283.
5. Joannon, S., Telouk, P., and Pin, C., *Spectrochim. Acta, Part B*, 1997, **52**, 1783.
6. Makishima, A., Nakamura, E., and Nakano, T., *Anal. Chem.*, 1997, **69**, 3754.
7. Hall, G. E. M., and Pelchat, J., *J. Anal. Atom. Spectrom.*, 1997, **12**, 103.
8. Crain, J.S., *Spectroscopy*, 1996, **11**, 30.
9. Erickson, M., Aldstadt, J., and Alvarado, J., *J. Haz. Mat.*, 1995, **41**, 351.
10. Heres, A. P., and Noe, M.C., *Nuclear Technology*, 1996, **115**, 146.
11. Liaw, M., Jiang, S., and Li, Y., *Spectrochim. Acta, Part B,* 1997, **52**, 779.
12. van den Broeck, K., Vandecasteele, C., and Geuns, J. M. C., *J. Anal. Atom. Spectrom.*, 1997, **12**, 987.
13. Rodushkin, I., and Ruth, T., *J. Anal. Atom. Spectrom.*, 1997, **12**, 1181.

14. Probst, T. U., Berryman, N. G., Lemmen, P., Lothar, W., Auberger, T., Gabel, D., Carlsson, J., Nóbrega, J., Gélinas, Y., and Krushevska, A., Barnes, R., *J. Anal. Atom. Spectrom.*, 1997, **12**, 1243.

15. Larsson, B., *J. Anal. Atom. Spectrom.,* 1997, **12**, 1115.

16. Bhattacharya, R. N., Wiesner, H., and Berens, T. A., *J. Electrochem. Soc.*, 1997, **144**, 1376.

17. Ajluni, C., *Electronic Design*, 1995, **43**, 38.

18. Morin, M., Kimura, T., and Koyanagi, M., *Solid State Tech.*, 1993, **36**, 45.

19. Fucsko, J., Tan, S., and Balazs, M., *J. Electrochem. Soc.*, 1993, **140**, 1105.

20. Lalchev, M., Ionov, I., and Daskalova, N., *J. Anal. Atom. Spectrom.*, 1997, **12**, 21.

21. Watling, R. J., Lynch, B. F., and Herring, D., *J. Anal. Atom. Spectrom.*, 1997, **12**, 195.

22. Lobinski R., *Applied Spectroscopy* 1997, 7, 260A

23. Shum S.C.K; Neddersen R. and Houk R.S, *Analyst* 1992 **117**, 577

24. Shum S.C.K. and Houk, R.S., *Anal. Chem.* 1993, **65** , 2972

25. Vela N.P; Olson L.K; and Caruso J.A., *Anal Chem.* 1993, **65**, 585A

26. Liu Y. lopez-Avila V. Zhu J.J Wiederin D.R. *Anal Chem.* 1995 **10**, 127

27. Corneils R. and De Kimpe J. *J. Anal. Atomic Spec,* 1994, 9 945; Seubert A., *Fresenius J. Anal. Chem.*, 1994 **350**, 210; Moens L. *Fresenius J. Anal. Chem.*, 1997, 359, 309

28. Greenfield, S., and Montaser, A., in *Inductively Coupled Plasmas in Analytical Atomic Spectrometry*, Montaser, A., and Golightly, D. W., eds., 2nd edn., VCH, London, 1992.

29. Allen L. A., Ph.D. Dissertation, Iowa State University, Ames, Iowa, 1996.

30. Niu, H., and Houk, R. S., *Spectrochim. Acta, Part B*, 1996, **51B**, 779.

31. Evans, E.H., Giglio J.J. Castillano T.M. and Caruso J.A. *Inductively Coupled and Microwave Induced Plasama Sources for Mass Spectrometry,* RSC, 1995 UK

32. Luc Moens, Ghent University (Belgium), Norbert Jakubowski, Institut fuer Spektrochemie und angewandte Spektroskopie (Germany) *Analytical Chemistry News & Features*, April, 1998; Giessmann, U. and Greh, U., *Fresenius J. Anal. Chem.*, 1994, **350**, 186

33. Turner, P.J. Haines, R.C. and Speakman, J. *5th International Conference on Plasma*

Source Mass Spectrometry, University of Durham, UK, 1996, **September;** Lynaugh, N; Turner, P.J; Speakman, J.; Haines, R.C. and Compson, K.R. *ICP Information Newsletter,* 1997 **23**, 319

34. Clifford, R. H., Montaser, A., and Dolan, S. P., *Anal. Chem.*, 1990, **62**, 2745.

35. Alives, L.C.; Wiederin, D.R; Houk, R.S. *Anal Chem.* 1992, **64**. 1164. Alives, L.C.; Minnich, M.G.; Wiederin, D.R; Houk, R.S. *J. Anal. Atomic Spectrum.* 1994, **9**,399.

36. McLaren, J. W. Lam, J.W. *Spectrochim. Acta*, Part B, 1990, **45B**, 1091; Botto R.I. and Zhu J.J , *J Anal. At. Spectrom.* 1994, **9**, 905

CHAPTER 2: IDENTIFICATION OF INORGANIC ELEMENTS IN PROTEINS IN HUMAN SERUM AND IN DNA FRAGMENTS BY SIZE EXCLUSION CHROMATOGRAPHY AND INDUCTIVELY COUPLED PLASMA MASS SPECTROMETRY WITH A MAGNETIC SECTOR MASS SPECTROMETER

A paper published in the Journal of American Chemical Society[1]

Jin Wang and R. S. Houk[2]; Dawn Dreessen and Daniel R. Wiederin

Abstract

A general method to identify trace elements in proteins and DNA is described. The method is sensitive enough to observe many unusual or difficult elements, such as Se, rare earths, Cd and U, at ambient levels bound to proteins in human serum. These measurements are made in only a few minutes without preliminary isolation and preconcentration steps. Binding of metal cations to DNA restriction fragments can be observed by similar procedures both for essential elements like Mn and Fe and toxic ones like Cd and Pb. In particular, trace Pb, Cd and Co are completely bound to DNA fragments. Reduction of chromate to a cation (probably Cr^{+3}) and subsequent binding of the Cr cation to DNA can also be detected by these procedures.

Inorganic elements play key roles in the function of many biological molecules[1]. Metal ions such as Zn and Cu, contribute to the structure and function of many enzymes, for example. The toxic activity of less abundant metals like Cd and Pb is thought to relate to their ability to compete with essential elements in proteins or to bind to DNA. There has been considerable recent interest in dietary selenium to prevent cancer[2] and delay the onset of AIDS symptoms.[3] Multielement analytical procedures are needed to study interactions between different trace elements. For example, occupational exposure to certain pairs of

---

[1] Reprinted with permission of J. Amer. Chem. Soc. 120: 5793-5799

[2] Author for correspondence

metals (e.g., Pb and Cu, Pb and Fe, or Fe and Cu) caused a much higher incidence of Parkinson's disease than exposure to any of the individual metals studied,[4] and selenium plays a role in the metabolism of iodine in thyroid hormones.[5]

With modern instrumentation for atomic spectroscopy, determination of the total amount of the elements of interest in a biological specimen is generally possible. Preparation of the sample and minimizing contamination, rather than the performance of the instrument per se, are often the limiting steps in the accuracy of the measured concentrations. This is particularly the case with inductively coupled plasma - mass spectrometry (ICP-MS) with a magnetic sector mass analyzer, which has very high sensitivity and sufficient spectral resolution to separate atomic analyte ions from polyatomic ions from other constituents of the sample. For example, detection limits for most elements are below 1 part-per-trillion, and the major isotopes $^{52}Cr^+$ and $^{56}Fe^+$ can readily be separated from the interferences ArC^+ and ArO^+.[6]

This paper describes methodology that combines these recent advances in ICP-MS with chromatographic separations for the study of inorganic ions directly in biological samples. Size exclusion chromatography (SEC) is chosen for these initial experiments because it operates near physiological pH and does not require organic solvents that might denature the biological molecules or otherwise remove the metals of interest. The SEC separation is also robust and can tolerate repeated injections of a difficult sample such as serum. The ICP-MS measurement then identifies the element(s) present in particular chromatographic peaks. Such combinations of chromatography and ICP-MS are presently considered the preferred general method for the measurement of the molecular forms of trace elements.

SEC has been used previously for ICP-MS with low resolution mass analyzers.[7] The main new aspects of the present paper are a) the extra sensitivity and spectral resolution provided by the magnetic sector MS, and b) further improvements in sensitivity and reduction of spectral interferences via the use of microscale nebulization and solvent removal for introducing virtually all of the column effluent into the ICP. The type of information provided by these capabilities is then illustrated for several elements of current interest in

proteins and DNA.

Instrumentation. The major instrumental components are a) SEC column,[8] b) microconcentric nebulizer and desolvation system,[9] c) ICP,[10] and e) magnetic sector MS.[11] Key operating conditions are identified in the appropriate footnotes. The compounds of interest are separated by SEC and injected on-line as discrete bands into the nebulizer. This particular nebulizer is designed for use at low liquid flow rates (typically 30 - 150 $\mu L\ min^{-1}$); it produces a mist of fine droplets that are efficiently transported out of the spray chamber. These droplets are then dried and most of the solvent is removed by a condenser. Desolvation has been shown by others to improve ion transmission dramatically for this type of ICP-MS device compared to the sensitivity obtained when the sample is introduced as wet aerosol droplets.[12] The dry aerosol particles from the sample then enters the hot argon ICP where they are converted into atomic ions. These ions are extracted through a molecular-beam sampling system and analyzed by a reverse geometry double focusing mass analyzer.

Two resolution settings were used for the mass analyzer. At low resolution, the peaks are flat-topped with a width of approximately 0.2 mass unit at the base of the peak. The nominal value of $m/\Delta m$ is 300, where Δm is the peak width. At medium resolution ($m/\Delta m$ = 3000), the narrower slits and the scanning process reduce the signal to about 10% of that obtainable at low resolution, so medium resolution is used only for elements such as Fe and Cr that suffer from spectral interference from polyatomic ions[13].

SEC Separations, The retention behavior of the SEC column is calibrated by analyzing synthetic samples of pure proteins known to contain particular elements. Basically, large proteins of high molecular weight are not retained and elute first, followed by smaller proteins, with small compounds eluting last. The calibration proteins, their molecular weights, and the elements monitored are thyroglobulin (670,000 g/mole or 670 kDa, I), ferritin (440 kDa, Fe, Cu and Zn), β-amylase (200 kDa, Cu), alcohol dehydrogenase (150 kDa, Zn and Cd) and carbonic anhydrase (29 kDa, Cu and Zn).

These pure proteins yield individual peaks with a width of 30-40 s at the base for a chromatographic resolution of ~1.0. Thus, the column and sample introduction system are capable of reasonable chromatographic resolution if a relatively simple sample is injected.

In particular, the extra dead volume added by desolvating the aerosol does not compromise the chromatographic peak shapes, at least when the bands from the column are already fairly wide (30-40 s). Heating the aerosol in the desolvation system can cause either memory or loss of volatile elements such as Hg and Os, however.

The observation that (a) these calibration mixtures yield single, sharp chromatographic peaks and (b) the retention times for the various calibration proteins fall on the same straight line when plotted vs molecular weight indicate that the SEC separation did not remove the inorganic elements from the proteins. We also injected blanks containing EDTA at ~ 1 mM several times to see if inorganic elements are retained by the column. Such elements could then be removed from the column by proteins in subsequent injections and appear falsely to be bound to protein in the original sample. Iron was the only element that gave a substantial chromatographic peak from the EDTA injection, and even that Fe peak was at a lower level than those from the serum or DNA samples. Thus, we believe the peaks shown below actually represent binding of the elements of interests or DNA in the original samples and are not merely due to artifacts of the SEC separation. Some elements (notably Pb) do produce an elevated, continuous background, however, as discussed below.

Samples. Human serum standard reference materials were obtained as freeze dried solids[14] and redissolved in 0.1 M tris-HCl buffer in deionized water to the same consistency as fresh serum. The pH of this reconstituted serum solution was approximately 7. It should be noted that these materials were not intended for use as either protein or trace metal standards; we analyzed them simply because they were available and could be handled readily with minimal precautions.

DNA restriction fragments were obtained commercially.[15] The DNA solution contained a range of fragments from 8 base pairs (molecular weight ~ 5 kDa) to 587 base pairs (MW ~ 387 kDa). It was diluted 1/50 in 25 mM tris buffer to a final concentration of 5 ppm DNA. This solution also contained 20 μM EDTA. The molecular weight calibrations derived for the proteins were assumed to be at least approximately valid for these DNA fragments.

The ICP produces primarily singly-charged atomic ions, regardless of the original

species in the sample solution. In the subsequent discussion, the ions observed by the mass spectrometer are are denoted by citing the isotope monitored, which distinguishes the ions formed in the ICP from those present in the sample solution. For example, $^{208}Pb^{+}$ is detected with the mass spectrometer from either free Pb^{+2} ions in solution or Pb bound to proteins in the sample.

Results and Discussions

Metal Ions in Proteins from Human Serum. Element-selective chromatograms for Zn, Cu and Pb are shown in Fig. 1A. The concentrations corresponding to the largest peaks are estimated in the captions to the figure. [16] The initial parts of these chromatograms show flat baselines, which have been deleted to conserve space. The major portions of these elements are present bound to proteins that elute in a retention window from 300 to 360 s, which corresponds to a molecular weight range of 200 to 20 kDa. The maximum of the SEC profile for these elements is at a molecular weight of roughly 70 - 80 kDa, which probably represents albumins, the most abundant proteins in serum. Copper and zinc also produce a small peak from a large protein(s) at ~600 kDa.

There is a substantial background for Pb, which is actually ions of $^{208}Pb^{+}$, for the following reason. This background at m/z = 208 dips briefly at 380 s, which is roughly when the Na and K from the serum sample elute from the column. Highly concentrated matrix elements typically suppress the signal for analyte ions in ICP-MS.(ref) The fact that this $^{208}Pb^{+}$ background is more or less flat in other regions means that the Pb does not come from the sample but is from the solvent, reagents, column or connecting tubing. Despite the perturbation of the $^{208}Pb^{+}$ background and signal at 380 s, there is a hint of a peak for "free" Pb, perhaps Pb^{+2}, at 400 s. Alternatively, this latter Pb chromatographic could represent a small (< 10 kDa) Pb-binding protein found previously in erythrocytes.[17] There is significant environmental and toxicological interest in determining what fraction of the Pb in blood and serum is free or is bound to cells or proteins.

These measurements show that nearly all the Cu and Zn and most of the Pb in serum is bound to proteins. In these and subsequent chromatograms, the SEC peaks shown from

serum are generally wider than those seen from pure proteins, probably because each SEC peak from serum probably represents a number of proteins. The chromatographic resolution provided by SEC is not capable of complete separations for such a complex sample as human serum. Also, the relative peak heights in the chromatograms do not directly reflect the relative concentrations.

The Cd chromatogram shown in Fig. 1B was obtained from the same injection and elution cycle as that in Figure 1A. Two $^{114}Cd^{+}$ peaks corresponding to Cd bound to proteins at ~ 600 kDa and 80 kDa are shown. There is little or no "free" Cd. Traditionally, Cd, Cu and Zn have been thought to be stored in metallothioneins.[18] However, parts A and B show that chromatographic peaks in the appropriate molecular weight range for metallothioneins (~10 kDa) are certainly not prominent and may not be present at all. Either these elements are not stored in metallothioneins in serum, or the metallothioneins are bound to other, larger proteins.

Another chromatogram for U and Th obtained from a different injection of serum is presented in Fig. 2. Three distinct fractions containing Th are observed at the molecular weights shown. The major Th fraction is at ~80 kDa, as is the case for U. There is some U bound to either small proteins or other small molecules as well.

For the elements shown previously, spectral overlap with polyatomic background ions is not a problem, so low resolution (i.e., wide slits in the MS) is used to provide maximum signal. Chromium is a different matter, as indicated in Fig. 3. A mass scan done at medium spectral resolution during the elution of the first Cr chromatographic peak is depicted in the insert to Figure 3. Spectral resolution of 3000 is sufficient to separate $^{52}Cr^{+}$ from $^{40}Ar^{12}C^{+}$. Not only is the signal from ArC^{+} much larger than that from $^{52}Cr^{+}$, but the ArC^{+} signal increases when proteins elute because they put more carbon into the plasma than the eluent alone. Thus, measurements at low spectral resolution would not suffice for the measurement of $^{52}Cr^{+}$ unless some other means was employed to remove ArC^{+}. Figure 3 also presents the reconstructed chromatogram for $^{52}Cr^{+}$, which shows Cr in two protein fractions at ~140 kDa and 10 kDa.

The reader should note that none of these elements have been spiked into these serum

samples. The signals shown represent the ambient levels of these elements in the samples as analyzed. It is possible that these reference serum samples were contaminated, either in production, during storage, or by us when they were re-dissolved. If so, the chromatograms still show that the extra trace metals added as contaminants bind to proteins. We have done some confirmatory experiments with fresh serum and found chromatographic binding patterns similar to those described in Figure 1-3, with lower concentrations for some elements, notably Cr and Th.

Selenium in Proteins from Human Serum.. Selenium is one of the most difficult elements for ICP-MS in that the ionization efficiency is low and the most abundant isotopes suffer from spectral overlap with the background ion Ar_2^+. The apparatus can barely resolve $^{78}Se^+$ from $^{38}Ar^{40}Ar^+$, at a cost of reduction of signal for $^{78}Se^+$ by a factor of ~1000 compare to the signal obtained at low resolution. We therefore use $^{82}Se^+$ at low spectral resolution despite overlap with $^{82}Kr^+$, a common contaminant of the argon used to operate the plasma. Fortunately, the total Se concentration in serum is fairly high, typically 90 ppb or more.[19]

A selenium chromatogram obtained in this fashion is shown in Fig. 4. Most of the Se is bound to three distinct protein fractions in the molecular weight ranges 760, 140 and 80 kDa. Some Se in small molecules also elutes after the proteins at a retention time of ~390 s.

The main selenoproteins that have been characterized are glutathione peroxidase (85 kDa), extracellular glutathione peroxidase (92 kDa), and selenoprotein P (three forms, 74, 61 or 57 kDa).[20] We see a chromatographic peak at ~80 kDa that could correspond to these species, in addition to peaks from two other, larger protein fractions that contain selenium.

With this system, calcium in serum elutes as a single chromatographic peak at about 320 S. Thus, $^{40}Ar^{42}Ca^+$ could contribute slightly to the chromatographic peaks labeled 140 and 80 kDa in figure 4. None of the other chromatographic peaks in Figure 4 are caused by this polyatomic ion.

Binding of Metal Ions to DNA Fragments. Element-selective chromatograms are shown for four elements in a solution of DNA restriction fragments in Fig. 5. In the first frame (Fig. 5a), chromatographic peaks for Pb and Cd occur at retention times that correspond to the elution of DNA fragments in the molecular weight ranges 7 - 41 kDa.

Again, these peaks represent the ambient concentrations of these elements in the DNA, solvent and buffers; none of these elements have been deliberately spiked into the samples. The chromatograms illustrate that these toxic elements are completely bound to DNA, at least at the trace levels encountered here.

The other frame of Fig. 5 shows that Fe and Mn also readily bind to DNA; Mn binds to larger fragments than does Fe. Three or four different size fragments containing Fe are partially separated by the SEC column. Medium spectral resolution is necessary here to separate $^{56}Fe^{+}$ from $^{40}Ar^{16}O^{+}$ and is helpful for the measurement of Mn. We also found a substantial amount of Co bound to DNA, much more so than in proteins from human serum. This latter observation is of interest because of other studies that show that cobalt binds readily to phosphodiesters similar to DNA[21]

Reactions and Binding of Cr (VI) and Cr (III) with DNA. Three chromatograms for Cr at medium spectral resolution are shown in Fig. 6. The DNA solution itself does not have appreciable levels of Cr, as shown by the dotted baseline in Fig. 6a. One aliquot of the DNA solution was then spiked with CrO_4^{-2}, i.e., the probable form of Cr (VI) at pH = 7, which was the pH value used for the separation. A second aliquot was spiked with Cr^{+3}. The two spikes contained roughly equal numbers of Cr atoms. Chromium from the CrO_4^{-2} spike is observed bound to DNA (Fig. 6a). Most of the Cr from the Cr^{+3} spike also binds to DNA (Fig. 6b), with a small subsequent peak for Cr bound to small molecules.

Other experiments show that the oxoanion MoO_4^{-2} shows little tendency to bind to these DNA fragments, as expected if the main metal binding sites are the negatively-charged phosphate groups. Thus, the original CrO_4^{-2} in the spike for Fig. 6a has been converted into a cation, otherwise the Cr from it would not bind to DNA.[22] One possible half reaction would be

$$CrO_4^{-2} + 8H^{+} + 3e^{-} \rightarrow Cr^{+3} + 4H_2O$$

If CrO_4^{-2} has been reduced, some other component of the solution has been oxidized, most likely the DNA. *Oxidation of DNA in this fashion is one possible process responsible for carcinogenesis by Cr (VI).*[23] Rather than oxidize DNA directly, chromate in actual biological systems could alternatively oxidize other compounds to produce reactive species

like O_2^- or OH^-, which then oxidize DNA.[23, 24] The present work shows that the Cr cation formed (probably but not necessarily Cr^{+3}) can bind to DNA during or after the oxidation of DNA.

Conclusion

The main results of this study can be summarized as follows:

1. Even though the chromatographic separation dilutes the sample, ICP-MS with a magnetic sector instrument can observe many elements at ambient levels in human serum and provides the spectral resolution necessary to measure Cr and Fe using their major isotopes.
2. Most of the metals studied remain bound to the biological molecules during the chromatographic separation. SEC provides a "soft" chemical separation that does not remove the metals from the proteins or DNA fragments. Eventually, better chromatographic separations (probably by a wholly different separation mechanism such as ion exchange, affinity chromatography, or electrophoresis) or an additional spectroscopic measurement (such as electrospray MS) will be necessary to identify individual proteins in samples of this complexity. The authors expect that SEC will continue to be valuable as a preliminary fractionation and desalting step, followed by a different separation procedure that has been fine-tuned to optimize chromatographic resolution for a particular set of compounds.
3. In human serum, alkali metals (Cs, Rb and Li) are observed as free metal ions, alkaline earths (Ba and Sr) are mostly free ions with some bound to proteins.[25] Most other metals are observed bound to proteins, even those elements normally considered toxic. For most elements, the main protein fraction containing metals is around 80 kDa, which probably corresponds to serum albumins.
4. Trace metal cations readily bind to DNA fragments. The Cr from a spike of CrO_4^{-2} also binds to DNA fragments, which indicates that the Cr (VI) has been reduced while the DNA has probably been oxidized. Such measurements are straightforward at Cr levels of ~50 ppb and could probably be performed at concentrations down near the present regulatory levels of Cr (VI) of ~ 1 ppb.
5. In principle, The ICP-MS device can measure several elements in the same molecules.

This capability would be useful for identifying enzymes that contain ions from different elements.

6. The purity of the blanks remains a problem at these concentrations, especially for Pb. Completely metal-free chromatographic systems are advisable, i.e., no stainless-steel columns. However, even if the samples are contaminated with additional metals at modest levels, the proteins and DNA fragments present therein readily bind the excess metals.

A number of valuable measurements should be possible based on the high selectivity and sensitivity of this general analytical method. These include: a) estimation of the strength of binding of the inorganic elements by addition of complexing reagents of known binding constants, followed by chromatographic separation of the products, b) comparison of binding patterns for metals in proteins that have had the disulfide bonds broken or have been denatured, and c) spike experiments in which a tracer in a particular oxidation state (e.g., Mn^{+2}) can be followed into particular biomolecules. Some such studies should be possible more or less directly on biological liquids or on extracts from tissues without the laborious isolation procedures normally employed, which may themselves contaminate or alter the metal binding characteristics of interest. Alternatively, the isolation procedures already developed can now be applied to very small samples. These types of experiments are underway in our laboratory.

Acknowledgements

The experiments are supported by the Ames Laboratory, U. S. Department of Energy, Office of Basic Energy Sciences, under Contract W-7405-Eng-82. The measurements were conducted at CETAC Technologies. The authors also thank Finnigan MAT for providing the mass spectrometer AND David E. Nixon (Mayo Clinic) and Nenad Kostic and Robert E. Serfass (Iowa State University) for many helpful discussions

References

1. (a) Chem. Reviews 1996, 96, November issue on bioinorganic enzymology and metalloenzymes, (b) Trace Elements in Human Nutrition and Health; World Health Organization, Geneva, Switzerland, 1996

2. L. C. Clark, G. F. Coombs, B. W. Turnbull, E. H. Slate, D. K. Chalker, J. Chow, L. S. Davis, R. A. Glover, G. L. Graham, E. G. Gross, A. Krongard, J. L. Lesher, H. K. Park, B. B. Sanders, Jr., C. L. Smith, and J. R. Taylor, J. Amer. Med. Assoc. 276, 1957 (1996); G. A. Colditz, J. Amer. Med. Assoc. 276, 1984 (1996); C. Ip and H. E. Ganther, Novel Strategies in Selenium Cancer Chemoprevention Research, in R. F. Burk, Ed., Selenium in Biology and Human Health, Springer-Verlag, New York, 1994 , Chap. 9.

3. E. W. Taylor, C. S. Ramanathan, R. K. Jalluri and R. G. Nadimpalli, J. Med. Chem. 27, 2637 (1994).

4. J. M. Gorell, C. C. Johnson, B. A. Rybicki, E. L. Peterson, G. X. Kortsha, G. G. Brown and R. J. Richardson, Neurology 48, 650 (1997).

5. J. R. Arthur and G. J. Beckett, Roles of Selenium in Type I Iodothronine 5 ′ -Deiodinase and in Thyroid Hormone and Iodine Metabolism, in R. F. Burk, Ed., Selenium in Biology and Human Health, Springer-Verlag, New York, 1994 , Chap. 5.

6. N. Bradshaw, E. F. H. Hall and N. E. Sanderson, J. Anal. Atomic Spectrom. 4, 801 (1989); I. Feldmann, W. Tittes, N. Jakubowski, D. Stuwer and U. Giessmann, J. Anal. Atomic Spectrom. 9, 1007 (1994).

7. S. C. K. Shum and R. S. Houk, Anal. Chem. 65, 2972 (1993); B. Gercken and R. M. Barnes, Anal. Chem. 63, 283 (1991); L. M. W. Owen, H. M. Crews, R. C. Hutton and A. Walsh, Analyst 117, 649 (1992).

8. SEC conditions for protein separations (Figs. 1-4): GPC 300 column (SynChrom Inc., 2 mm ID x 25 cm long), eluent aqueous tris-HCl buffer (0.1 M) at 160 μL/min, pH = 6.9. Conditions for DNA separations (Figs. 5 and 6): packing from GPC 300 column removed and packed into PEEK column by Keystone Scientific, Inc. (2 mm ID x 25 cm long), same eluent with tris buffer at 0.025 M.

9. MCN and desolvation conditions: MCN (CETAC Technologies) with single pass conical spray chamber, aerosol gas flow rate 0.7 L min^{-1}, make up gas flow rate 0.5 L min^{-1}, heater temp 140 °C, condenser temp 0 °C.

10. ICP conditions: outer gas flow rate 14 L min^{-1}, auxiliary gas flow 0.8 L min^{-1}, forward power 1.25 kW, sampling position 10 mm from load coil, on center.

11. MS conditions: Along with the ICP conditions, ion lens voltages etc. were adjusted to maximize the signal for analyte ions from standard solutions injected post-column before the chromatographic experiments. The accelerating voltage was nominally 4095 volts.

12. Hutton, R.C., personal communication, 1996. Dry ICP-MS sensitivity

13. The m/z value transmitted during a chromatographic peak can be readily changed in the low resolution mode by changing the accelerating voltage with very little dead time between such hops. In the present work, this electrostatic peak switching procedure is generally done over a limited m/z range at a fixed magnetic field setting, although both the accelerating voltage and magnetic field strength can be switched in tandem. In medium resolution, the magnetic field is kept at a preset value corresponding to the middle of the mass region of interest. The accelerating voltage is then scanned and resulting chromatogram is reconstructed for the ions of interest.

14. Standard reference material 1263a, Freeze-Dried Human Serum, National Institute of Standards and Technology (NIST).

15. PBR322 HaeIII digest, Boehringer Mannheim.

16. These estimates are based on the typical sensitivity of the instrument for the isotopes monitored. They have not been derived from the rogorous calibrations and are provided primarily for the general information of the reader. These measurements are not meant to represent accurate, quantative measurement of concentration.

17. I. A. Bergdahl, A. Schutz and A. Grubb, J. Anal. Atomic Spectrom. 11, 735 (1996); Y. Lolin and P. O'Gorman, Ann. Clin. Biochem. 25, 688 (1988); H. J. Church, P. Day, R. A. Braithwaite and S. S. Brown, J. Inorg. Biochem. 49, 55 (193); S. R. V. Raghavan, B. D. Culver and H. C. Gonick, Environ. Res. 22, 264 (1980).

18. K. T. Suzuki, N. Imura, M. Kimura, Metallothionein III, Birkhauser Verlag, Basel, Switzerland, 1993; M. J. Stillman, C. F. Shaw III, K. T. Suzuki, Metallothioneins: Synthesis, Structure and Properties of Metallothioneins, Phytochelatins and Metal-Thiolate Complexes, VCH, New York, 1992.

19. Total Se level in serum

20. R. F. Burk, Ed., Selenium in Biology and Human Health, Springer-Verlag, New York, 1994.

21. J. K. Barton, Metal-Nucleic Acid Interactions, in I. Bertini, H. B. Gray, S. J. Lippard and J. S. Valentine, Bioinorganic Chemistry, University Science, Mill Valley, CA, 1994, p. 486; D. R. Jones, L. F. Lindoy and A. M. Sargeson, J. Amer. Chem. Soc. 106, 7807 (1984); S. H. Gellman, R. Petter and R. Breslow, J. Amer. Chem. Soc. 108, 2388 (1986); J. Chin and X. Zhou, J. Amer. Chem. Soc. 110, 223 (1988); J. R. Morrow and W. C. Trogler, Inorg. Chem. 27, 3387 (1988).

22. A. S. Hneihen, A. M. Standeven and K. E. Wetterhahn, Carcinogenesis 14, 1795 (1993).

23. M. Misra, J. A. Alcedo and K. E. Wetterhahn, Carcinogeneis 15, 2911 (1994); E. J. Dudek and K. E. Wetterhahn, Metal Ions in Biology and Medicine 3, 175 (1994).

24. S. A. Katz and H. Salem, Biological and Environmental Chemistry of Chromium, VCH. New York, 1994, p. 89; J. Molyneux and M. J. Davies, Carcinogenesis 16, 875 (1995).

25. Wang J.; Houk, R.S.; Dreessen, D.; Wiederin, D.R.; Inorg. Biochem., in preparation.

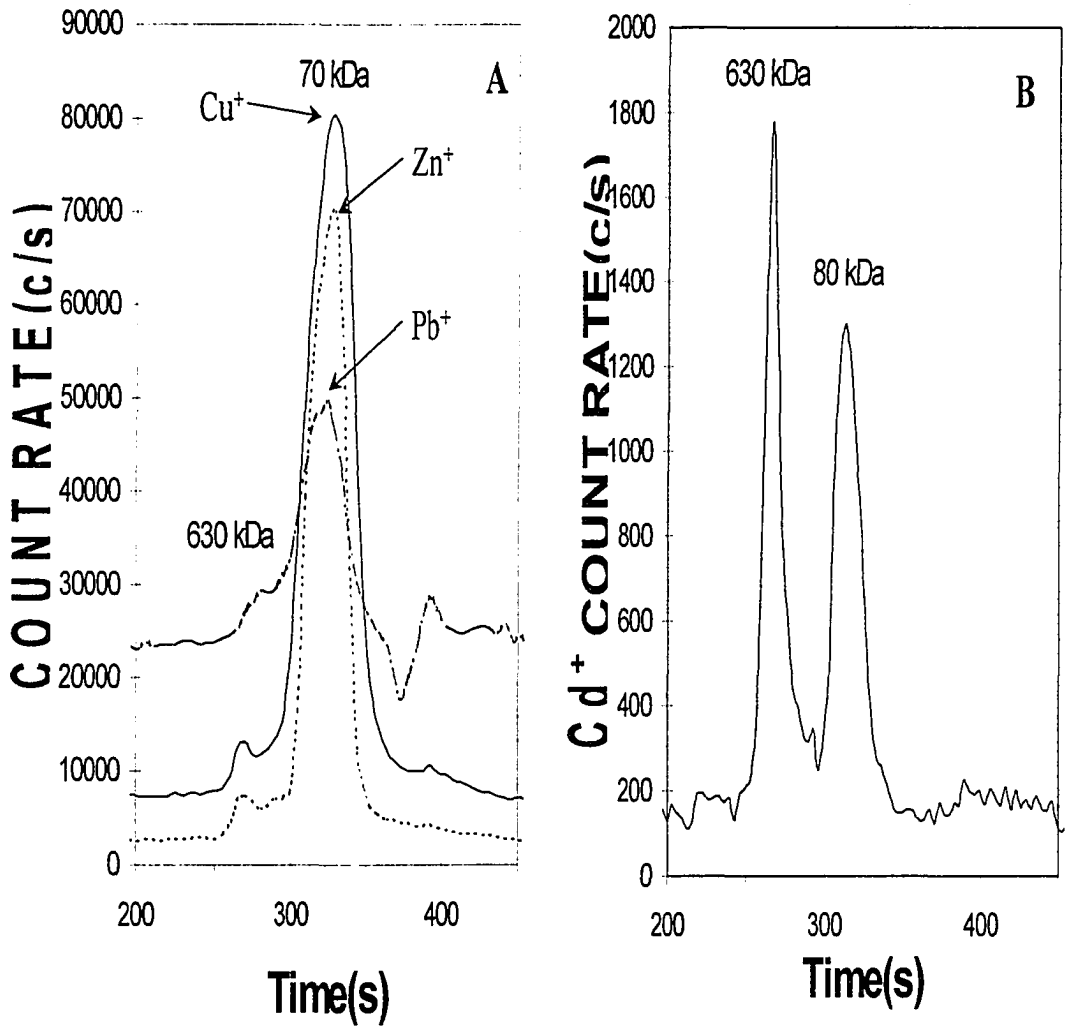

Fig. 1. Element-selective chromatograms for $^{64}Zn^{+}$, $^{63}Cu^{+}$ and $^{208}Pb^{+}$ (Fig. 1a) and $^{114}Cd^{+}$ (Fig. 1b) on proteins from a single injection of NIST 1263a human serum. Molecular weights of the measured protein fractions are determined by calibration with known proteins and are indicated on the figures. Approximate concentrations for the largest chromatographic peaks are ~3 ppb Zn, 1 ppb Cu, 1 ppb Pb and 90 ppt Cd. Spectral resolution = 300. The GPC column (see reference 8) was used for Figs. 1-4.

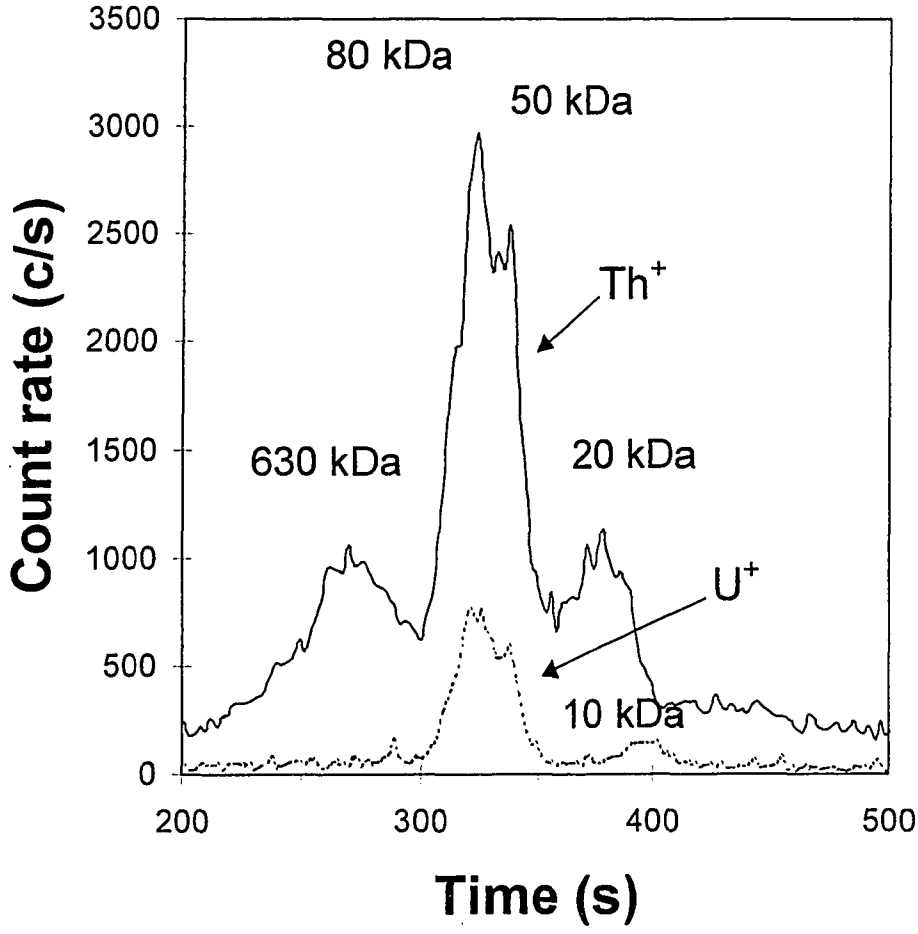

Fig. 2. Chromatograms for $^{232}Th^{+}$ and $^{238}U^{+}$ on proteins in NIST 1263a human serum. Concentrations for the largest peaks are ~ 3 ppt Th and 1 ppt U. Spectral resolution = 300.

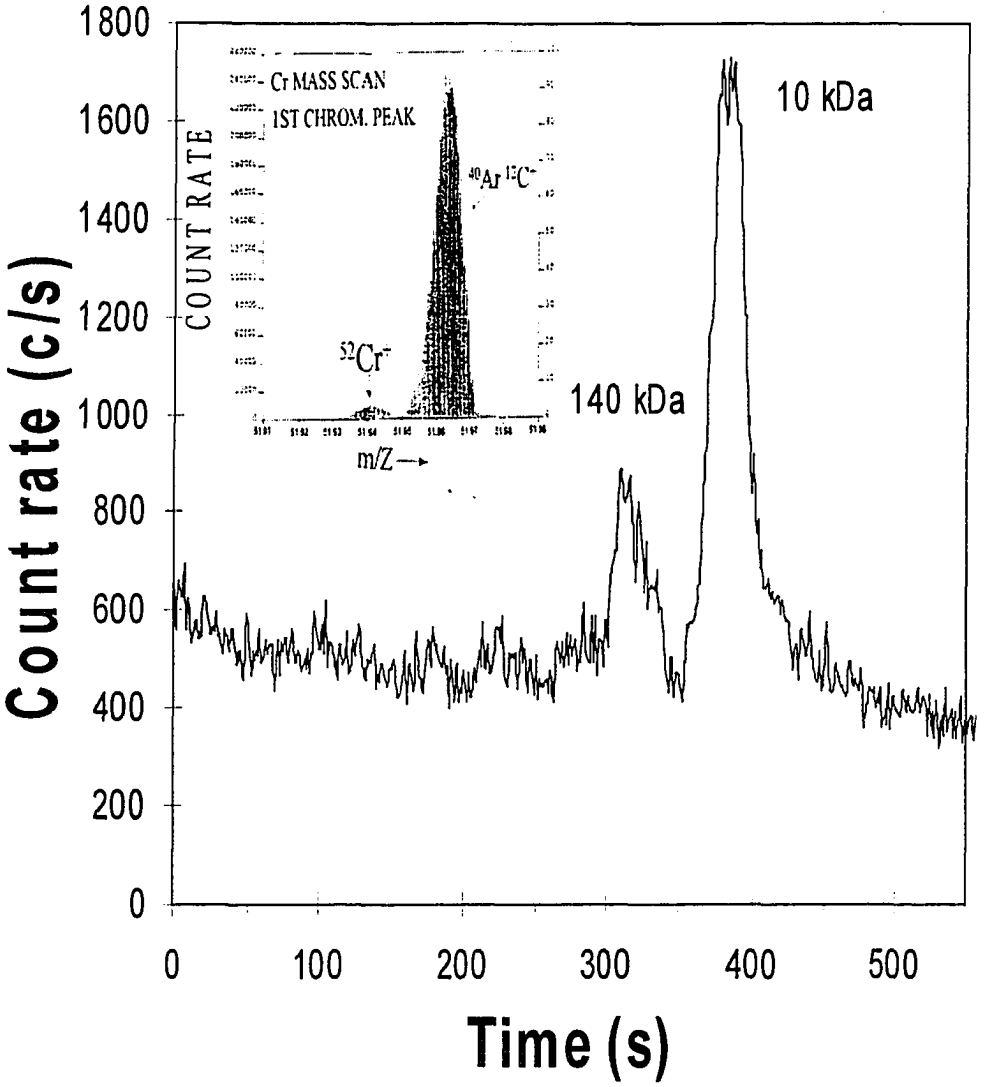

Fig. 3. Chromatogram for $^{52}Cr^{+}$ in proteins from NIST 1263a human serum, spectral resolution = 3000. The inset shows the mass spectral separation between $^{52}Cr^{+}$ and $^{40}Ar^{12}C^{+}$. The Cr concentration in the largest peak is ~0.1 ppb.

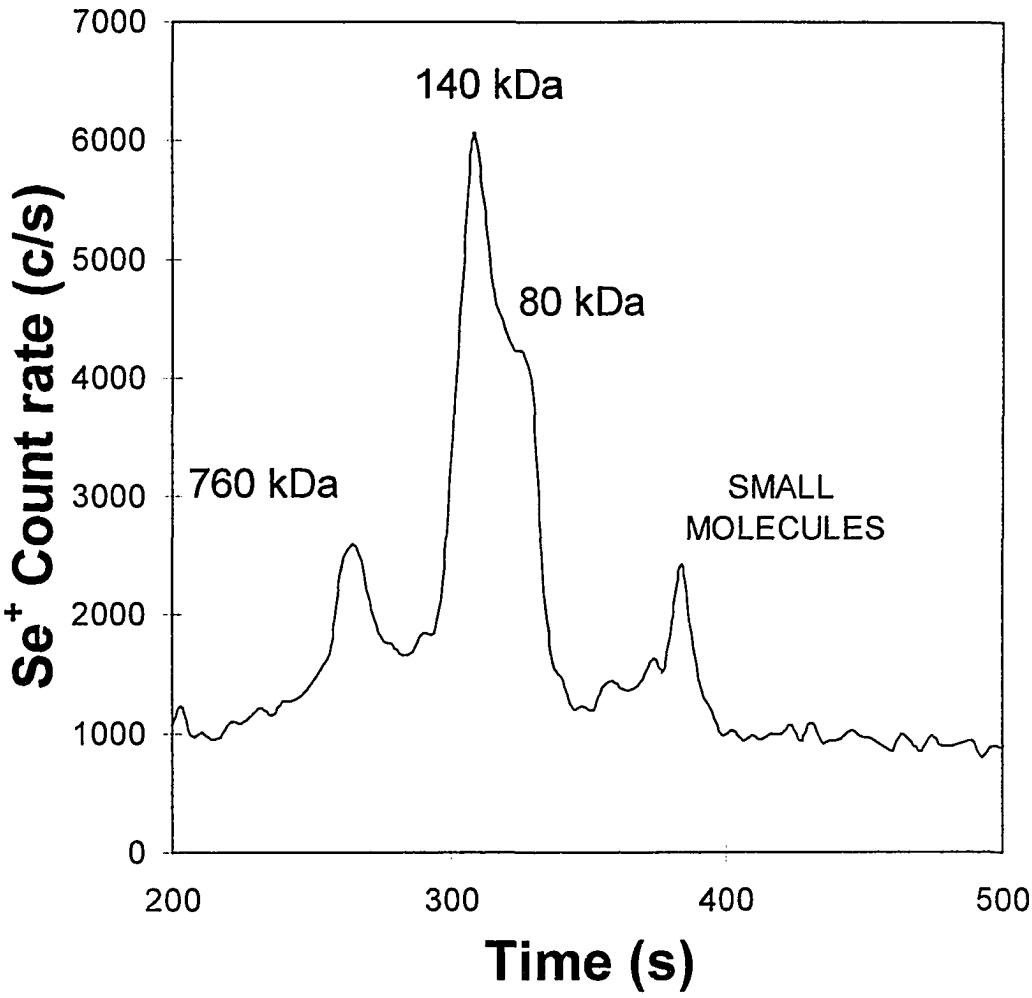

Fig. 4. Chromatogram for $^{82}Se^{+}$ in proteins from NIST 1263a human serum, spectral resolution = 300. The Se concentration in the largest peak is approximately 40 ppb.

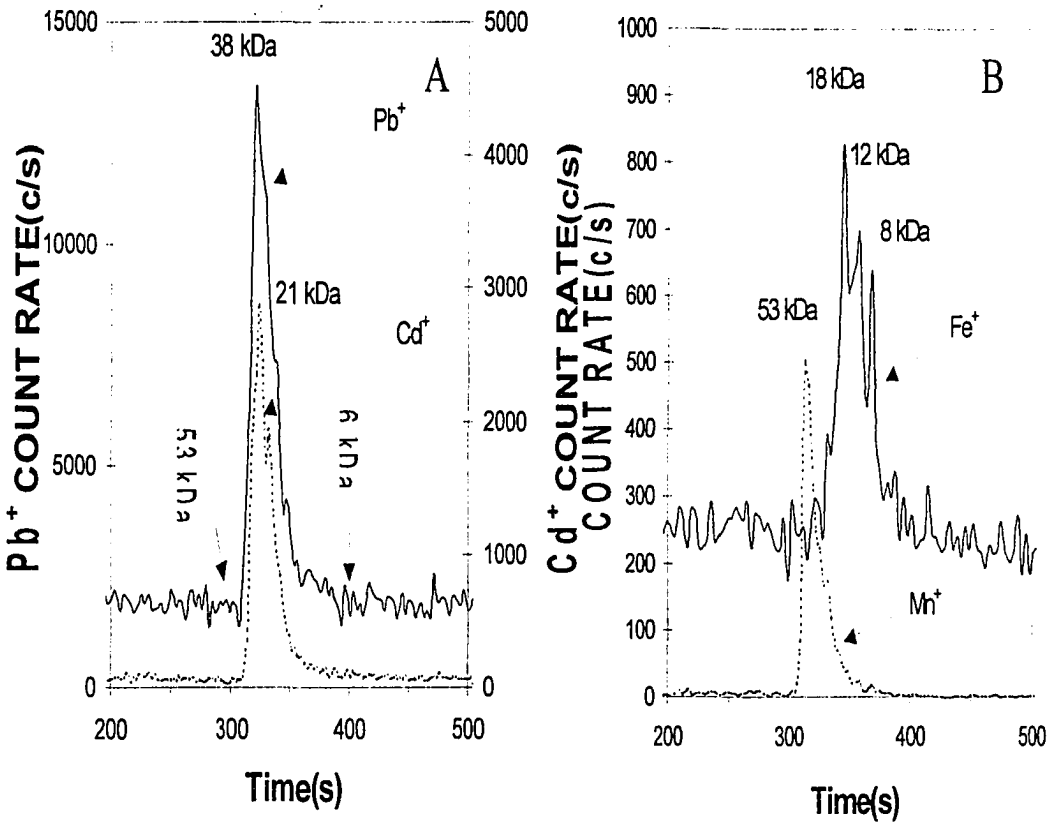

Fig. 5. Chromatograms for $^{114}Cd^{+}$, $^{208}Pb^{+}$, $^{56}Fe^{+}$ and $^{55}Mn^{+}$ bound to DNA restriction fragments. For Cd and Pb, spectral resolution = 300; for Fe and Mn, resolution = 3000. These metal ions are impurities in the samples or solvents, not spikes. Concentrations are roughly 12 ppb each for Fe, mn and Pb and 50 ppb for Cd. The homemade PEEK column [8] was used for the results shown in this and the final figure.

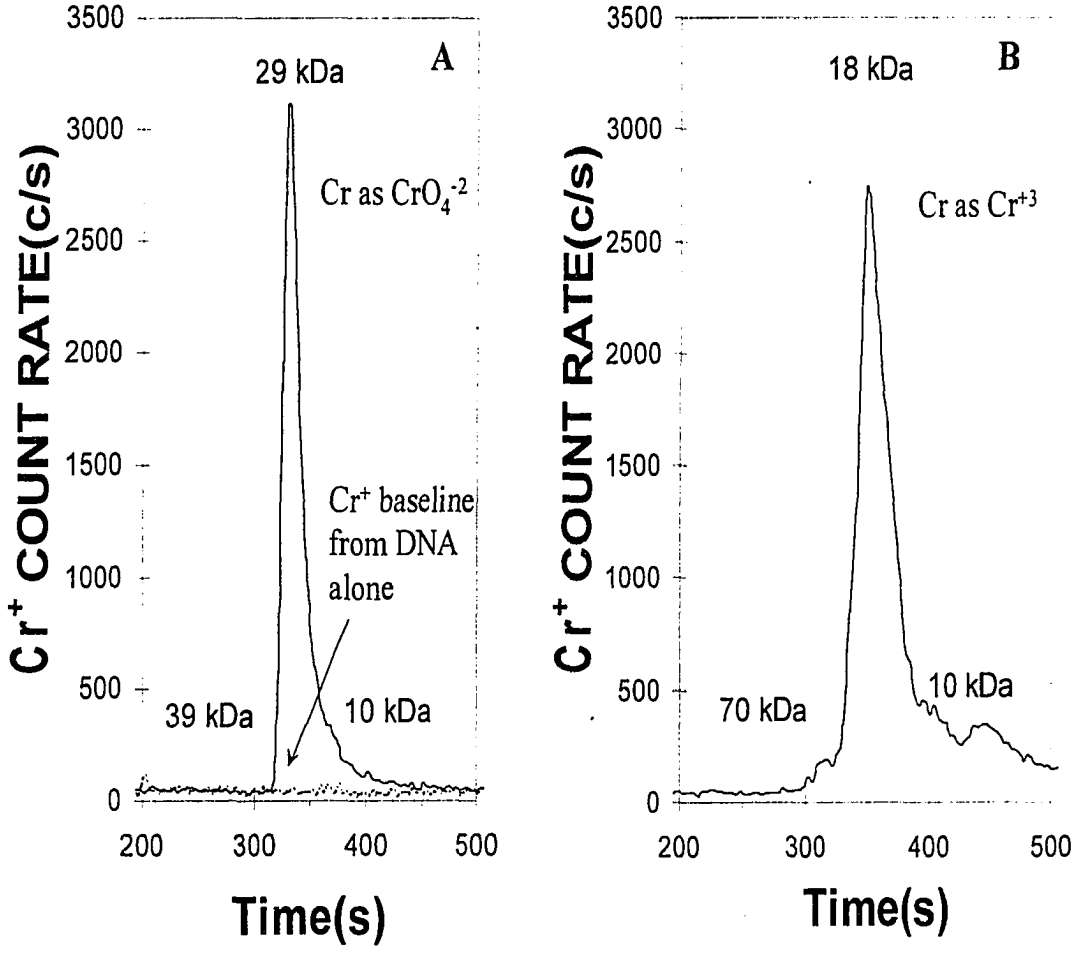

Fig. 6. Chromatograms for $^{52}Cr^{+}$ from unspiked DNA fragments (baseline at bottom of frame a), DNA fragments spiked with CrO_4^{-2} at 33 ppb (a) and DNA fragments spiked with Cr^{+3} at 66 ppb (b). Spectral resolution = 3000.

CHAPTER 3: SPECIATION OF TRACE ELEMENTS IN PROTEINS IN HUMAN AND BOVINE SERUM BY SIZE EXCLUSION CHROMATOGRAPHY AND INDUCTIVELY COUPLED PLASMA – MASS SPECTROMETRY WITH A MAGNETIC SECTOR MASS SPECTROMETER

A paper submitted to Journal of Biological Inorganic Chemistry, March 1999

Jin Wang and R. S. Houk *, Dawn Dreessen and Daniel R. Wiederin

Abstract

Proteins are separated by SEC while atomic ions from the inorganic elements are detected on-line by ICP-MS. A double focusing mass analyzer provides very high sensitivity, low background and sufficient spectral resolution to separate the atomic ions of interest from most polyatomic ions at the same nominal m/z value. The chromatograms show the distribution of the elements of interest between protein-bound and free fractions and provide the approximate molecular weights of those protein fractions that contain the elements monitored. The distributions of various elements, including V, Mo, Fe, Co, Mn, and lanthanides, in human or bovine serum samples are shown. Alkali metals and Tl are present primarily as free metal ions and are not bound to proteins. Inorganic elements spiked into the serum samples can be followed into various proteins. EDTA does not remove Fe, Pb, Sn or Th from the proteins but does extract Mn from some proteins. Procedures for determining the effects of breaking disulfide linkages on the metal binding characteristics of proteins are also described.

Key words: metalloproteins, ICP-MS, SEC,

Abbreviations: ICP-MS inductively coupled plasma – mass spectrometry, SEC size exclusion chromatography, NIST National Institute of Standards and Technology, EDTA ethylene diamine tetraacetic acid

* Corresponding author

Introduction

The identification of trace metals in proteins and other biological molecules remains an important task. For example, several enzymes involving molybdenum [1,2] and tungsten [3] have recently been studied intensively. These elements are present at lower overall concentrations than the traditional levels previously associated with essential elements. Some important biological molecules contain several different metals such as Zn and Cu in superoxide dismutase [4] and Fe (III) and Zn (II) in kidney bean purple acid phosphatase [5]. Thus, multielement analytical methods capable of measuring all the metals in biomolecules at ambient levels are necessary.

The present work describes procedures for identifying whether particular trace elements are bound to proteins in biological fluids (such as serum) and for measuring the approximate molecular weights of such proteins. The measurements are performed without preliminary extraction or preconcentration procedures. Several experiments for estimating the strength with which metals are bound to proteins and for examining the effects of breaking disulfide linkages are also demonstrated.

SEC has been used previously with ICP-MS for the analysis of biological fluids [6-8]. The present work is unique in that it employs a double focusing mass spectrometer, which has better ion transmission and sufficient spectral resolution to separate atomic analyte ions from polyatomic ions at the same nominal m/z value. Other experiments along these lines are described in a companion paper [9] and by Sanz Medel and co-workers [10].

Materials and Methods

Samples and Reagents. In the present work, the samples are either bovine or human serum reference materials (NIST 1598 and 909b, respectively). The freeze-dried samples are reconstituted in aqueous tris/HCl buffer (0.1 M) at pH = 7.0. The proteins are separated at physiological pH, and organic solvents are not used. Thus, the separation conditions are selected to minimize changes in the proteins from their native states. The total solute level in the reconstituted serum is similar to that in the actual serum sample before freeze drying. For breaking disulfide linkages, 2-mercaptoethanol (abbreviated 2-ME, Fisher Biotech) was used without further purification. Metal spikes were obtained by diluting aqueous ICP

standards (PLASMACHEM) with deionized water to the desired concentrations.

Chromatographic Separations. The basic instrument and operating conditions have been described previously [9]. To minimize metal contamination during the separation, a so-called "metal free" pump (Acuflow Series III) and a column packed in PEEK are used. For the chromatograms shown below, the eluent flow rate is either 100 or 160 μL/min. The calibration between retention time and molecular weight axis is determined by injecting simple mixtures of standard proteins of known molecular weight. The retention times for peaks for the unique elements, such as Fe in ferritin, Cu in β-amylase, or I in thyroglobulin, are noted. It is assumed that sample proteins of similar size as the standard proteins elute at similar retention times. This calibration procedure provides only an approximate estimate of molecular weight, so the values are cited to only one or at most two significant figures.

ICP-MS. The mass spectrometer is a Finnigan MAT ELEMENT double focusing device [11,12]. Operating conditions for the ICP and sample introduction device are similar to those described previously [9]. Ion optic voltages of the MS are selected to maximize signal from an element in the middle of the mass range, such as $^{115}In^{+}$, while injecting a standard solution of 10 ppb In.

The MS can be operated in either of two resolution modes. At low resolution ($R = m/\Delta m = 300$), the device produces flat-topped peaks approximately 0.2 Dalton (Da) wide at the base. The ion transmission and sensitivity are maximal in this mode. At R = 3000 (medium resolution), triangular peaks are obtained. The device can separate atomic analyte ions from many polyatomic interfering ions at this resolution setting. This medium resolution mode is used to resolve such spectral overlap interferences for the first row transition metals, especially for $^{51}V^{+}$ ($^{35}Cl^{16}O^{+}$), $^{52}Cr^{+}$ ($^{40}Ar^{12}C^{+}$), $^{55}Mn^{+}$ ($^{39}K^{16}O^{+}$ and $^{37}Cl^{18}O^{+}$) and $^{56}Fe^{+}$ ($^{40}Ar^{16}O^{+}$). The major interfering ions in these cases are noted in parentheses. The resolution is increased by decreasing the slit widths in fixed increments, which reduces the ion transmission and sensitivity to approximately 10% of that at R= 300. The high resolution mode (R ~ 8000) was not necessary for the elements studied in the present work. Note that almost all the ions observed from the ICP are singly charged, regardless of the oxidation state of the element in the sample.

Results

Speciation of Vanadium, Molybdenum and Lanthanide Elements. This paper and its companion [9] illustrate the detection capabilities of the double focusing ICP-MS device by reporting element-selective chromatograms for some unusual trace elements. Fig. 1 shows such data for vanadium in human serum. Vanadium is found in two protein fractions with molecular weights of 70 kDa and 30 kDa. There is little evidence for a chromatographic peak at long retention time from either "free" vanadium, such as the various vanadium cations (V^{3+}, VO^{2+} or VO_2^+) or other small molecules containing vanadium. Medium spectral resolution (R = 3000) was used here because of possible interference between $^{51}V^+$ and $^{35}Cl^{16}O^+$.

Spectral interferences are less severe for heavier elements, so the slits are widened to R = 300 to maximize sensitivity for chromatograms for Mo (Fig. 1) and the light lanthanides (Fig. 2). Like V, Mo is also found in two distinct protein fractions (100 kDa and 30 kDa, Fig. 1), with the larger one at somewhat higher molecular weight than that for V.

The lanthanides (Fig. 2) are mostly bound to several distinct protein fractions, with the highest levels in the fraction at 90 kDa. Different lanthanides produce the same chromatographic pattern. The ionization efficiencies of the lanthanides are similar in the ICP, and there should be little difference in mass bias between these three isotopes, so correction for isotopic abundance allows direct comparison of the relative concentrations from the peak areas. Thus, the lanthanide concentrations decrease in the order [Ce] > [La] > [Pr], which is the same trend seen in the abundances of these elements in most geological materials [13]. There is a significant peak at long retention time for "free" lanthanides, which is not seen for most of the transition metals studied.

These chromatograms show that the lanthanides are primarily bound to proteins in human serum. Even though these elements are usually considered nontoxic, the results in Fig. 2 are of interest in that lanthanides are often believed to be nonradioactive analogs for the environmental behavior of some actinides, particularly those with 3+ oxidation states [14,15].

Thallium and Alkali Metal Ions. There is considerable interest in monitoring alkali metal ions other than Na and K. For example, lithium is used to treat manic depression, and the radioactive isotopes of Cs (especially ^{137}Cs) are of great environmental interest in the

remediation of nuclear waste. The most common form of the toxic element Tl in aqueous solution is the cation Tl^+, which has the same charge as the alkali metals. If the Tl^+ concentration becomes too high, then Tl^+ interferes with the biological functions of K^+ [15].

The chromatogram in Fig. 3 shows that Tl^+ elutes at long retention time, like the alkali metals Cs^+ and Rb^+, which themselves co-elute with Na^+ and K^+ (not shown). Elements that produce broad, tailed peaks at long retention time ($\geq$ 400 s) are present either as free ions or are bound to small molecules, not proteins. Thus, all the Tl in this sample is present as aqueous Tl^+ and is "free" to mimic Na^+ and K^+ biologically. None of the Tl^+ is bound to serum proteins. Fortunately, the overall concentration of Tl in the sample is low, ~ 1 ppt.

Metal Spike Experiments. Results for two spike experiments in bovine serum are shown in Fig. 4. The solid line in each figure represents the chromatogram obtained from the original serum sample, while the dotted line is the new chromatogram obtained when a fresh sample is spiked with the element indicated. The spike chromatogram is measured just after the first one, so the signal levels can be compared.

Fig. 4a shows such results for Co. Two protein fractions containing Co are observed, with perhaps a hint of some free Co. When 20 ppb of Co^{2+} are added, the amount of additional Co that binds to the two protein fractions is about the same, and the free Co fraction is more noticeable. A 0.2 ppb spike of Cd^{2+} also binds more or less uniformly to the two protein fractions that originally contained Cd (Fig. 4b). The increases in total signal for each element also show that the concentrations of Co and Cd in the original sample are ~ 0.5 and 0.07 ppb, respectively.

A different situation is seen for Mn in human serum (Fig. 5). The chromatogram for the original sample shows Mn in three protein fractions (440, 80 and 25 kDa) and a peak for "free" Mn. When the sample is spiked with 4 ppb Mn^{2+}, most of the added Mn goes into the third protein fraction. The third peak shifts to slightly longer retention time, which apparently indicates that adding the Mn^{2+} lowers the average molecular weight of this third protein fraction. The retention times of the other three peaks remain the same as those obtained from the unspiked sample, so this shift is not just the uncertainty in retention time between two injections in this case.

Effect of EDTA. Initial experiments with EDTA were performed by adding it only to the sample at 1 mM, which is comparable to the total molar concentration of the various proteins present. After the samples were spiked with EDTA, they were allowed to stand for at least one hour at room temperature before injection onto the column.

As shown in Fig. 6, EDTA added to the serum samples does not remove Sn, Pb or Th from the proteins. Otherwise, the protein peaks would disappear and be replaced by peaks of similar height at much longer retention time ($\geq$ 400 s). Slight shifts in the retention times of the major peaks just represent the reproducibility of injection and elution. Thorium especially has a very high formation constant with EDTA ($K_f = 1.6 \times 10^{23}$), yet Th still remains bound to the protein molecules!

As shown in Fig. 7a, the situation is similar for Fe even when a large excess of EDTA (1 mM) is added to the eluent, i.e., the column is being flushed continually with 1 mM EDTA. Two protein fractions containing Fe are seen at 500 and 80 kDa regardless of whether the eluent contains EDTA or not. The formation constants for Fe^{3+} and Fe^{2+} with EDTA are 1.3×10^{25} and 2.1×10^{14}, respectively. Of course, this experiment does not identify the oxidation state of the Fe in the proteins.

For the elements shown so far, EDTA does not remove either essential metals or ambient levels of toxic ones from proteins in serum. This observation is surprising given the use of EDTA to treat heavy metal toxicity. Perhaps metal therapy with EDTA chelates the *excess* metals present, not those already bound to proteins.

As was the case in the spike experiments, somewhat different behavior is seen for Mn (Fig. 7b). Three Mn peaks are seen from bovine serum. There could be a fourth peak at long retention time that is largely obscured by background. Addition of excess EDTA to the mobile phase removes Mn from the first peak. The second, major peak becomes moderately more intense. There is still little evidence for Mn bound to EDTA, as if the Mn removed from the large protein responsible for the first peak did not remain bound to EDTA but wound up on the second, medium-sized protein. However, the signal levels and Mn concentrations are low and much of the increase could just be Mn impurity from the EDTA, so this latter interpretation must be treated with caution.

Changes in Conformation of Metalloproteins. The conformations of the proteins in the serum samples were altered by adding 2-ME at 11 mM. This reagent should break the disulfide linkages and unfold the proteins without diluting the final sample appreciably, so the metal signals obtained in the presence of 2-ME can be compared directly to those from the original sample.

The results are shown for Fe in Fig. 8. The solid line is the original chromatogram obtained with no additive. As noted above, two protein fractions containing Fe at 500 and 80 kDa are observed. Addition of 2-ME removes Fe from the large protein fraction and shifts the remaining Fe toward the fraction at 80 kDa. There is no Fe peak at long retention time, so little or no free Fe is present.

The total Fe signal (i.e., the peak areas in Fig. 8) remains the same within ±1 %. Thus, the 2-ME did not contain Fe at levels comparable to that in the serum sample. This result also indicates that that response for Fe is the same for Fe in various proteins, which is expected because of the high temperatures and efficient atomization conditions in the ICP.

Results for a similar experiment involving Mn are shown in Fig. 9. The original sample gives three Mn peaks, all bound to proteins. Addition of 2-ME removes the Mn from the largest protein (i.e., the first peak) and increases the amount of Mn in the smallest protein. The total Mn level, measured by the total net signal in all chromatographic peaks for Mn, increases by ~ 10% when 2-ME is present. This additional Mn probably comes from Mn impurity in the 2-ME additive.

Differences between Metal-Containing Proteins in Human and Bovine Serum. There are some interesting differences between the two serum samples studied in the present work. There is much more Co in the bovine serum sample (Fig. 4a) than in the various human sera we have analyzed. There is much more Mn in human serum (Fig. 5) than in bovine serum (Figs. 7b and 9).

Discussions

This paper demonstrates methodology to study the binding of trace metals to proteins in biological fluids. Other inorganic elements such as Se can be measured as well [9]. The measurements have high sensitivity and elemental selectivity. Thus, many such experiments

are possible without preliminary separation and isolation procedures. Alternatively, purified proteins can be characterized using only minute amounts of sample.

Several additional experiments are suggested by the present work. Generally, the response of the ICP-MS device is not strongly dependent on the chemical form of the element, so quantification of the inorganic element(s) in biomolecules should be possible using simple inorganic standards. Measurement of binding capacity should be possible by titrating the protein with metal spikes, for example. The reader should also note that ICP-MS is a multielement measurement, so identification of various elements in given proteins should be possible. The quality of the chromatographic separation is clearly one area of improvement. These and other related experiments are under investigation.

Acknowledgements

Two of the authors (JW and RSH) are supported by the Ames Laboratory, U. S. Department of Energy, Office of Basic Energy Sciences, under Contract W-7405-Eng-82. The measurements were conducted at CETAC Technologies. The authors also thank Finnigan MAT for providing the mass spectrometer.

References

1. Hille R (1996) Chem Rev. 96: 2757-2816.
2. Burgess B, Lowe D (1996) Chem Rev. 96: 2983-3012.
3. Johnson M, Rees D, Adams M (1996) Chem Rev. 96: 2817-2840.
4. Lipscomb W, Strater N (1996) Chem Rev. 96: 2375-2433
5. Wilcox D (1996) Chem Rev. 96: 2435-2458.
6. Shum S, Houk R (1993) Anal. Chem. 65: 2972-2976.
7. Gercken B, Barnes R (1991) Anal. Chem. 63: 283-287.
8. Owen L, Crews H, Massey R., Bishop N (1995) Analyst 120: 705.
9. Wang J, Houk R, Dreessen D, Wiederin D (1998) J. Amer. Chem. Soc. 120: 5793-5799.
10. Cabezuela A, Bayon M, Gonzalez E, Sanz Medel, A (1998) Analyst 123: 865-870.
11. Feldmann I, Tittes W, Jakubowski N, Stuewer D, Giessmann U. (1994) J. Anal. Atomic Spectrom. 9: 1007-1014.
12. Moens L, Jakubowski N (1998) Anal. Chem. 70: 251A-256A.

13. Date A, Hutchison D (1987) J. Anal. Atomic Spectrom. 2: 269-276.
14. Choppin G, Riszalka E (1994) Solution Chemistry of Actinides and Lanthanides, Handbook of Chemistry and Physics of Rare Earths, Vol. 18, Chap. 128, Gschneidner, K Jr., Eyring L, Choppin G, Lander G. Eds., North Holland: Amsterdam.
15. Katz J, Morss L, Seaborg G (1987) The Chemistry of the Actinide Elements, Chapman and Hall: London, pp. 9, 14, 1122.
16. da Silva J, Williams R (1991) The Biological Chemistry of the Elements, Clarendon: London, p. 539.

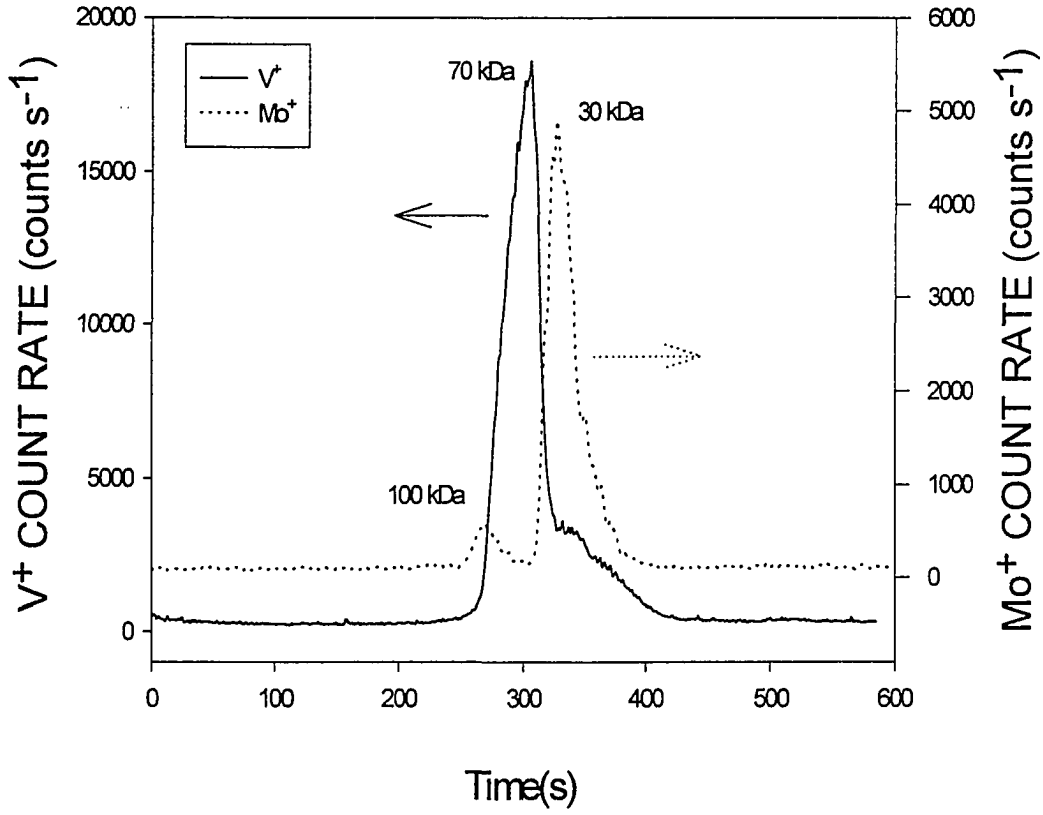

Fig. 1. Chromatograms for ^{51}V in human serum (NIST 909b, spectral resolution = 3000) and ^{98}Mo (12 ppb) in bovine serum (NIST 1598, spectral resolution = 300). Approximate molecular weights for the main fractions are listed in this and subsequent figures. Certified or information values for total concentrations of the elements are given where available.

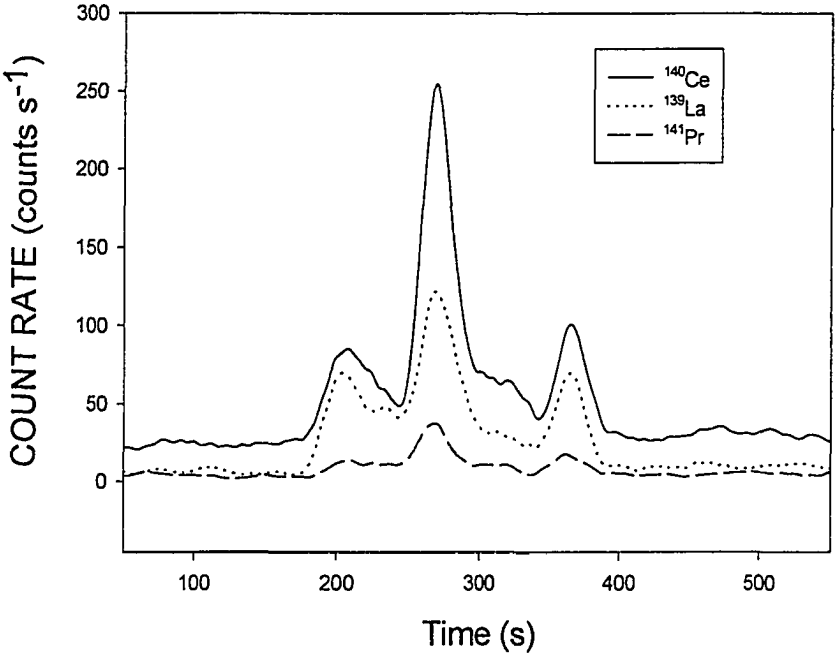

Fig. 2. Chromatograms for ^{139}La, ^{140}Ce, and ^{141}Pr in bovine serum (NIST 1598), spectral resolution = 300. All four chromatograms were obtained from the same injection. Note the peaks from "free" lanthanide ions at ~ 370 s.

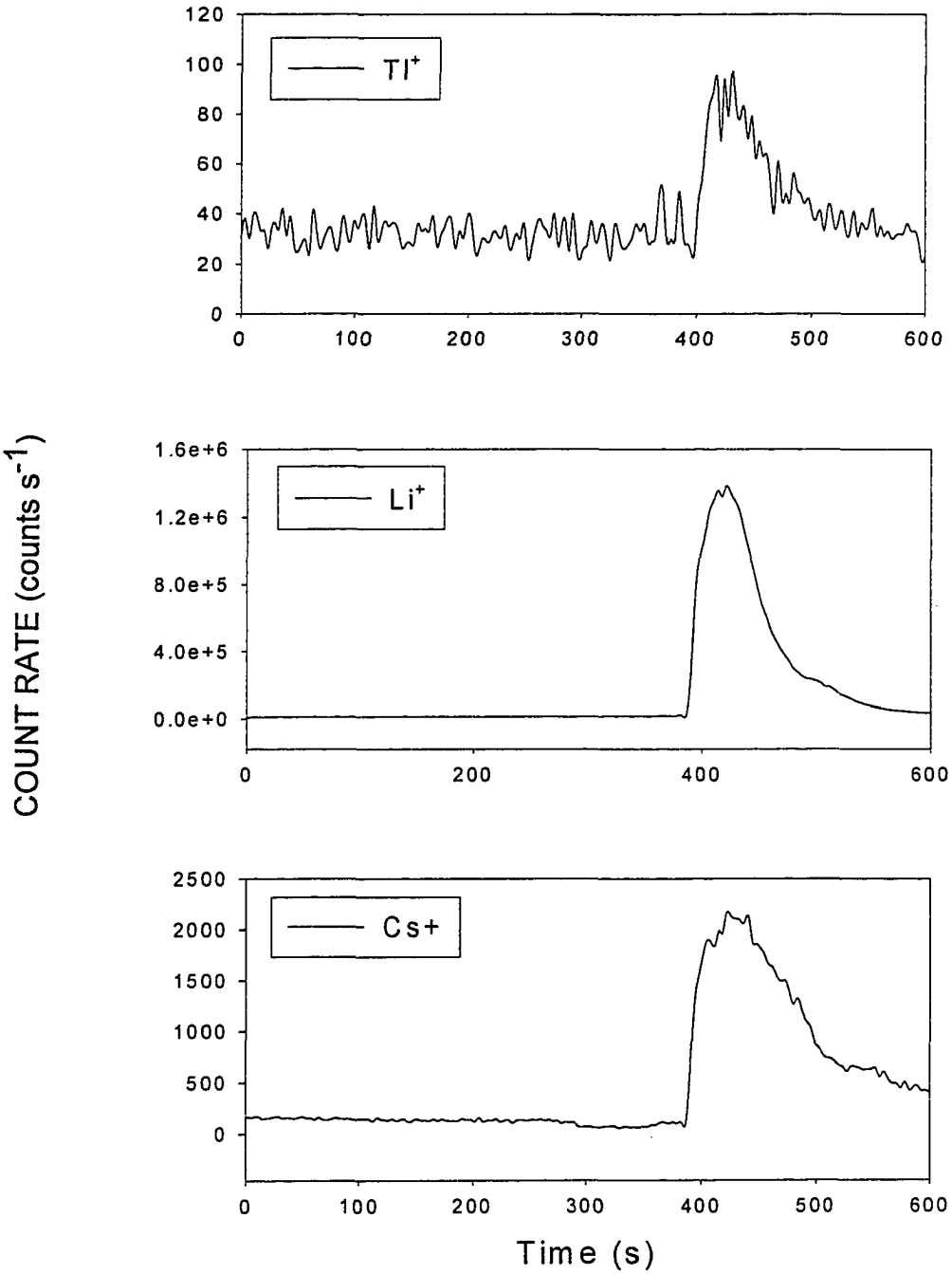

Fig. 3. Chromatograms for ^{205}Tl(~0.4 ppb), ^{7}Li and ^{133}Cs in bovine serum (NIST 1598), spectral resolution = 300

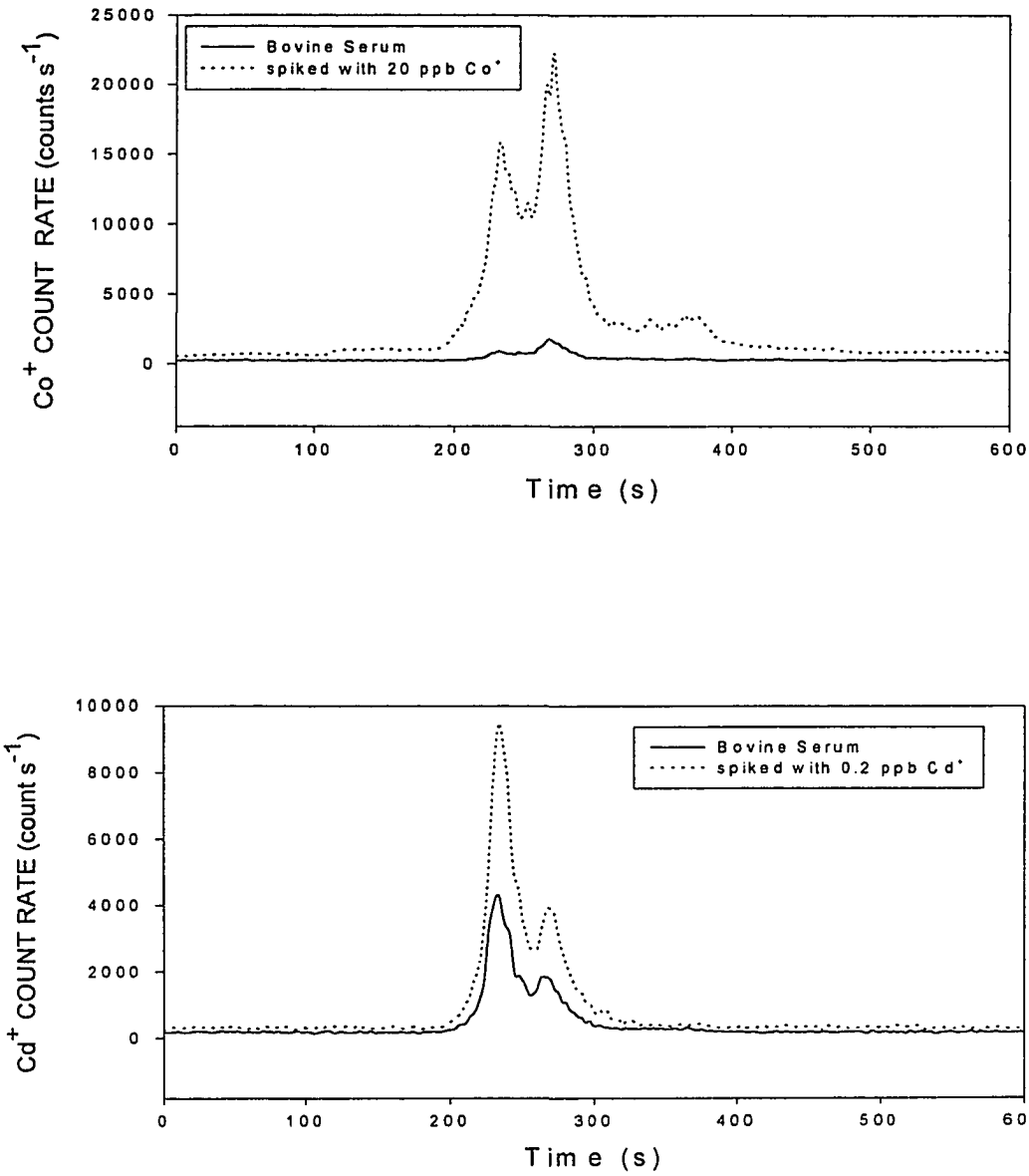

Fig. 4. Chromatograms illustrating spike experiments for ^{59}Co (1.2ppb) and ^{114}Cd (0.09 ppb) in bovine serum (NIST 1598), spectral resolution = 300.

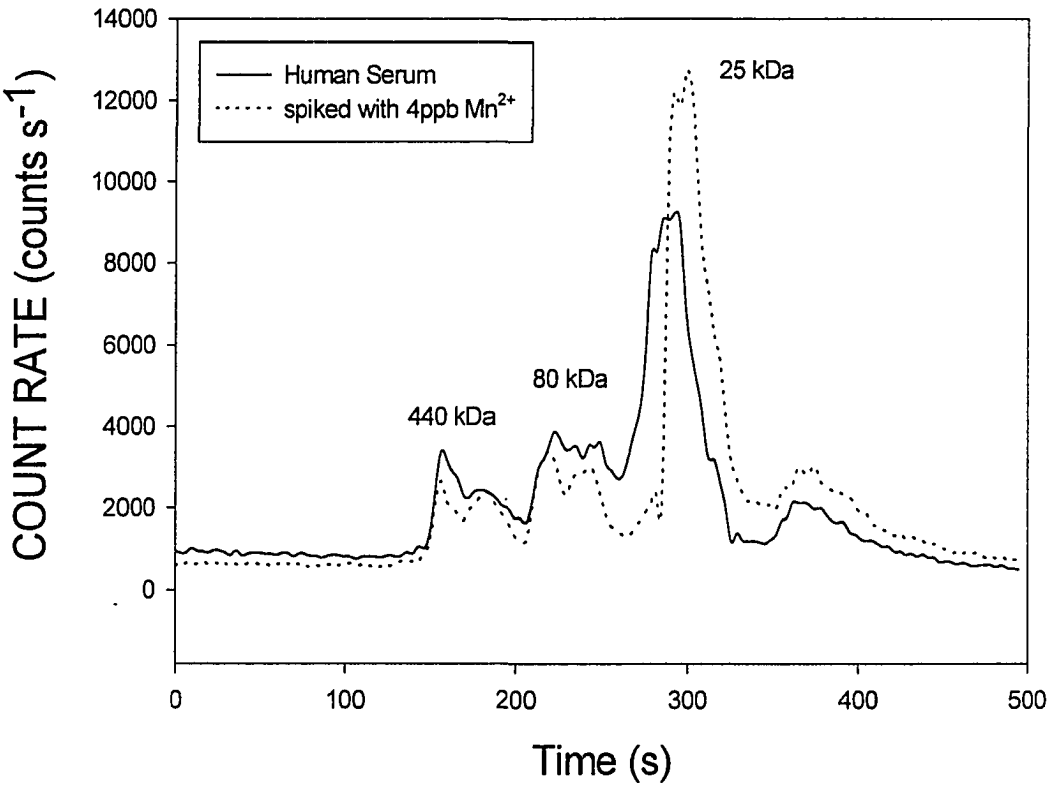

Fig. 5. Chromatogram for spike experiment for ^{55}Mn in human serum (NIST 909b), spectral resolution = 3000.

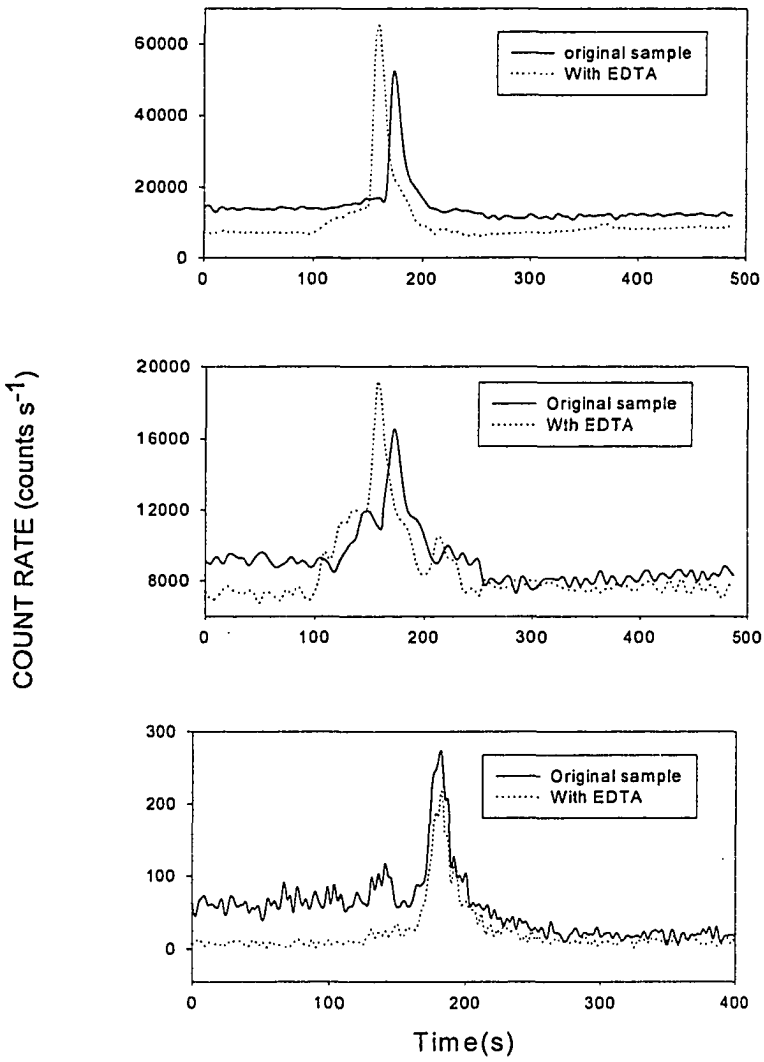

Fig. 6. Effect of EDTA at 1 mM in sample on chromatograms for ^{120}Sn (top), ^{208}Pb (middle) and ^{232}Th (bottom), spectral resolution = 300. Bovine serum (NIST 1598)

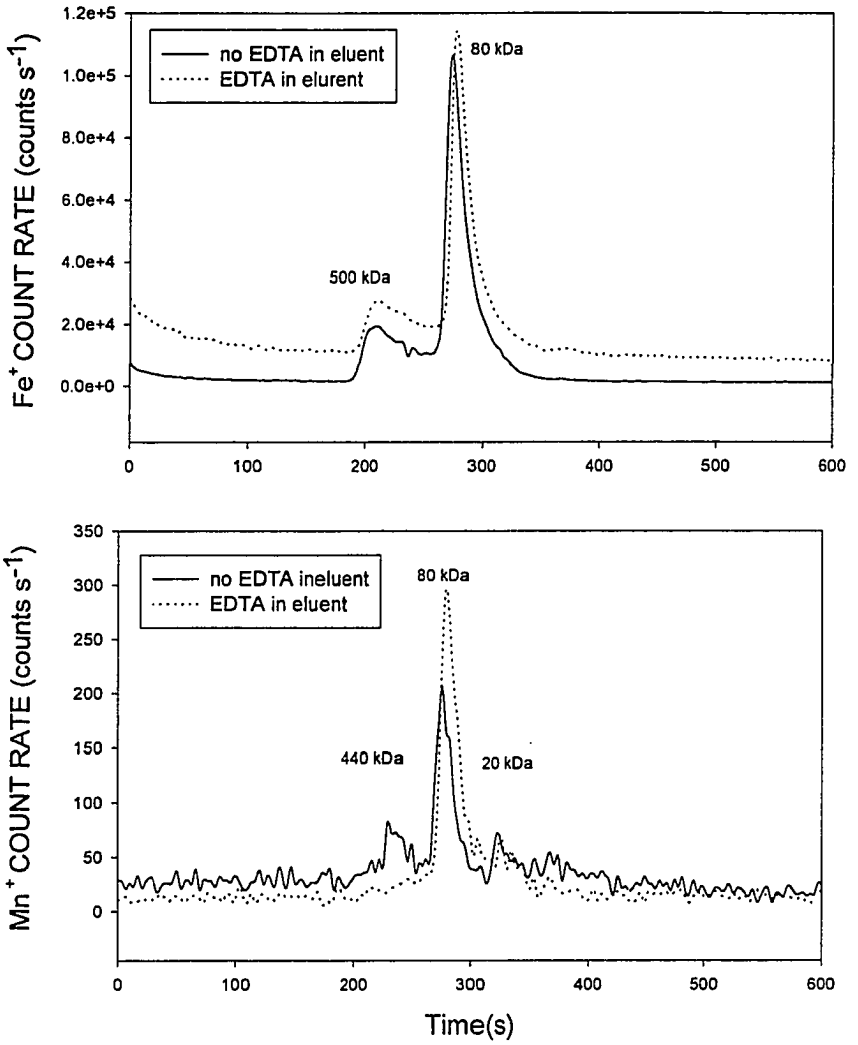

Fig. 7. Effect of EDTA at 1mM in eluent on chromatograms for ^{56}Fe (2.55 ppm) and ^{55}Mn (3.8 ppb) in bovine serum (NIST 1598). The spectral resolution is 3000 in this and subsequent figures.

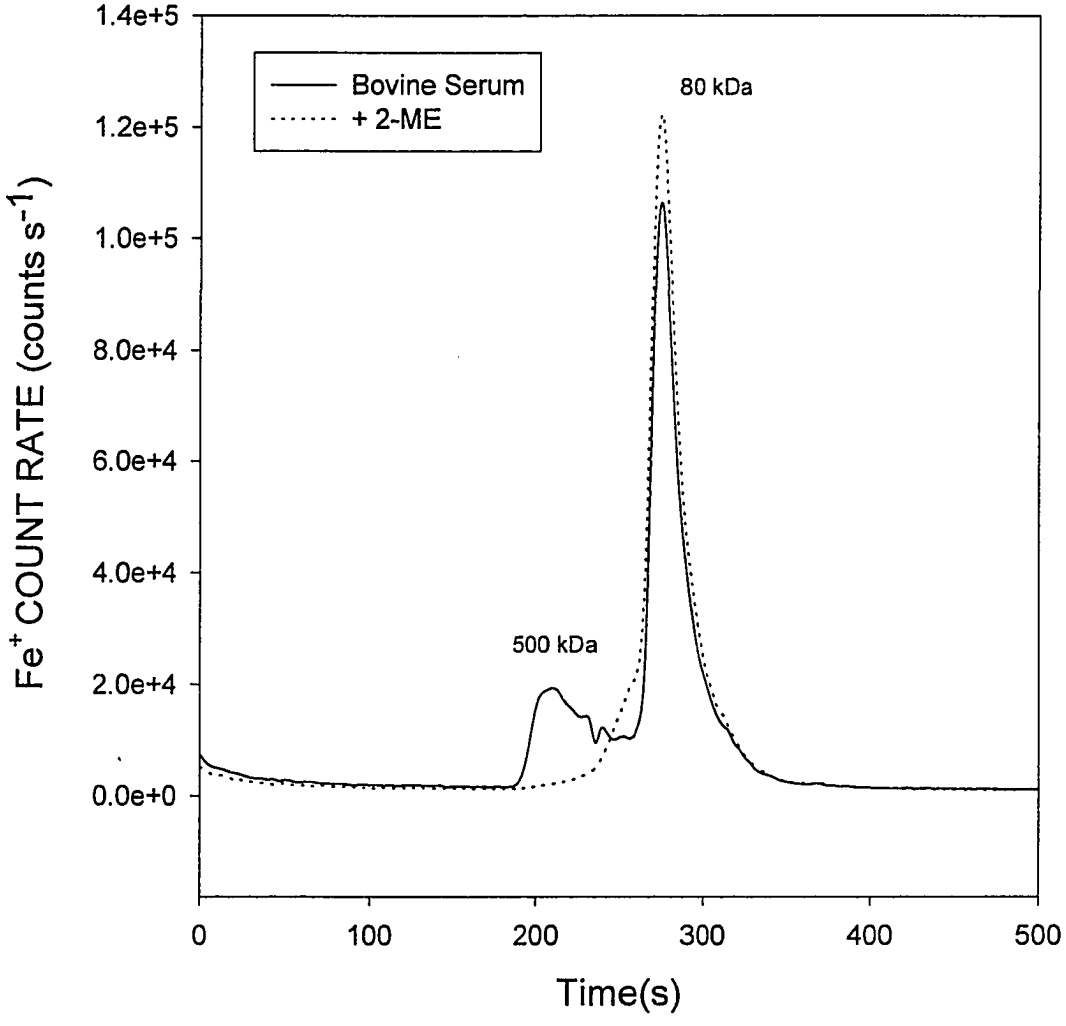

Fig. 8. Effect of 2-ME (11 mM) on chromatograms for ^{56}Fe (2.55 ppm) in bovine serum (NIST 1598).

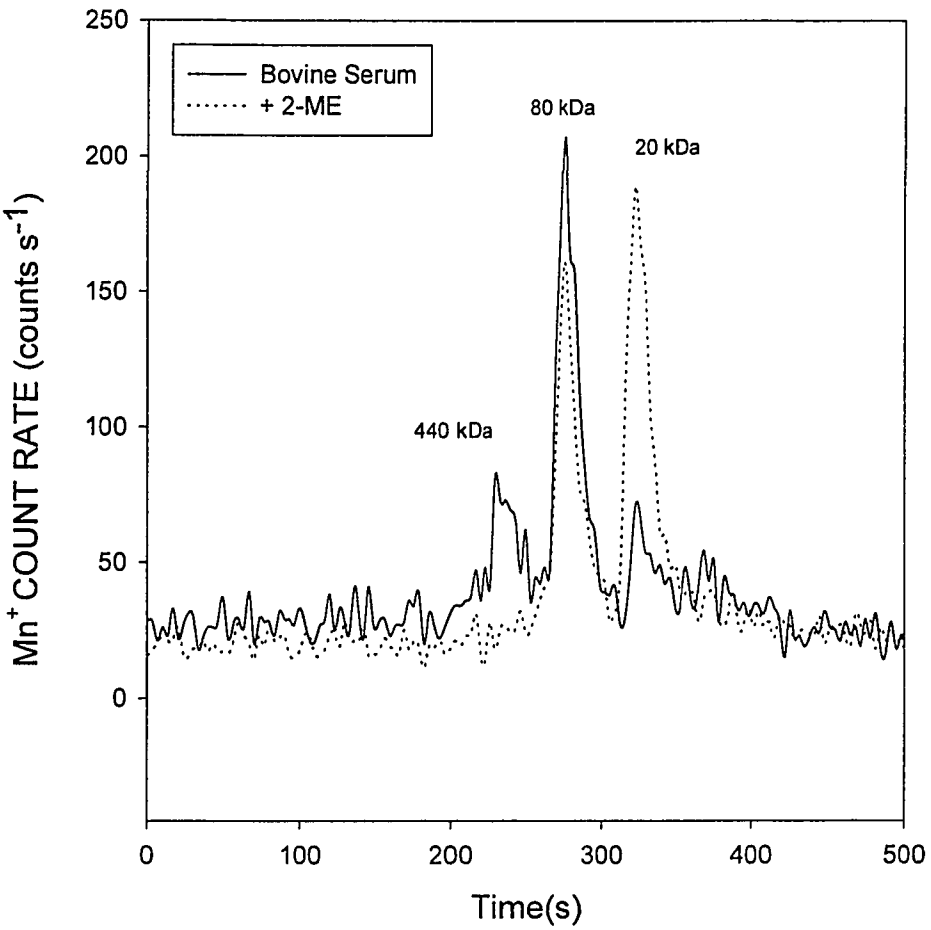

Fig. 9. Effect of 2-ME (11 mM) on chromatograms for ^{55}Mn (3.8 ppb) in bovine serum (NIST 1598).

CHAPTER 4: APPLICATION OF HIGH-PERFORMANCE SIZE EXCLUSION CHROMATOGRAPHY- INDUCTIVELY COUPLED PLASMA MASS SPECTROMETRY WITH A MAGNETIC SECTOR MASS SPECTROMETER TO THE INVESTIGATION OF ELEMENTAL DISTRIBUTION IN LIVER EXTRACT

A paper is to be submitted to Analyst

Jin Wang, Dawn Dreessen, Daniel R. Wiederin and R S. Houk*

Abstract

High-performance size exclusion chromatography- inductively coupled plasma mass spectrometry with a magnetic sector mass spectrometer has been used for the determination of trace elemental distribution in liver extract. The experimental setup provides sufficient chromatographic resolution and very good signal sensitivity. Measurements at high spectral resolution help to remove polyatomic interferences for some difficult elements like copper and zinc. Some elements are found in different molecular weight proteins, for example, cadmium binds to four different protein fractions (>400 kDa, 70 kDa and 13 kDa). Other elements like molybdenum are found to be completely in low molecular weight fractions.

Introduction

Elemental speciation in biological samples provides the crucial evidence for the judgment of the toxicity, bioavailability and environmental behavior of the different species.[1] Not all chemical forms of the inorganic elements are equally biologically active. For example, methyl mercury is more toxic than inorganic mercury salts, arsenobetaine is much less toxic than inorganic arsenic, heme iron is much more valuable biologically than inorganic iron salts, and cobalt as cyanocobalamin in liver is an important vitamin. [2]

The liver is an important organ that performs many metabolic functions. It synthesizes serum proteins (albumin, antibodies, fibrinogen), urea, prothrombin, and other coagulation factors. The liver, being a detoxification center, clears exogenous loads as well as endogenous load. It plays a key role in the intermediary metabolism of carbohydrates,

* Corresponding author

lipids, and protein. It is important for the metabolism of hormones. The liver also plays a role in vitamin economy by serving as a storage organ for vitamin A and B12. It also stores glycogen, fat and probably proteins. Liver, with its function as a storage organ, responds to chronic situations by either repleting or depleting its reserves over extended periods. The results of animal feeding experiments in which orally administrated Cd û metallothionein (Cd-MT) and ionic cadmium are transported differently following absorption, the former being deposited in the kidney (the target organ for cadmium toxicity) and the latter in liver. [3]

Investigation of elemental speciation in food has revealed that the metals are not only present in the ionic form but are also complexed to various binding proteins.[4] Analytical information can contribute to identifying cases of suspected malnutrition or excessive intake of potentially toxic elements before the clinical symptoms are manifest, or it may be used to define populations at risk.

It is necessary to understand the chemical forms and mechanism of accumulation of metal ions in liver. The lack of sensitive and selective analytical methods that can distinguish trace metal species has been the main obstacle. The ICP-MS interfaced to size exclusion chromatography provides such a technique. SEC has been used previously for ICP-MS with a low resolution mass analyzer in the elemental speciation studies of biological samples.[5] ICP-MS with a quadrupole mass analyzer suffers from polyatomic interference problems. High resolution ICP-MS with magnetic and electric sector field can overcome interference problem. The advantages of high resolution ICP-MS include extremely low instrumental background; improved sensitivity in low resolution for non-interfered isotopes; extremely low detection limits for nearly all elements down to the ppt region and multi-element capabilities. Here we describe a method to determine the elemental distribution of trace level elements in proteins in liver extract. In this work a high resolution ICP-MS was used as HPLC detector in the speciation studies of liver extract in order to cope with interference problems for some elements under investigation.

Experimental Section

Bovine Liver 1577a standard reference material [National Institute of Standards and Technology (NIST)] was obtained as freeze dried solid, 1.3 g batches were dissolved in 30

ml of 50 mM tris-HCl buffer. The solution was ultracentrifuged at 25 000 rpm and 10°C for 2 hours. The supernatant was decanted and the rest of the solution was filtered with 0.45 μm filter, then the remaining solution can be injected to the column without further treatment.

A Finnigan MAT high resolution ICP-MS was used.[6] ICP conditions: outer gas flow rate 14 L min^{-1}, auxiliary gas flow 0.8 L min^{-1}, forward power 1.25 kW, sampling position 10 mm from load coil, on center. Along with the ICP conditions, ion lens voltages etc. were adjusted to maximize the signal for analyte ions from standard solutions injected post-column before the chromatographic experiments. The accelerating voltage was usually 4095 volts.

SEC conditions for protein separation: TSK-GEL G3000SW_{XI} column (Tosohaas, Montgomeryville, PA) 5 μm particle size, 7.8 mm ID x 30 cm long. The eluent is 50 mM aqueous tris-HCl buffer with 0.05% sodium azide (NaN_3) at 0.5 mL/min, pH = 7.3. The column is suitable for separating proteins with molecular weight (MW) from 10,000 to 500,000 (globular protein).

Microconcentric nebulizer (MCN) and desolvation conditions: MCN (CETAC Technologies) with single pass conical spray chamber, aerosol gas flow rate 0.80 L min^{-1}, make up gas flow rate 0.10 L min^{-1}, heater temperature 140 °C, condenser temperature 0 °C. UV-vis absorbance at 280 nm was measured with a Rainin Dynamax UV-C type UV-vis detector and data was acquired by Labview program.

Fig. 1 shows the experimental setup for SEC-ICP-MS. More detail about experimental procedures can be found in reference 7

Results and Discussions

Fig. 2 shows the chromatograms of several standard proteins recorded by UV-vis absorption at 280 nm. The concentration of each protein is approximately 1mg/ml. Injection volume is 20 μl. Since the molecular weight range that can be separated by this column is 10 kDa û 500 kDa, the larger protein thyroglobin (669 kDa) elutes in the exclusion volume. Other smaller proteins then elute based on their apparent molecular weight, each with a certain retention time. The good separation performance of this column is shown in Fig. 2. By plotting the molecular weight versus the retention time, a calibration curve can be established for the relationship between the retention time and molecular weight of protein.

The ionic strength of mobile phase buffer plays an important role in maximizing molecular sieving mechanism and minimizing secondary effects such as ionic and hydrophobic interactions between the sample and the column packing materials. Under conditions of high ionic strength hydrophobic interactions may occur, while under low ionic strength, ionic interactions take place more often with small solutes. Fig. 3 shows the effect of salt strength of the mobile phase on the separation of proteins in liver extract. With 50 mM tris/HCl and 0.05 % NaN_3 as mobile phase, several fractions can be separated for liver extract. With 0.1 M NaCl and 1 mM EDTA added to the mobile phase, the chromatogram shows no significant changes. For ICP-MS the salt load of the mobile phase should be kept as low as possible in order to minimize interferences and matrix effects and the risk of deposits in the ICP-MS orifices. The mobile phase of choice for this work is 50 mM tris/HCl with 0.05% NaN_3 .

Fig. 4 shows Cu and Zn chromatograms in liver extract. For the detection of $^{63}Cu^+$ and $^{64}Zn^+$, medium resolution ($R = m/\Delta m = 3000$) is need to separated analyte signals from interferences such as $^{31}P^{16}O_2^+$ and $^{32}S^{16}O_2^+$. For Cu there is one sharp peak corresponding to MW >500 kDa, one larger peak corresponding to MW = 13 kDa and two small peaks corresponding to MW < 10 kDa.). Most of copper exists in smaller protein fractions. The concentration of copper corresponding to the major peak corresponding to MW = 13 kDa is estimated to be 5 ppb.

For Zn there is one main peak corresponding to MW = 13 kDa. Zinc is mainly bound to MW = 13 kDa protein. Almost all of zinc exists in smaller molecular weight fraction. The concentration of zinc corresponding to the major peak corresponding to MW = 13 kDa is estimated to be 4 ppb.

Templeton et al. studied excess iron accumulation in human and animal tissues by chromatographic separation of proteins and detection by ICP-MS and reported the iron distribution in healthy rat liver.[8] The measurement of iron in the present work exhibits improved sensitivity and spectral resolution. Fig. 5 shows the Mn and Fe chromatograms in liver extract. For Mn and Fe, medium resolution is used here to separate analyte signal from interferences, mainly $^{39}K^{16}O^+$ and $^{40}Ar^{16}O^+$. There is only one peak corresponding to MW = 13 kDa for Mn^+. Almost all of Mn exists in small protein fractions (MW = 13 kDa). The

corresponding concentration of Mn is about 3 ppb. For iron there are two small peaks corresponding to MW > 500 kDa and MW = 150 kDa, the third peaks corresponding to MW = 10 kDa. Only a small amount of iron is bound to larger protein fractions (MW > 500 kDa and MW = 150 kDa), most of iron exist in small protein fractions (MW = 10 kDa). The estimated concentration of iron corresponding to the major peak at MW = 13 kDa is estimated to be 3.5 ppb.

Cadmium speciation in cooked pig kidney was carried out by Crews et al. by size exclusion chromatography coupled directly to ICP-MS. [9] The measurement of cadmium in this work provides better sensitivity and improved spectral resolution. Fig. 6 shows the chromatogram of $^{112}Cd^{+}$ and $^{114}Cd^{+}$ in liver extract detected at low resolution. Four peaks are well separated: two small peaks corresponding to MW >500 kDa, one small and wide peak corresponding to MW = 70 kDa, and one sharp peak corresponding to MW = 13 kDa. Thus the results show that cadmium binds four different fractions: two high molecular weight (MW > 500 kDa) protein fractions, MW = 70 kDa protein fraction and low molecular weight fraction (MW = 13 kDa). More cadmium is found in small protein fraction. The concentration of cadmium corresponding to the major peak at MW = 13 kDa is estimated to be 2 ppb.

High resolution ICP-MS is also advantageous in determining non-metallic elements such as sulfur and phosphorous. Comparison of the sulfur and metallic chromatograms may reveal the relationship between sulfur-rich proteins and the metallothioneins. Fig. 7 shows the chromatogram of S in liver extract using medium resolution. With the high resolution ICP-MS, the background is relatively low. The analyte signal from ^{34}S can be distinguished clearly. There are three S^{+} peaks with the corresponding molecular weight: >500 kDa, 13 kDa and 10 kDa. Most of the sulfur is bound to low molecular weight protein fractions. The concentration of sulfur corresponding to the last peak corresponding to MW = 10 kDa is estimated to be 0.4 ppb. Fig. 8 show the chromatogram of P^{+} measured using high resolution. There is one small peak corresponding to MW > 500 kDa, one small and wide peak corresponding to MW = 70 kDa, and one larger peak corresponding to MW = 11 kDa, following by a large peak from smaller molecules. Only a small amount of phosphorus is bound to larger protein fractions (MW > 500 kDa and MW = 80 kDa); most of phosphorus

exists in small protein fractions (MW = 11 kDa). The concentration of phosphorus corresponding to the peak at MW = 11 kDa is estimated to be 20 ppb. Phosphorus is also found in the MW = 70 kDa protein fraction where no sulfur is found.

Fig. 9 shows the Co and Mo chromatograms in liver extract. There is only one sharp Mo peak at MW = 11 kDa. The result shows that Mo is completely in small fraction (MW = 11 kDa), and Mo is not bound to high molecular weight proteins. The concentration of Mo corresponding to the major peak corresponding to MW = 11 kDa is estimated to be 2 ppb. There is one very sharp Co peak corresponding to MW = 155 kDa and several small peaks corresponding to MW < 10 kDa. The first peak corresponds to the protein fraction with a molecular weight of 155 kDa. Most of the cobalt is bound to larger protein fraction (MW = 155 kDa) and only a small amount of cobalt exists in smaller protein fractions. The concentration of cobalt bound to protein is estimated to be 0.4 ppb. Very sharp peak shows that column is capable of good separation.

The measurement for Ca and Mg were completed with a different column: GPC 300 at 0.1ml/min. Fig. 10 shows the $^{42}Ca^{+}$ and $^{44}Ca^{+}$ chromatograms of liver extract. For Ca, medium resolution is need to separate analyte signal from interferences from $^{40}Ar^{1}H_{2}^{+}$ and $^{12}C^{16}O_{2}^{+}$. There is only one Ca^{+} peak corresponding to small molecule. Calcium exists only in small molecule and is not protein bound. The concentration of calcium is estimated to be 3.8 ppb. Similar chromatogram is obtained for magnesium in medium resolution (Fig. 11). There is also only one Mg^{+} peak corresponding to small molecules (Fig. 11). Mg is not protein bound. The concentration of Mg is estimated to be 70 ppb.

Conclusion

Size exclusion chromatography with a double focusing ICP-MS detection has been successfully applied to the study of elemental distribution in liver extract. High resolution ICP-MS eliminates polyatomic interferences and provides high sensitivity in low resolution mode. Because of the high sensitivity provided by present work, sample preconcentration is not needed, only simple sample preparation that should not dilute species is used here. Information about approximate molecular weight of protein in the sample can be obtained without using standard of that protein. This is one of the advantages for using SEC

comparing with using other separation modes such as reverse phase HPLC and ion exchange chromatography. In the present work better separations are achieved by using a longer column with a narrow molecular weight separation range than in earlier paper.[7] However, the separation take a long time with a larger void volume. The results present useful information about trace elemental distribution among proteins in liver extract. A sensitive detection method is provided for elemental distribution in liver extract, which is important in monitoring elemental uptake and distribution. The applicability of ICP-MS as a sensitive, multielement detector in the field of biological research has been demonstrated.

Acknowledgements

The experiments are supported by the Ames Laboratory, U. S. Department of Energy, Office of Basic Energy Sciences, under Contract W-7405-Eng-82. The measurements were conducted at CETAC Technologies. The authors also thank Finnigan MAT for providing the mass spectrometer.

References

1. Sergio Caroli Ed. *Element Speciation in Bioinorganic Chemistry.* Chemical Analysis Series, Vol.135, John Wiley & Sons, Inc. 1996; Ure, A.M. and Davidson, C.M., Ed. *Chemical Speciation in the Environment.* Blackie Academic & Professional 1995.
2. Subramanian, K. S., Iyengar, G.V. and Okamoto, K., *Biological Trace Element Research Multidisplinary Perspectives.* ACS Symposium Series 445, 1991.
3. Kendrick, M.J., May, M.T., Plishka, M.J. and Robinson, K.D., *Metals in Biological Systems*, Ellis Horwood 1992.
4. *Elemental Analysis of Biological System Vol. 1 Biomedical, Environmental, Compositional, and Methodological Aspects of Trace Elements.* Venkatesh Iyengar. G., CRC Press, Inc.,1989.
5. Owen, L.M.W., Crews H.M., Massey R.C. and Bishop, N.J., *Analyst* 1995 **120**, 705; Owen, L.M.W., Crews, H. M., Huttton, R. C. and Walsh, A., *Analyst* 1992 **117**, 649; Leopold, I. and Gunther, D., *Fresenius J. Anal. Chem.* 1997, **359**, 364

7. Stuewer, D. and Jakubowski, N., *J. of Mass Spectrometry*, 1998, **33**, 579 and references herein.

8. Wang J.; Houk R.S.; Dreessen D.R.; Wiederin D. *Journal of the American Chemical Society*. 1998, Volume **120,** No. 23 5793-5799.

9. Stuhne-Sekalec, L., Xu, S.X., Parke, J.G., Olivieri, N.F. and Templeton, D.M., *Anal. Biochem.,* 1992, **205,** 278

10. Crews, H.M., Ebdon, L., and Massey, R.C., *Analyst,* 1989, **114**, 895

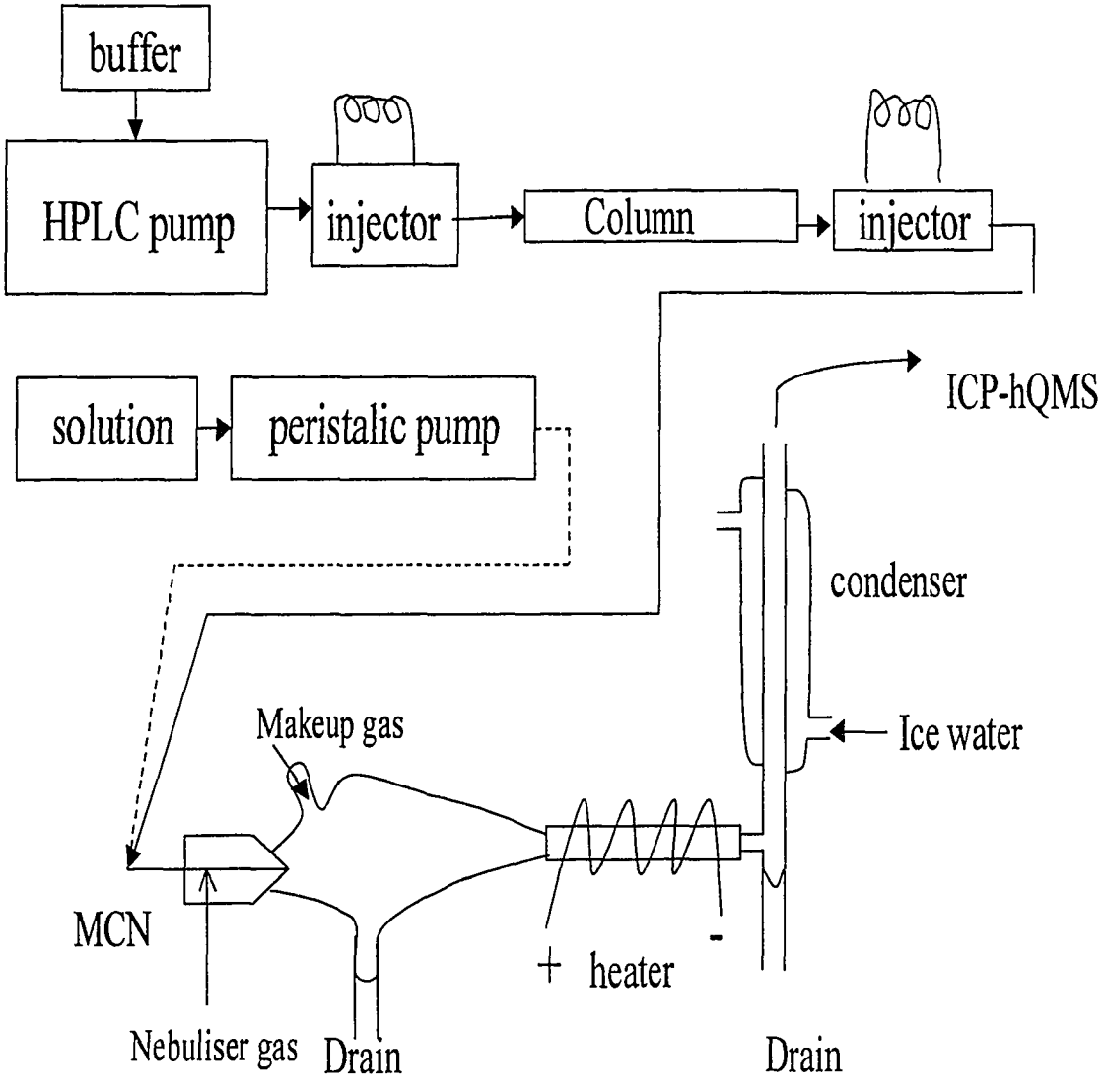

Fig. 1. Experimental setup for size exclusion chromatography-ICP-MS.

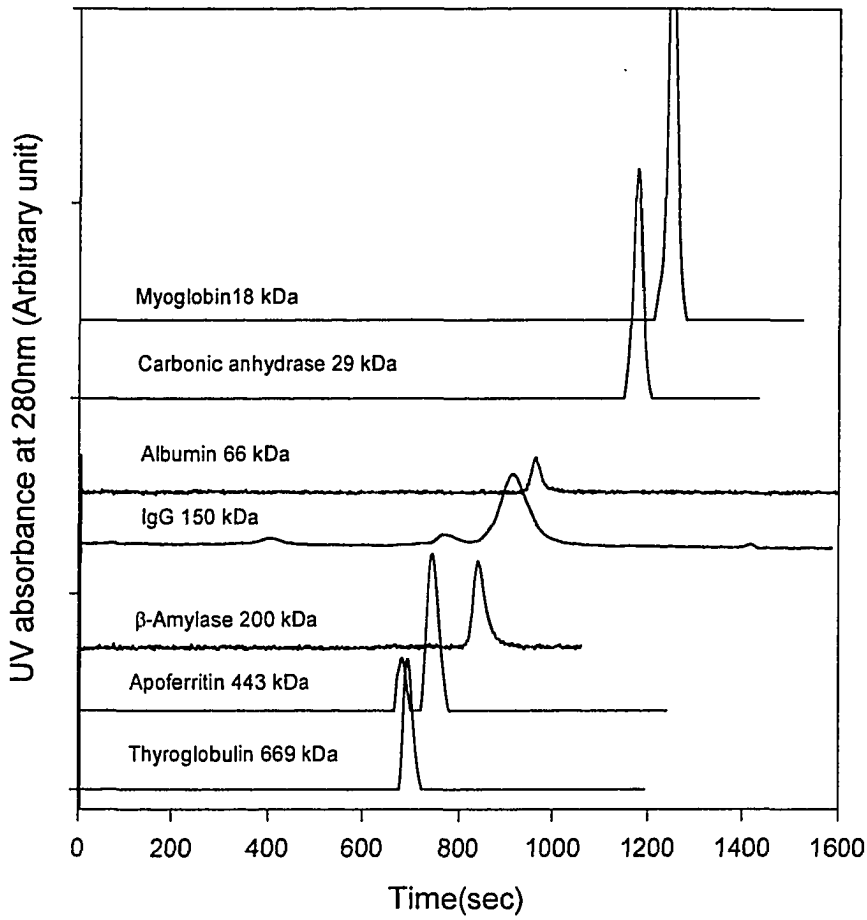

Fig. 2. Shows the chromatograms of several standard proteins recorded by UV-vis at 280 nm. The concentration of each protein is approximately 1mg/ml. Injection volume is 20 μl.

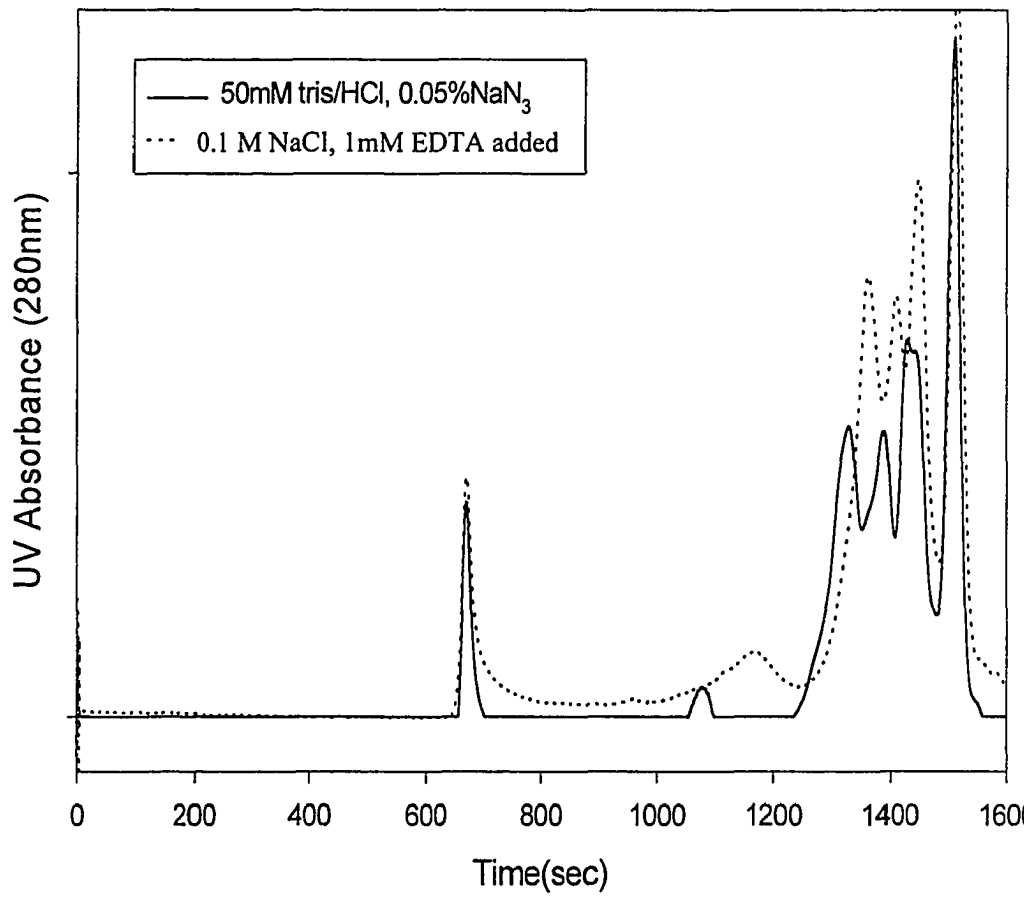

Fig. 3. Effect of salt strength of mobile phase on the separation of proteins in liver extract.

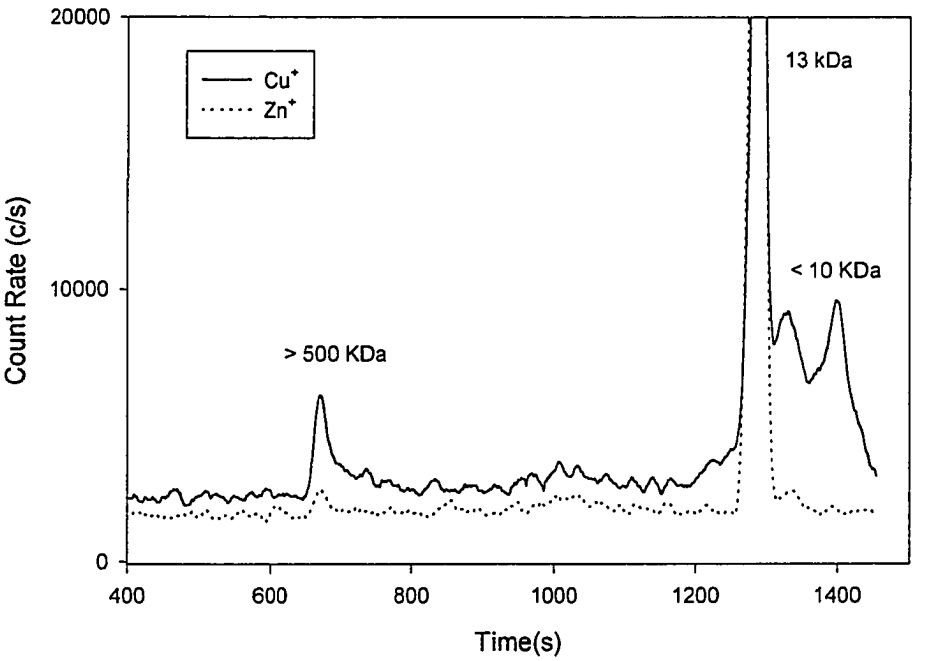

Fig. 4. ^{63}Cu and ^{64}Zn chromatograms in liver extract, spectral resolution = 3000.

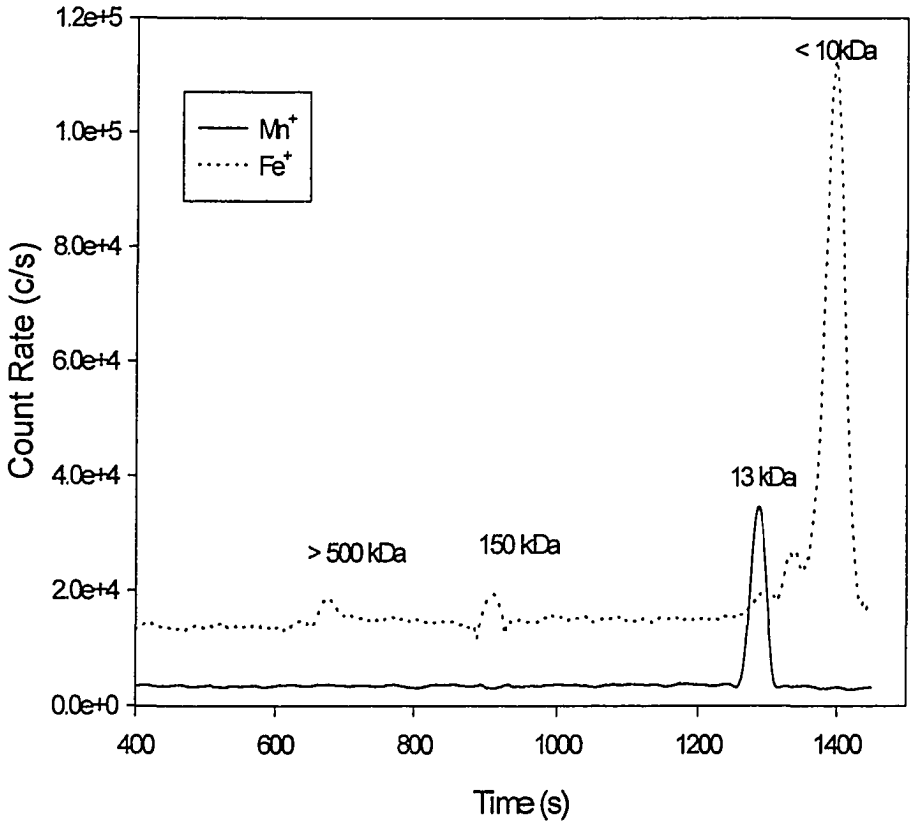

Fig. 5. ^{55}Mn and ^{56}Fe chromatograms in liver extract, spectral resolution = 3000.

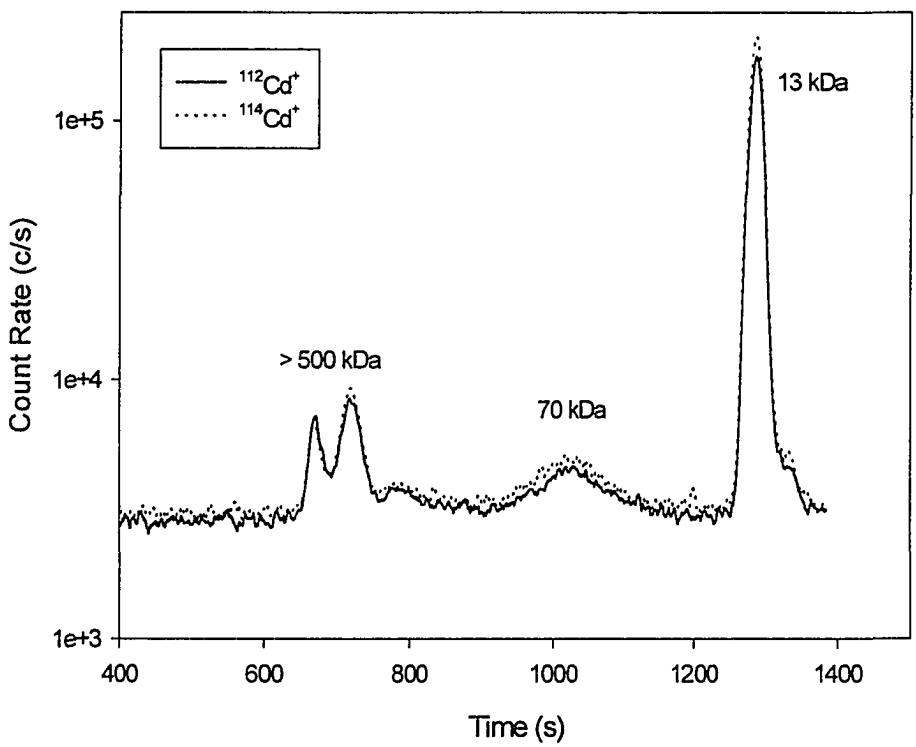

Fig. 6. ^{112}Cd and ^{114}Cd chromatogram in liver extract, spectral resolution = 300.

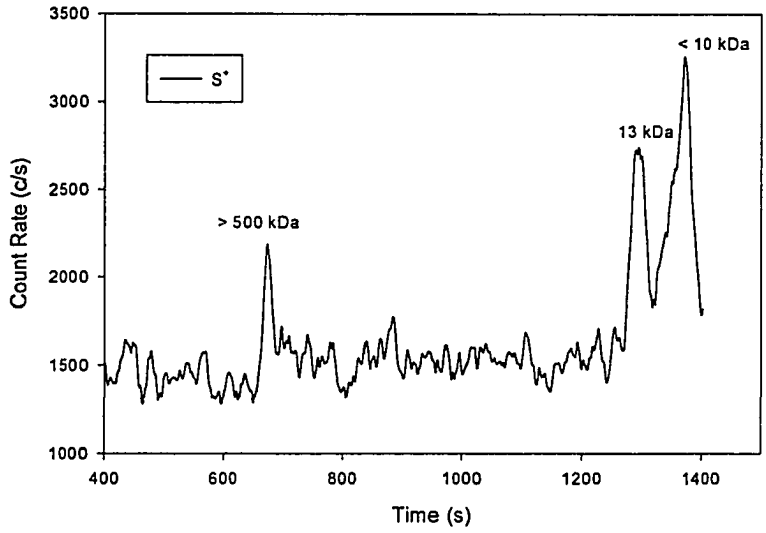

Fig. 7. ^{34}S chromatogram in liver extract, spectral resolution = 3000.

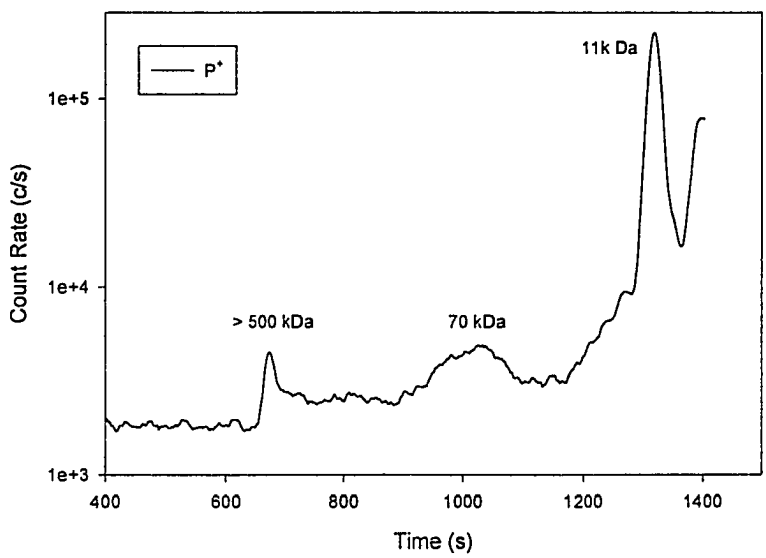

Fig. 8. ^{31}P chromatogram in liver extract, spectral resolution = 3000.

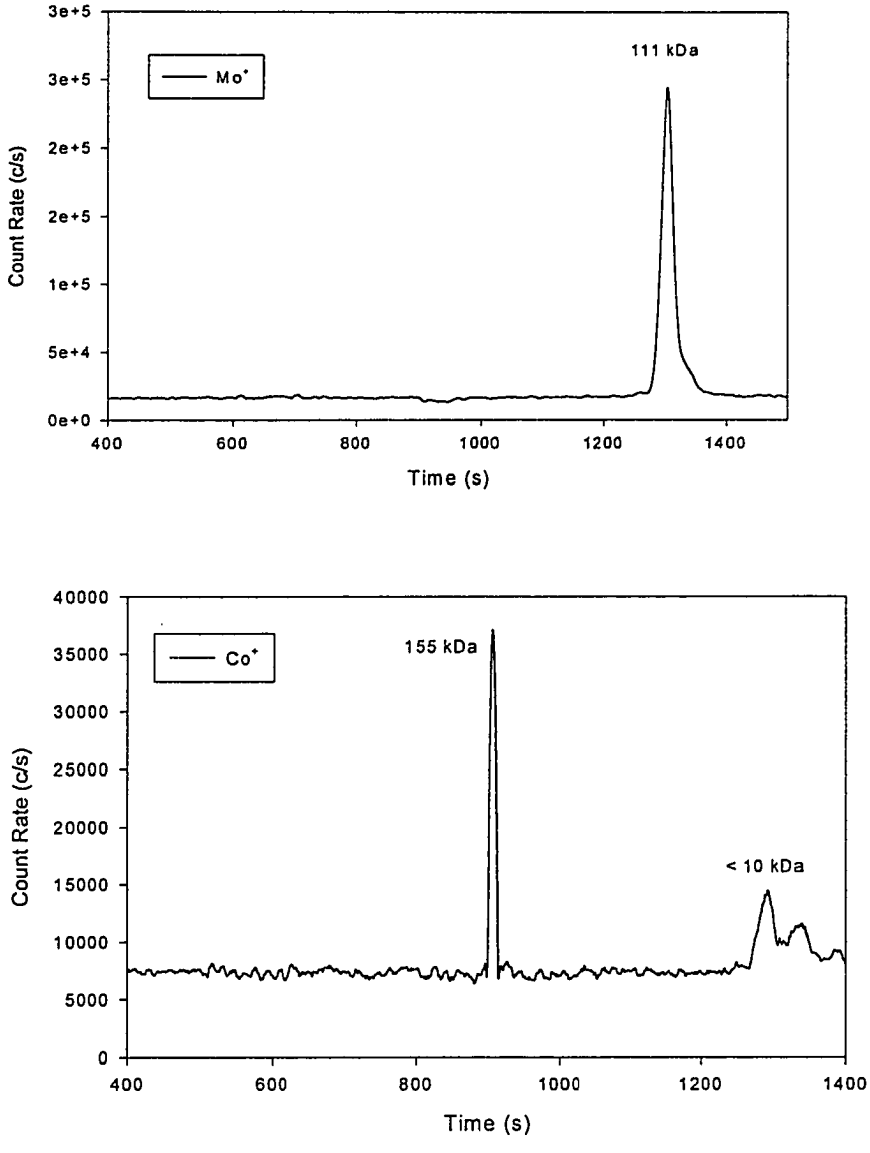

Fig. 9. ^{59}Co and ^{98}Mo chromatograms in liver extract, spectral resolution = 300.

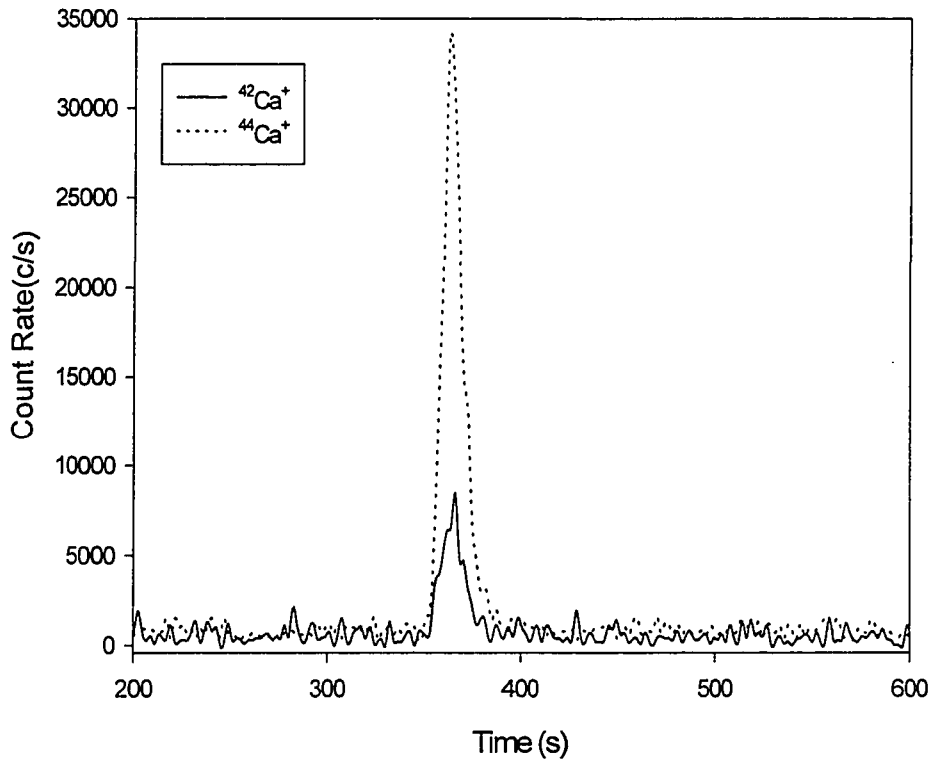

Fig. 10. $^{42}Ca^{+}$ and $^{44}Ca^{+}$ chromatograms of liver extract, spectral resolution = 3000.

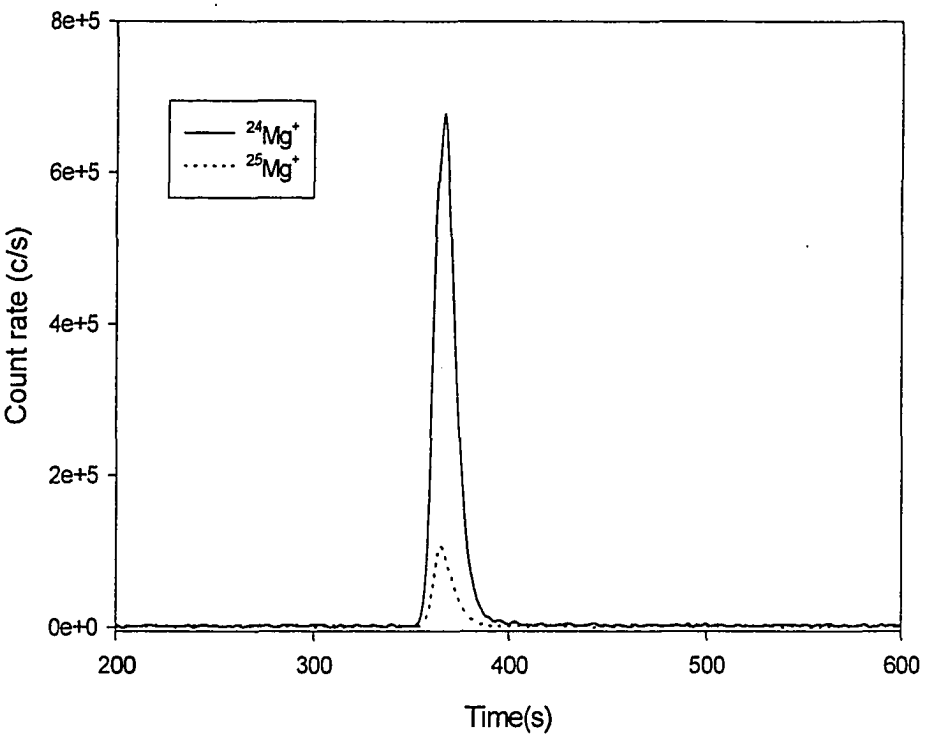

Fig. 11. $^{24}Mg^{+}$ and $^{25}Mg^{+}$ chromatograms of liver extract, spectral resolution = 3000.

CHAPTER 5: FUNDAMENTAL STUDIES ON RESOLVING POLYATOMIC INTERFERENCES, IMPROVING ION TRANSMISSION AND USING DIFFERENT COLLISION GASES BY ICP-MS WITH A COLLISION CELL

A paper is to be submitted to Analytical Chemistry

Jin Wang and R. S. Houk*

Abstract

ICP-MS with a collision cell can remove or reduce argon-related interferences. In this fundamental study, hydrogen, methane and xenon have been used as collision gas to reduce or remove polyatomic interferences. Helium is used to improve ion transmission. Hydrogen, methane and xenon are all effective to reduce polyatomic interferences, With He in the cell the value of hexapole bias voltage is closely related with the ion signals, a certain value of hexapole bias voltage gives the maximum ion signal. Ion energy is also an important parameter influencing ion transmission. With He in collision cell the ion energy spread is smaller and ion signal is improved. The experiments also illustrate how collision gases (hydrogen, methane and xenon) separate analyte signals from the interferences. The results here provide some guidance for optimizing operating conditions with this kind of instrument.

Introduction

In argon ICP-MS polyatomic ions overlap with and obscure some analyte ions such as $^{40}Ar^+$ interferences with $^{40}Ca^+$, $^{40}Ar^{16}O^+$ interferences with $^{56}Fe^+$, $^{40}Ar_2^+$ interferences with $^{80}Se^+$. Many approaches have been used to solve these interference problems. Some approaches are focused on the sample introduction system: desolvation was used to minimize solvent load into the plasma; chromatographic separation[1] and ETV[2] were used to separate analyte ions with interference ions. Other techniques are focused on the modification of ICP plasma to reduce the formation of polyatomic interferences like cool plasma[3] and mixed gas plasma[4]. Only using sector double focusing instrument or high-resolution quadrupole can

* Corresponding author

truly separate analyte signal from interferences in a nominal mass. The disadvantage with high-resolution system is lower sensitivity under high resolution.

Another approach is to put a collision cell in front of the mass analyzer; polyatomic interferences may be reduced or removed by collision with a neutral molecular gas, while analyte ions are not affected by this collision process. A collision cell interface may substantially modify the ion transmission in ICP-MS. Addition of neutral reactant gases into the collision cell can be used to selectively remove some polyatomic interference ions while affect little or none to analyte ions. The first concept was first demonstrated by Houk [5]and by Douglas[6] for ICP-MS. The work by Douglas described the attenuation of polyatomic ion interferences by collision cell in Ar ICP-MS, which showed not much success in removing polyatomic ions.[6] Rowan and Houk [5] employed a RF-only quadrupole cell as the first stage of double-quadrupole arrangement. Low energy gas phase collisions with Xe or CH_4 were used for reducing polyatomic ion interferences in Ar ICP-MS. Koppenaal and coworkers also observed that many polyatomic ions were essentially eliminated from the mass spectrum of their ion trap ICP-MS and an octopole collision cell instrument.[7] Tuner and coworkers at Micromass have developed the first commercial ICP-MS with a hexapole collision cell. By using He, Ar or N_2 in the cell, the energy spread of ions can be reduced to less than 1V, and the transfer efficiency of the instruments is extremely high. With hydrogen added to the cell the argon-based interference molecular ions can be removed or reduced.[8] Collision cell interface ICP-MS instrument offer interesting development for high intensity and interference-free ICP-MS. There is still a lot work needed regarding the fundamental mechanism of collision reduction of interferences and the possibility of other novel gases as collision gas to achieve better sensitivity and better removal of interferences

Experimental Section

A Micromass Platform ICP-hQMS was used for the measurement. In the platform ICP-hQMS a hexapole RF collision cell was placed between the skimmer cone and the quadrupole mass filter. Ions from the MS interface were forced onto the entrance aperture of the hexapole array by the extraction voltages; the hexapole array was surrounded by a jacket into which different types of gas could be admitted. The gas flow was controlled by separate

mass flow controller. The use of the jacket around the hexapole produces an independently controllable atmosphere for thermalization and gas phase reaction. The standard Meinhard nebuliser and cooled double pass Scott type spray chamber were used. The nebuliser uptake rate is 0.5 ml/min. The nebulizer flow rate is around 0.85 l/min. The optimum operating parameters of ICP- hQMS are listed in Table 1.

TABLE 1 Typical operating parameters of ICP-hQMS

Gases			Analyzer			Torch		
Cool	14.00	L/min	Cone	590	V	X posn	0.5	
Interm.	1.00	L/min	Hex Exit	330	V	Y posn	0.27	
Neb1.	0.85	L/min	Hex Bias	-2.5	V	Z posn	0.1	
			LM Res	20.1	V	Power	1300	W
He	4.33	ml/min	HM Res	20.1	V			
H2	2.0	ml/min	Ion Energy	1	V			
SC Temp	4	°C	Multiplier	502	V			

All working standards were prepared from 1000 mg/l high purity stock standard (Plasma Chem) and diluted to the appropriated concentration with 1% (v/v) high purity HNO_3. Helium (99.995%) and hydrogen (99.9995%) were from Air Products. Xenon (99.999%) and methane (99.995%) were from Matheson Gas Products. These gases were used without further purification and introduced into collision cell by a mass flow controller, which are also controlled by computer. 10ppb Be, Co, In, Pb, U standards in 1% HNO_3 were used for the optimization of plasma conditions. The highest signal of $^{208}Pb^+$ was obtained by adjusting helium flow. A 10 ppb Co in deionized water solution was used to adjust H_2 flow to reach highest ratio of signal at 59 (m/z) to signal at 56 (m/z), a optimal H_2 flow was reached when sensitivity at 59 (m/z) is the highest and background signal at 56 (m/z) and 80 (m/z) are minimum.

Results and Discussions

H_2 as a collision gas

Figure 1a and 1b show the spectra of 10 ppb Cobalt in 1% HNO_3 solutions with increasing amount of hydrogen in the collision cell. Without hydrogen in the cell there are huge peaks from Ar_2^+ at m/z = 80; ArO^+ at m/z = 56; ArN^+ at m/z = 54; ArH^+ at m/z = 41; Ar^+ at m/z = 40, 39 and 38, C^+ at m/z = 12; N^+ and NH^+ at m/z = 14 and 15 respectively; O^+ at m/z = 16; OH^+, OH_2^+ and OH_3^+ at m/z = 17,18 and 19 respectively. With adding H2 at the flow rate of 6 ml/min, dramatic changes occur in the spectra. The peak from $^{40}Ar_2^+$ was basically removed, argon oxide $^{40}Ar^{16}O^+$ and argon nitride $^{40}Ar^{14}N^+$ were significantly reduced, and argon ^{40}Ar and argon hydride $^{40}Ar^1H^+$ were also reduced a lot, which indicates that hydrogen is very effective in reducing these interferences. Analyte signal $^{59}Co^+$ was increased meanwhile, which indicates that hydrogen has a certain collision focusing effect resulting in improved ion transmission. It is interesting to notice the changes in the low mass range: $^{12}C^+$, $^{14}N^+$, $^{14}N^1H^+$, $^{16}O^+$ and $^{16}O^1H^+$ were also reduced. With adding more hydrogen, the Co^+ signal decreases due to the ion loss from too many collisions. Other interference signals continue to decrease including argon hydride ArH^+ at m/z = 39, OH_2^+ and OH_3^+ peaks at m/z = 18 and 19 remain the same. Here the reaction cross-sections (reaction rates) for ArX^+ (and some other ions) with H_2 is very high, the products of these reactions are lower molecular weight ions which can be defocused from the cell. Figure 2a and 2b show the intensity changes of some typical interferences with different amount of hydrogen in the cell. This kind of time resoled analysis clearly demonstrated how fast the reducing process of interferences by hydrogen will take effect. It takes less than 20 s for completion of reduction of most interferences and at most 30 s for oxygen related interferences. The chromatograms also show how much hydrogen is needed to reduce the interferences to a certain extent. It can be seen that different amount of hydrogen is need for different elements, if hydrogen added too much the analyte signals will also be sacrificed.

H_2 separate analyte signals from interferences

The effect of hydrogen in the cell on the interferences $^{38}Ar^1H^+$, $^{40}Ar^+$, $^{40}Ar^{16}O^+$ and $^{40}Ar_2^+$ is studied. Figure 3 presents the negative attenuation percentage of these four interferences change with hydrogen flow rate. The solution analyzed here is just a deionized water solution; thus the intensity for each m/z represents the sum of the signal from corresponding background and possibly the signal from impurity in the water. With increasing H_2 flow all the interferences were attenuated. Ar^+ and Ar_2^+ were quickly reduced to ~ 100% with a H_2 flow of 2 ml/min. Due to the Fe contamination in the water the curve for ArO^+ can only reach ~85% with the same amount of H_2. Because of formation of ArH^+ with addition of H_2 the attenuation for ArH^+ is not very effective. Intensities from Ar_2^+ and Ar^+ decrease more rapidly than the signals from ArO^+ and ArH^+. With sufficient amount of H_2 added, the curves tend to be flat which reflect the contribution from the impurity in the solvent.

Figure 4 shows how hydrogen can separate Ca^+ from the interference Ar^+. The intensities at m/z = 40 were measured from two solutions: A deionized water which gives mainly the intensity of interference Ar^+ and a 0.4 ppb Ca^+ in 1% HNO_3 solution which gives the intensity of both analyte Ca^+ and interference Ar^+. The figure shows clearly the different response of two curves with H_2 flow rate. Without H_2 in the cell, the intensities from two solutions are basically the same. The analyte signal of Ca^+ is just obscured by the huge background signal from Ar^+ interference. With increasing H_2 flow, at first two intensities are decreased to the same level. At this time H_2 flow is not larger enough to reduce Ar^+ to the level the Ca^+ can show up. With more H_2 (3 ml/min), two curves begin to gradually separate. At H_2 = 5 ml/min the upper curve tend to level off representing the signal of Ca^+, the lower curve continue to drop representing the reducing interferences. Now Ar^+ is reduced enough so Ca^+ can be seen. This indicates that H_2 can selectively react with Ar^+ without too much loss of Ca^+; with Ar^+ reduced by reacting with H_2, Ca^+ can be differentiated from the background, and finally separated from the background. With even more H_2, each curve will be flat. The intensity of flat parts of upper curve comes from 0.4ppb Ca^+. The intensity of flat parts of lower curve comes from Ca^+ impurity of the water.

The same methodology applies to the experiment showing how hydrogen can separate Fe^+ from interference ArO^+ (Figure5). The intensities at m/z = 56 were measured from two solutions: A deionized water which gives mainly the intensity of interference ArO^+ and a 10 ppb Fe^+ in 1% HNO3 solution which gives the intensity of both analyte Fe^+ and interference ArO^+. It can be seen that only a much smaller H_2 flow (1ml/min) can differentiate Fe^+ from interference ArO^+. This is due to the fact that ArO^+ interference is far less than Ar^+ interference. The results also indicate that H_2 can selectively react with ArO^+ with only small loss of Fe^+. With ArO^+ reduced by reacting with H_2, Fe^+ can be differentiated from the background, and finally separated from the background.

A similar experiment shows how hydrogen can separate Se^+ from the interference Ar_2^+ (Figure 6). The intensities at m/z = 80 were measured from two solutions: A deionized water which gives mainly the intensity of interference Ar_2^+ and a 10 ppb Se^+ in 1% HNO_3 solution which gives the intensity of both analyte Se^+ and interference Ar_2^+. The results here also indicate that H_2 can selectively react with Ar_2^+ with no significant loss of Se^+, with Ar_2^+ reduced by reacting with H_2, Se^+ can be differentiated from the background, and finally separated from the background.

The amount of H_2 needed to get a net Se^+ signal three time the Ar_2^+ interference is larger than that needed to get a net Fe^+ signal three times ArO^+ interferenece, while less than that need to get a net Ca^+ signal. This is reasonable due to the fact that Ar_2^+ interference is more than ArO^+ interference but less than Ar^+ interference.

He as a collision gas

Effect of ion energy on ion transmission with helium in the cell

Since the scattering rate is normally much faster than the fragmentation rate with helium as collision gas, helium is also not chemically reactive, helium is not effective at reducing the polyatomic ion interference. Figure 7 shows the signal changes of several typical elements with ion energy with helium and without helium in the cell. Without helium in the cell, the signal û ion energy curves show slow increase before the plateau, the energy spread of ions is large with a value in the range of 10 eV, and the maximum intensity only can reach 60 %. With helium in the cell all other elements except low mass $^9Be^+$ exhibit

increased sensitivity with increasing ion energy. Ion signals increase more steeply with ion energy before the plateau. The energy spread of ions is decreased to the value of about 3 eV, and the maximum intensity can reach 100 %.

Effect of hexapole bias voltage on the ion transmission with He in the cell

With a neutral gas in the collision cell, the ions with higher atomic weight relative to the collision gas tend to lose kinetic energy and migrate toward to the axis as a result of collision. This is the so-called collision focusing. If the molecular weight of collision gas is too large the ion will be scattered out of the cell. Usually for most of collision gases the scattering cross-section for polyatomic ions in the ICP is greater than the fragmentation cross-section, so most of the polyatomic ions will be scattered out instead of being dissociated. Thus collision-induced dissociation with He is not efficient for minimizing polyatomic interferences. There may be some ion-molecular reactions happened in the process.

Figure 8 shows the signal changes of several typical elements with hexapole bias voltage with helium and without helium in the cell. Without collision gas in the cell the ion signals are not affected by the hexapole bias. With the addition of helium into the cell, all the other elements except $^{9}Be^{+}$ show the increased signals and reach the maximum intensity at a certain hexapole bias voltage value. Figure 8b demonstrates such improvement by plotting the ratio of the intensity with helium in the cell to the intensity with no helium in the cell versus hexapole bias. An increase factor of 4 - 8 can be obtained. The results show that helium can be used to focus the ions into the center by the collisions and improve the ion transmission. Thomson et al. observed that the effect of collisional focusing is great for very heavier ions (protein ions) on a triple quadrupole mass spectrometer[9]. Here the effect of focusing is great for middle mass ions. By monitoring the changes of the ion signal with different amount of helium in the cell, it can be observed that too much helium added will generate too much collision, which scatter out analyte ions and decrease the ion signal. With the normal amount of helium that increase the analyte ion signal, some interference signal like $^{40}Ar_2^{+}$ also increased by a smaller factor. Thus helium can increase both interferences and analyte signal at normal operating gas flow!

Mixture of He and H_2 as collision gas

Effect of ion energy on ion transmission with He and H_2 in the cell

Mixture of He and H_2 is normally used in the collision cell of ICP-hQMS thus the effect of this mixture collision gas on the ion transmission is investigated. All other elements except $^{9}Be^{+}$ show an S-shape curve with increasing ion energy (Figure9). The ion energy spread of ion obtained for this mixture gas system is of 2-3 eV. The use of this collision gas mixture also decreases the ion energy spread and improves the ion transmission.

Effect of ion energy on hexapole bias voltage with He and H_2 in the cell

Similarly the effect of hexapole bias voltage on the ion signal are examined for this mixture gas system (Figure 10). All ion signal increase with hexapole bias. For low mass $^{9}Be^{+}$ and Co^{+} hexapole bias voltage of û1 corresponds the maximum of the intensity; for middle mass $^{115}In^{+}$ and $^{140}Ce^{+}$ hexapole bias voltage of 0 corresponds the maximum of the intensity; for high mass $^{208}Pb^{+}$ and $^{238}U^{+}$ hexapole bias voltage of 1 corresponds the maximum of the intensity. With this mixture collision gas, elements with high mass usually need larger value of hexapole bias voltage in order to acquire enough energy to pass through the collision cell and quadrupole. In this case the effects of collisional focusing are great for middle mass ions. Multiple collision in the hexapole cell result in two effects that are advantageous for transmission of ions into the quadrupole: the first: the ions are focused toward the center, where the ions will better enter the quadrupole, thus the ion beams better match the acceptance aperture of the quadrupole, resulting in better transmission. And the second: the axial ion energy and energy spread is also decreased. Thus the kinetic energy of the ions entering the quadrupole is more uniform, resulting in the mass independent resolution.

CH_4 as a collision gas

The potential of removing polyatomic interferences using methane as a collision gas was studied. The results obtained here with a commercial device agree well with the results of Rowan and Houkæs work[5] with a home made device.

Methane separate analyte signals from interferences

Similar experiment is designed to demonstrate how methane separate analyte signals from the interference. In Figure 11 the intensities at m/z = 56 were measured from two solutions: A deionized water which gives mainly the intensity of interference ArO^+ and a 10 ppb Fe^+ in 1% HNO_3 solution which gives the intensity of both analyte Fe^+ and interference ArO^+. The figure shows clearly the different response of two curves with methane flow rate. Here methane flow used is relatively smaller than the previous H_2 flow. At CH_4 = 0.4 ml/min Fe^+ signal can be separated from ArO^+ signal. The results indicate that CH_4 can selectively react with ArO^+ with only small loss of Fe^+, with ArO^+ reduced by reacting with CH_4, Fe^+ can be differentiated from the background, and finally separated from the background. The similar methodology applies to the experiment showing how methane can separate Se^+ from the interference Ar_2^+.

In Figure 12 the intensities at m/z = 80 were measured from two solutions: A deionized water which gives mainly the intensity of interference Ar_2^+ and a 10 ppb Se^+ in 1% HNO_3 solution which gives the intensity of both analyte Se^+ and interference Ar_2^+. The figure shows clearly the different response of two curves with methane flow rate. At CH_4 = 0.6 ml/min Se^+ signal can be separated from Ar_2^+ signal. The results indicate that CH_4 can selectively react with Ar_2^+ with no significant loss of Se^+. With Ar_2^+ reduced by reacting with CH_4, Se^+ can be differentiated from the background, and finally separated from the background. The amount of methane needed to get a net Se^+ signal three time the Ar_2^+ interference is larger than that needed to get a net Fe^+ signal three times ArO^+ interfernece, since Ar_2^+ is usually usually larger than ArO^+.

The similar methodology applies to the experiment showing how methane can separate Ca^+ from the interference Ar^+. In Figure 13 the intensities at m/z = 40 were measured from two solutions: A deionized water which gives mainly the intensity of interference Ar^+ and a 10 ppb Ca^+ in 1% HNO_3 solution which gives the intensity of both analyte Ca^+ and interference Ar^+. The figure shows clearly the different response of two curves with methane flow rate. At CH_4 = 0.8ml/min Ca^+ signal can be separated from Ar^+ signal. The results indicate that CH_4 can selectively react with Ar^+ without too much loss of

Ca^+, with Ar^+ reduced by reacting with CH_4, Ca^+ can be differentiated from the background, and finally separated from the background. The amount of methane needed to get a net Ca^+ signal three time the Ar^+ interference is larger than that needed to get a net Se^+ signal three times Ar_2^+ interference, since Ar^+ is usually larger than Ar_2^+.

The formation of methane clusters with ArO^+ and Ar_2^+ was examined in Figure 14. ArO^+ methane clusters and Ar_2^+ methane clusters signal do not increase instead decrease with increasing methane flow. This indicates that the no ArO^+ methane clusters and Ar_2^+ clusters as produced by the addition of methane. The apparent cluster signals are just from background or impurities. The formation of methane clusters with analyte signal Co^+ was examined in Figure15. Co^+ methane cluster remains approximately the same with increasing methane flow. This indicates that the not much Co^+ methane clusters produced by the addition of methane. The loss of Co^+ signal due to Co^+ methane cluster is minimal. The formation of hydride with methane in the cell is examined (Figure16). SeH^+ and FeH^+ signal remains approximately the same with increasing CH_4 flow. This indicates that no Ar_2^+ hydride and ArO^+ hydride produced by the addition of methane. The original SeH^+ and FeH^+ signals are believed to be produced by hydrogen already in the plasma.

Xe as a collision gas

The potential of removing polyatomic interferences using xenon as a collision gas was studied. It was found that with adding xenon into the collision cell a relatively clean spectrum was obtained. Peak at m/z = 80 almost disappears and peaks at m/z = 56, 54 also decreased to a significant extent.

Xe separate analyte signals from interferences

The following experiments demonstrate how xenon separate analyte signals from the interference. In Figure 17 the intensities at m/z =56 were measured from two solutions: A deionized water which gives mainly the intensity of interference ArO^+ and a 10 ppb Fe^+ in 1% HNO_3 solution which gives the intensity of both analyte Fe^+ and interference ArO^+. The figure shows clearly the different response of two curves with methane flow rate. Here xenon flow used is relatively smaller than H_2 flow. At Xe = 0.2ml/min Fe^+ signal can be separated

from ArO^+ signal. The results indicate that Xe can selectively react with ArO^+ with small loss of Fe^+. With ArO^+ reduced by reacting with Xe, Fe^+ can be differentiated from the background, and finally separated from the background.

The similar experiment showing how xenon can separate Se^+ from the interference Ar_2^+. In Figure 18 the intensities at m/z = 80 were measured from two solutions: A deionized water which gives mainly the intensity of interference Ar_2^+ and a 10 ppb Se^+ in 1% HNO_3 solution which gives the intensity of both analyte Se^+ and interference Ar_2^+. The figure shows clearly the different response of two curves with xenon flow rate. At Xe = 0.3 ml/min Se^+ signal can be separated from Ar_2^+ signal The results indicate that xenon can selectively react with Ar_2^+ with no significant loss of Se^+, with Ar_2^+ reduced by reacting with Xe, Se^+ can be differentiated from the background, and finally separated from the background.

The results from similar experiments showing how xenon can separate Ca^+ from the interference Ar^+ is shown in Figure 19, the intensities at m/z = 40 were measured from two solutions: A deionized water which gives mainly the intensity of interference Ar^+ and a 10 ppb Ca^+ in 1% HNO_3 solution which gives the intensity of both analyte Ca^+ and interference Ar^+. The figure shows clearly the different response of two curves with methane flow rate. At Xe = 0.4 ml/min Ca^+ signal can be separated from Ar^+ signal. The results indicate that Xe can selectively react with Ar^+ without too much loss of Ca^+, with Ar^+ reduced by reacting with Xe, Ca^+ can be differentiated from the background, and finally separated from the background.

Conclusion

ICP-MS with a collision cell provides a powerful tool to remove or reduce interferences and improve sensitivity. The experimental results show that hydrogen in the cell is very effective in removing or reducing polyatomic interferences. An appropriate amount of helium (He) introduced into the cell increase ion transmission of the elements in the middle and high mass range. The focusing effect of collision gases is demonstrated based on the experiments with collision gas in the cell and no collision gas in the cell. The enhancement of ion transmission is closely related with the nature and flow rate of collision gas, collision energy and ion energy. Without gas in the cell, hexapole bias voltage basically

has no significant effect on ion transmission; With He in the cell the value of hexapole bias voltage closely related with the ion signals, a certain value of hexapole bias voltage gives the maximum ion signal. Ion energy (IE) is also an important parameter influencing ion transmission. With He in the collision cell the ion energy spread is smaller. Up to now He and H_2 are still the first choice of collision gas used in the routine analysis for ICP-MS with a collision cell. Xenon and methane both demonstrate the promising potential in removing interferences without lost much of analyte ions. The works also successfully illustrate how collision gases such as hydrogen, methane and xenon separate analyte signals from corresponding interferences.

Acknowledgements

The experiments are supported by the Ames Laboratory, U. S. Department of Energy, Office of Basic Energy Sciences, under Contract W-7405-Eng-82. The authors also thank Micromass Inc. for providing the mass spectrometer.

References

1. Hutton and Ebdon, *J. Anal. At. Spectrom.*, 1987, **2**, 595.
2. Beres, Thomas, Denoyer and *Brudeer, Spectroscopy, 1994, 9(1), 20.*
3. *Jiang, Houk, Stevens, Anal.* Chem., 1988, **60**, 1217.
4. Smith, Wiederin and Houk, Anal. Chem., 1991, **63**, 1458; Lam and Horlick, Spectrochemica Acta, 1990, **45B**, 1313; Hill, Ford and Ebdon, J. Anal. Atomic Spectrom., 1992, **7**,1157.
5. Rowan, J.T., *MS thesis.* Department of Chemistry, Iowa State University, Ames 1988; Rowan, J.T. and Houk, R.S., *Appl. Spectrosc.* 1989, **43**, 976.
6. Douglas, D. J. *Can J. Spectrosc.* 1989, **34**, 38.
7. Eiden G.C., Barinaga C.J. and Koppenaal D.W., *Rapid Commun. Mass Spectrum* 1997, **11**, 37; Gregory, C.E. Barinaga C.J., and Koppenaal D.W., *J. Anal. At. Spectrom.* 1996, **11**, 317
8. Turner P.J., Haines R.C. and Speakman J., *the 5th International Conference on Plasma Source Mass Spectrometry*, University of Durham, September 1996, 16-20.

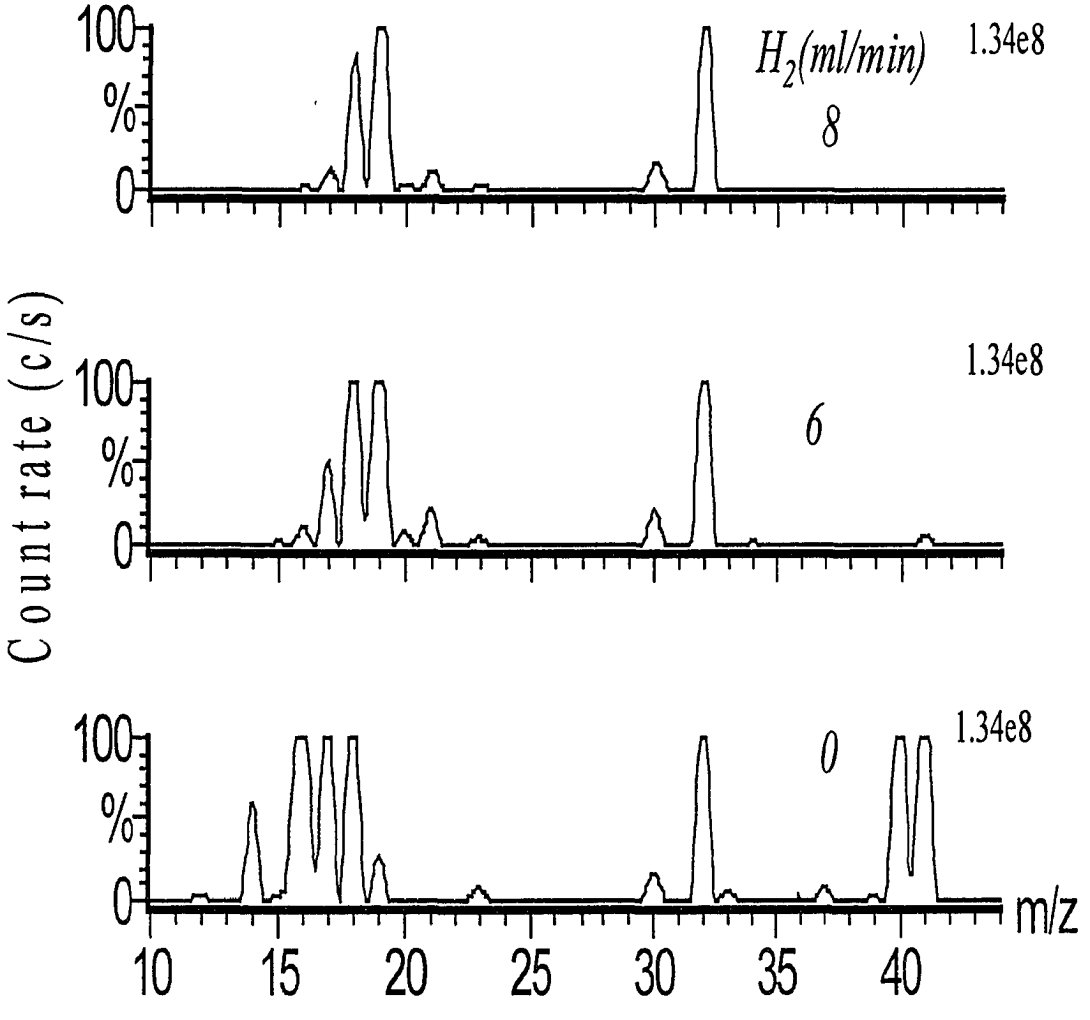

Fig. 1A. the spectra of 10 ppb Co in 1% HNO_3 solutions with increasing amount of hydrogen in the collision cell.

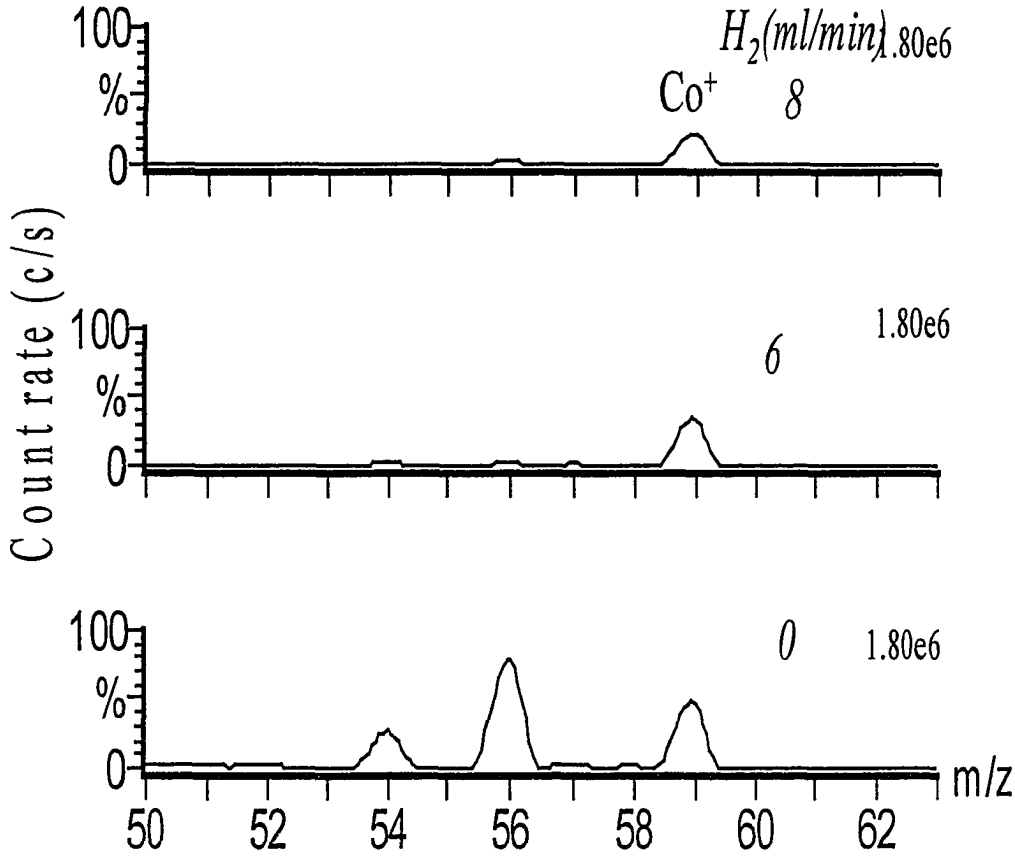

Fig. 1B. continued.

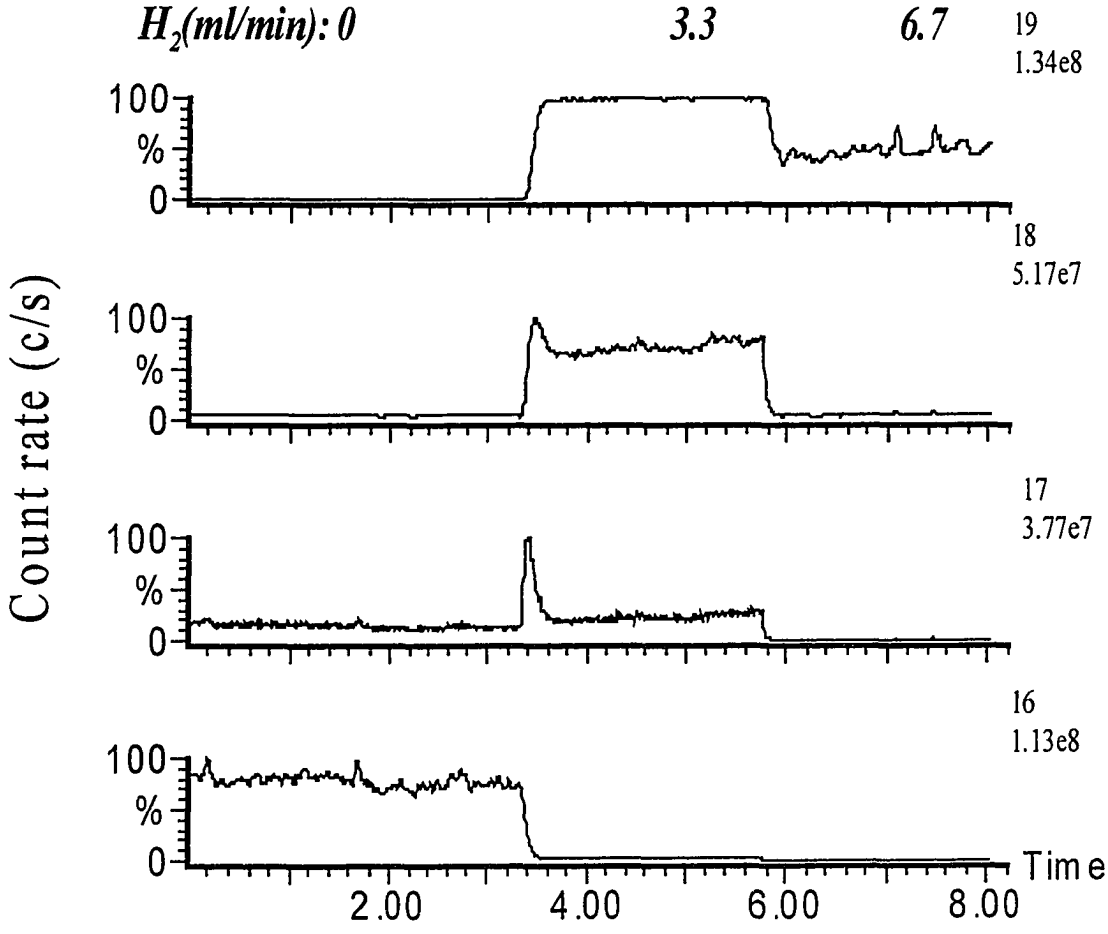

Fig. 2A. The intensity changes of some typical interferences with different amount of hydrogen in the cell.

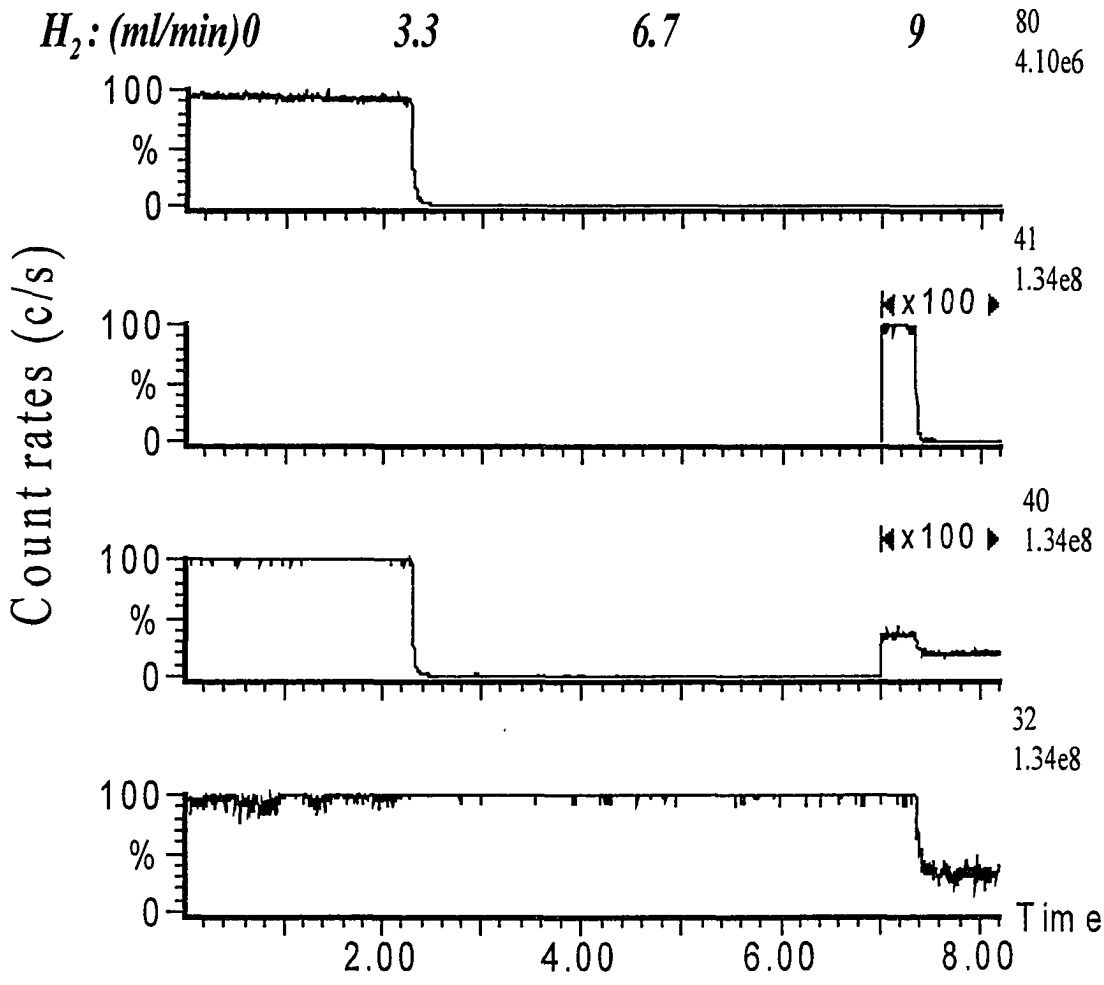

Fig. 2B. continued.

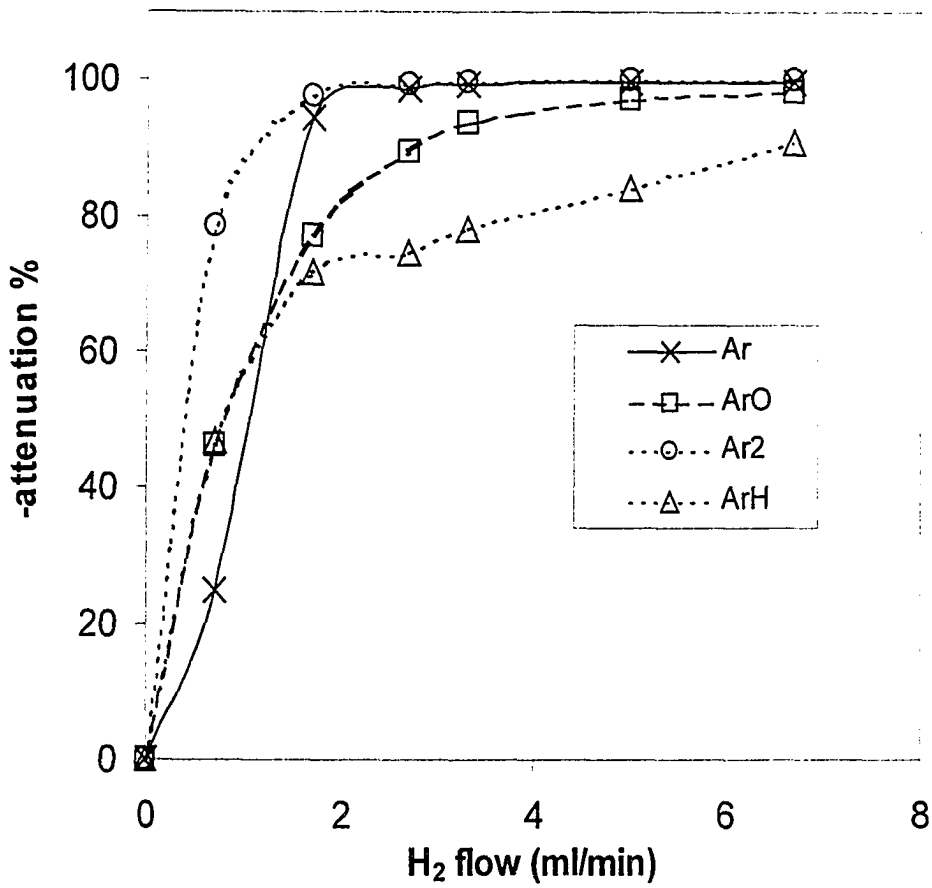

Fig. 3. The effect of hydrogen in the collision cell on the intensity of argon adducts at m/z = 40, 41, 56, 80 from a deionized water solution.

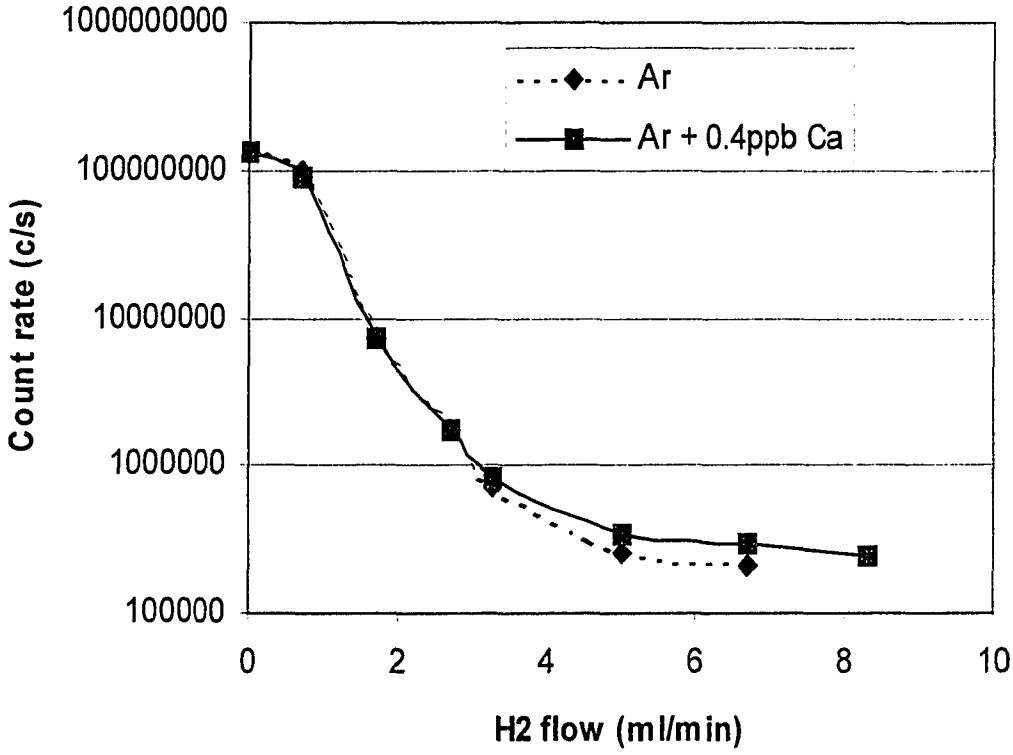

Fig. 4. The effect of hydrogen in the collision cell on the signal at m/z = 40 from a deionized water solution(dash curve) and a 0.4ppb Ca^+ in 1% HNO_3 solution (solid curve).

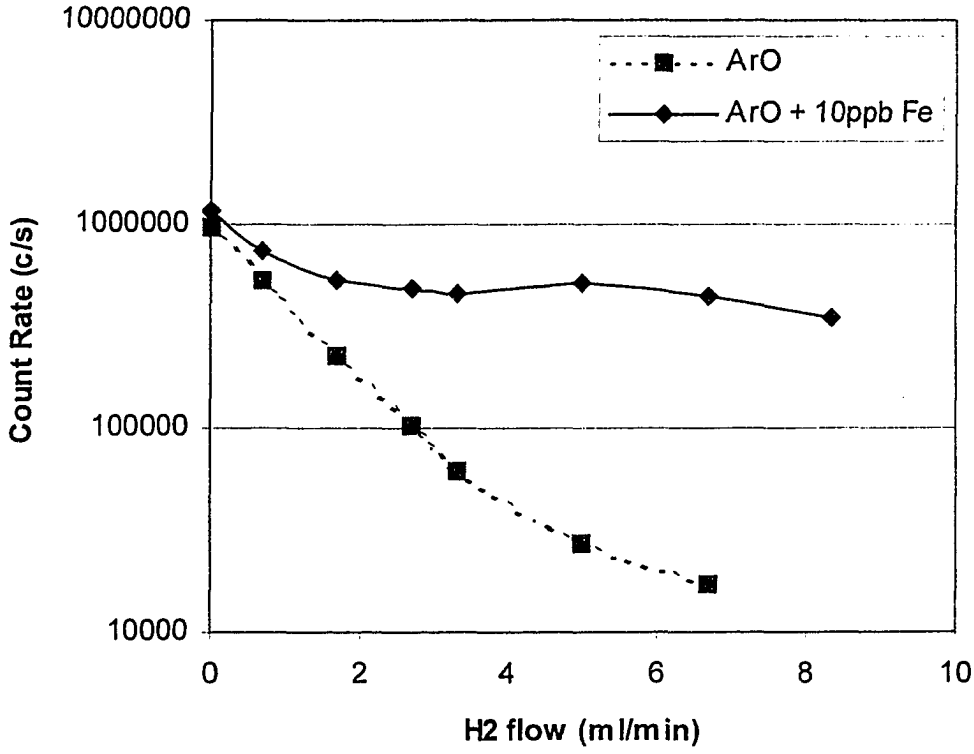

Fig. 5. The effect of hydrogen in the collision cell on the signal at m/z = 56 from a deionized water solution(dash curve) and a 10ppb Fe^{+} in 1% HNO_3 solution (solid curve).

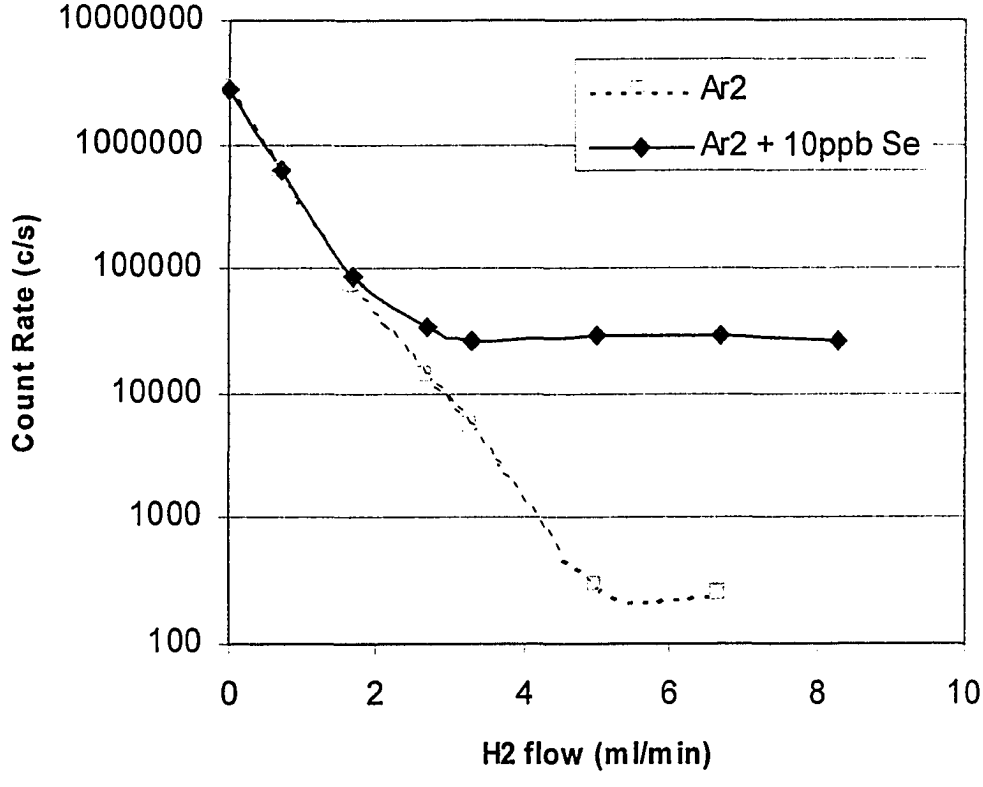

Fig. 6. The effect of hydrogen in the collision cell on the signal at m/z = 80 from a deionized water solution(dash curve) and a 10ppb Se^{+} in 1% HNO_3 solution (solid curve).

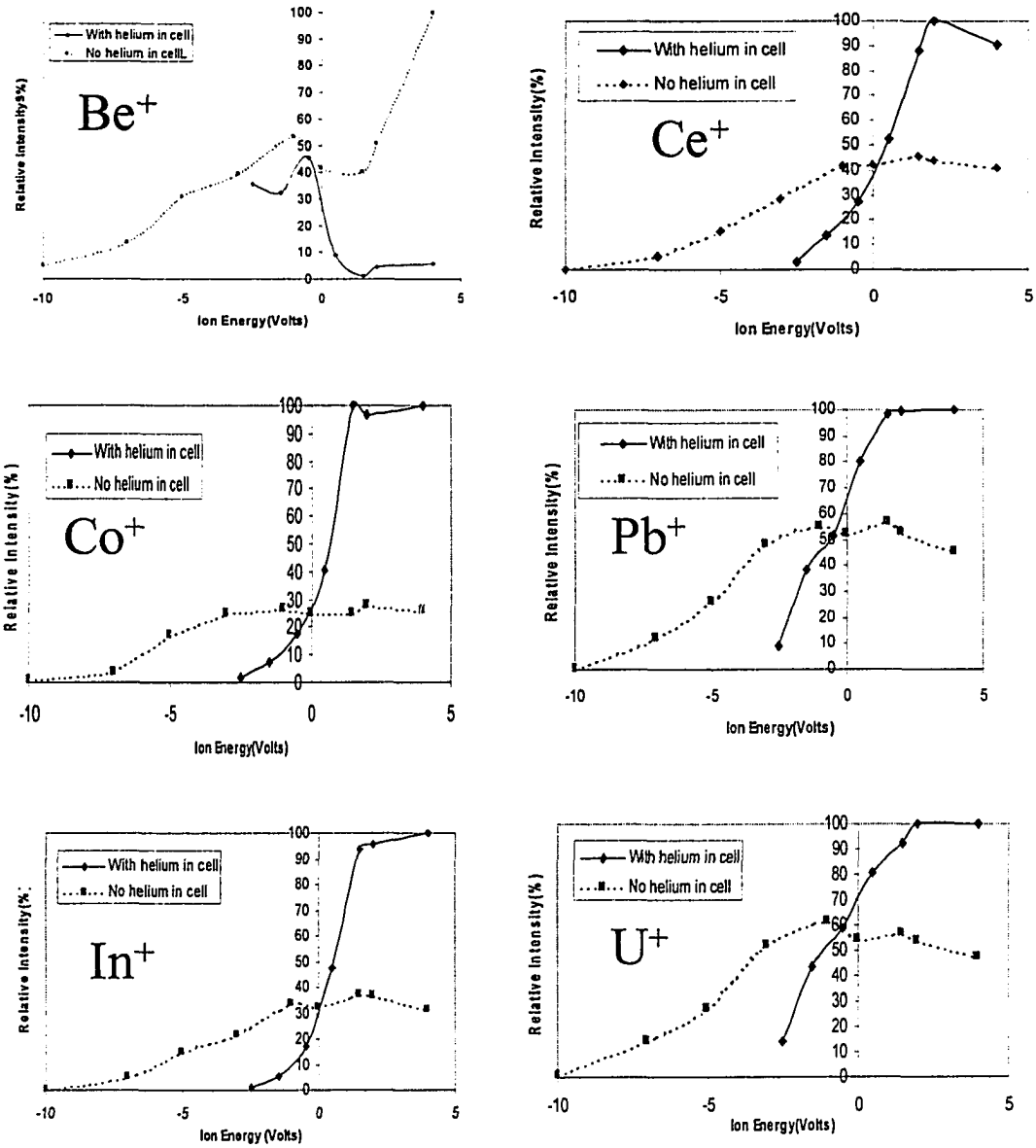

Fig. 7. The signal changes of several typical elements with ion energy with helium and without helium in the cell.

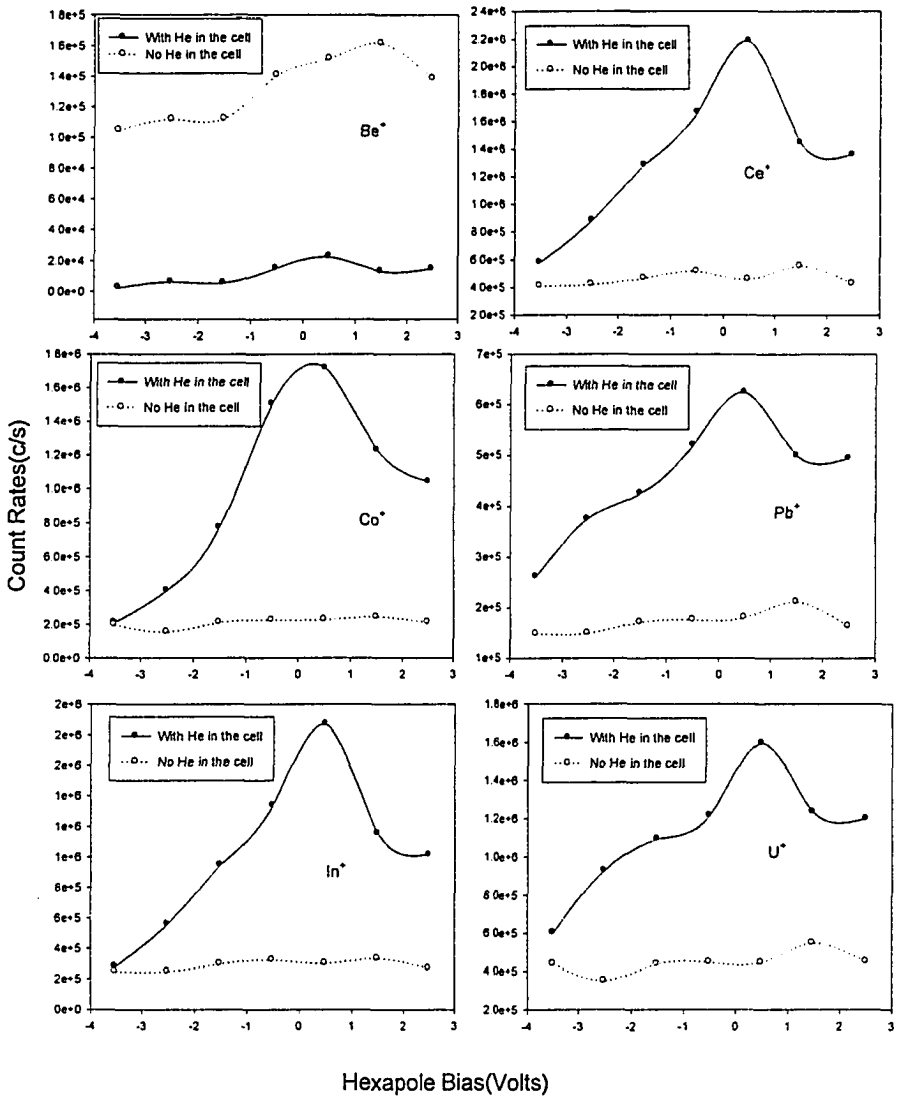

Fig. 8A The signal changes of several typical elements with hexapole bias with helium and without helium in the cell.

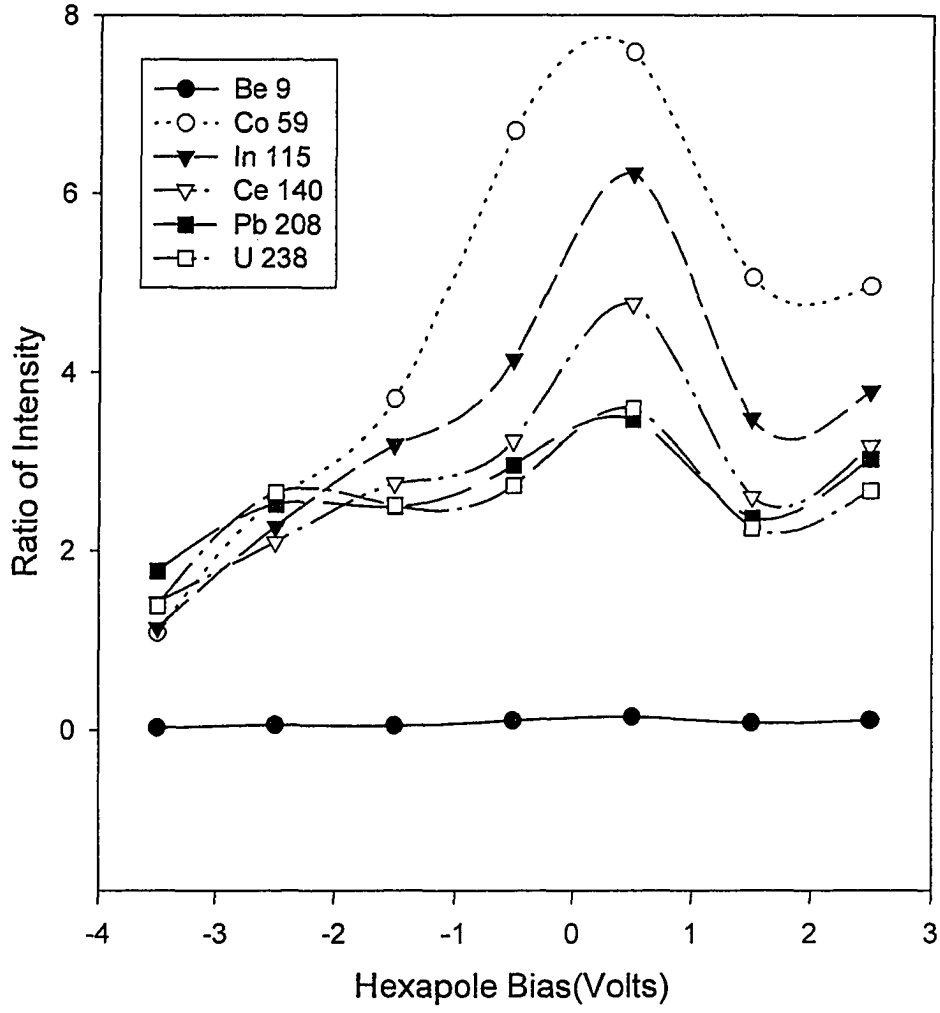

Fig. 8B. Effect of hexapole bias on the ration of the intensity with helium in the cell to the intensity with no helium in the cell.

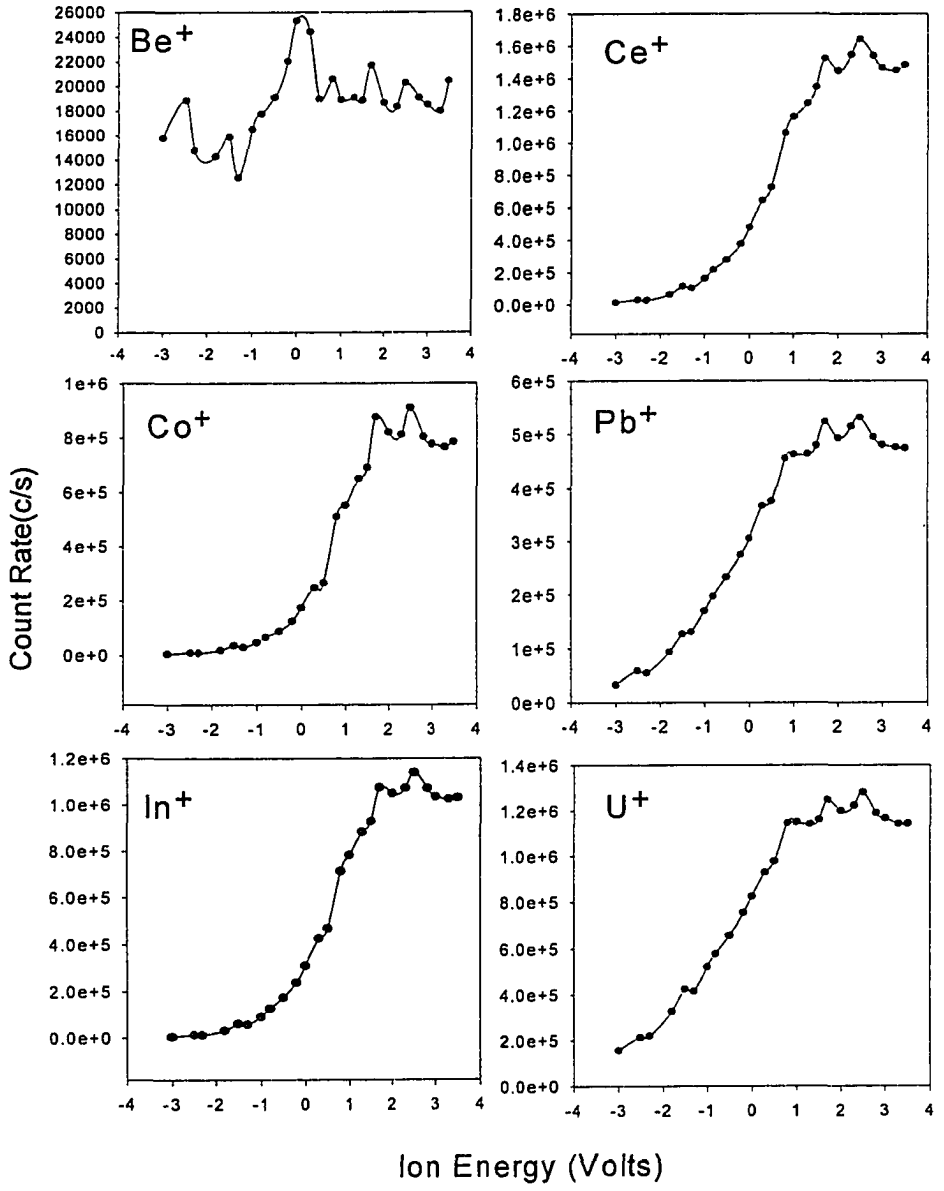

Fig. 9. The signal changes of several typical elements with ion energy with helium and Hydrogen in the cell.

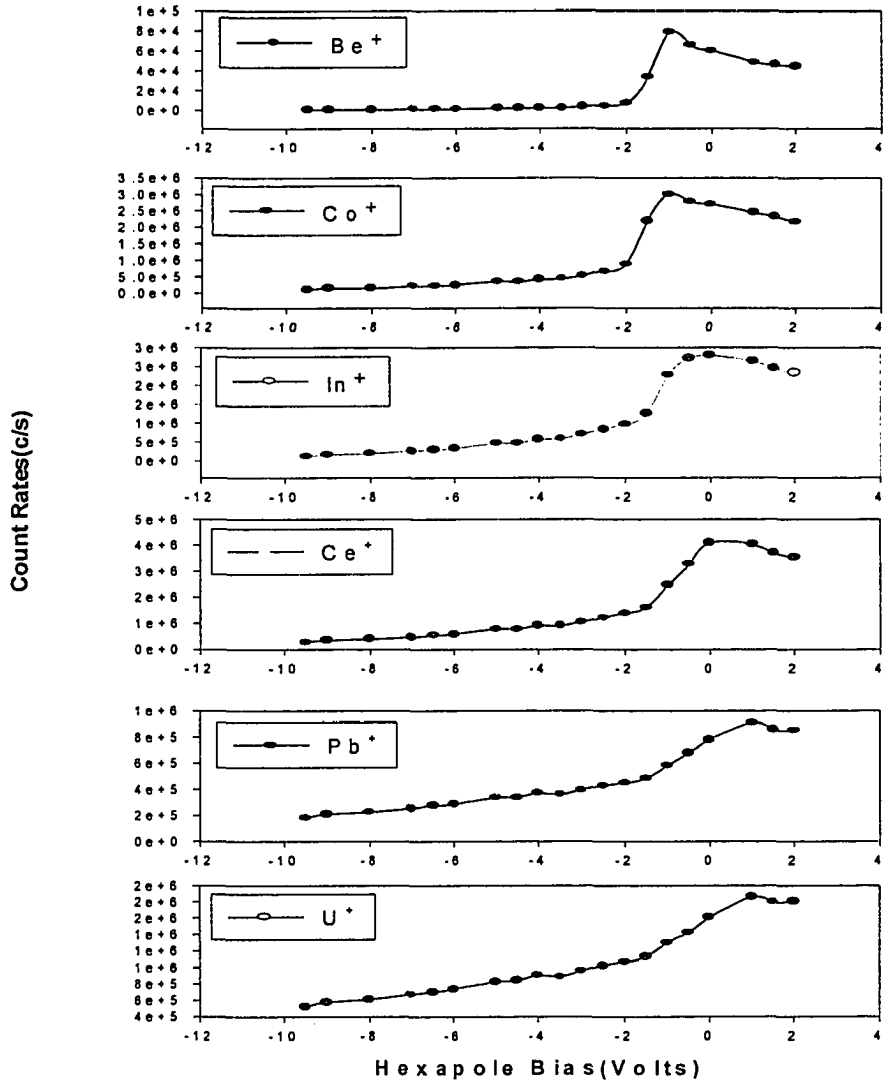

Fig. 10. The signal changes of several typical elements with hexapole bias with helium and Hydrogen in the cell.

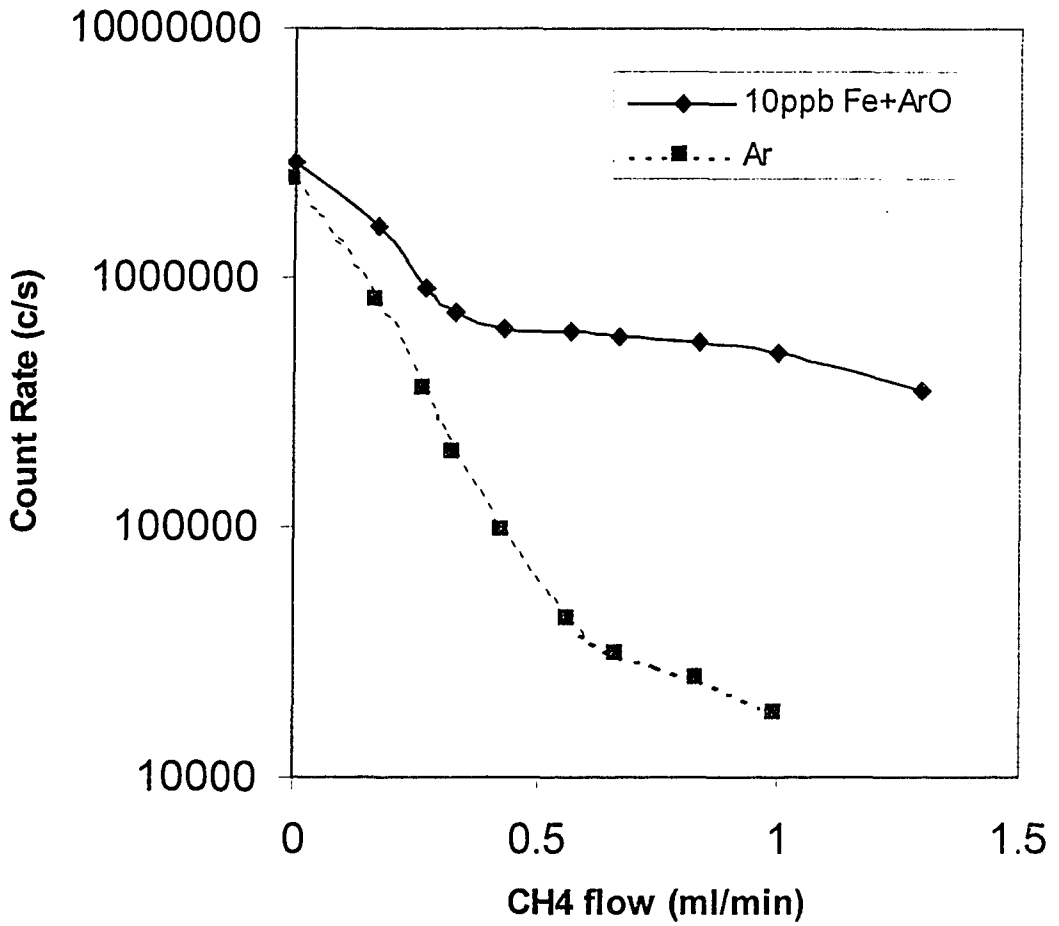

Fig. 11. The effect of methane in the collision cell on the signal at m/z = 56 from a deionized water solution(dash curve) and a 10ppb Fe^{+} in 1% HNO_3 solution (solid curve).

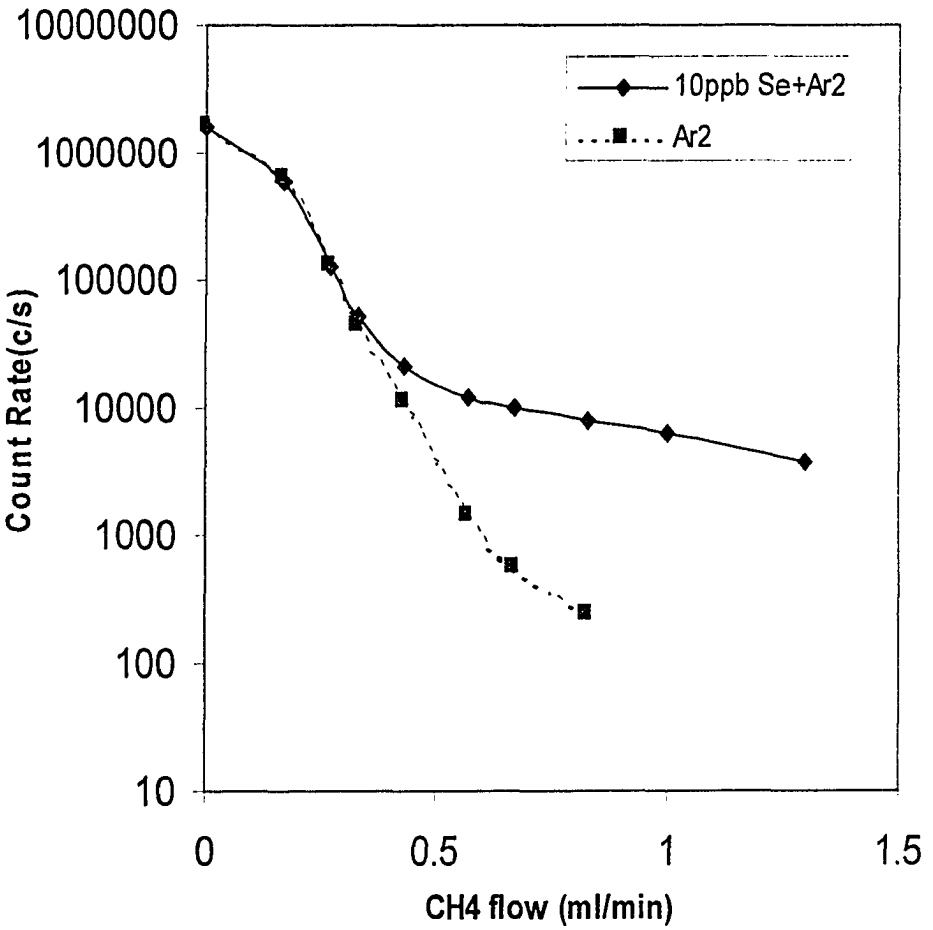

Fig. 12. The effect of methane in the collision cell on the signal at m/z = 80 from a deionized water solution(dash curve) and a 10ppb Se^{+} in 1% HNO_3 solution (solid curve).

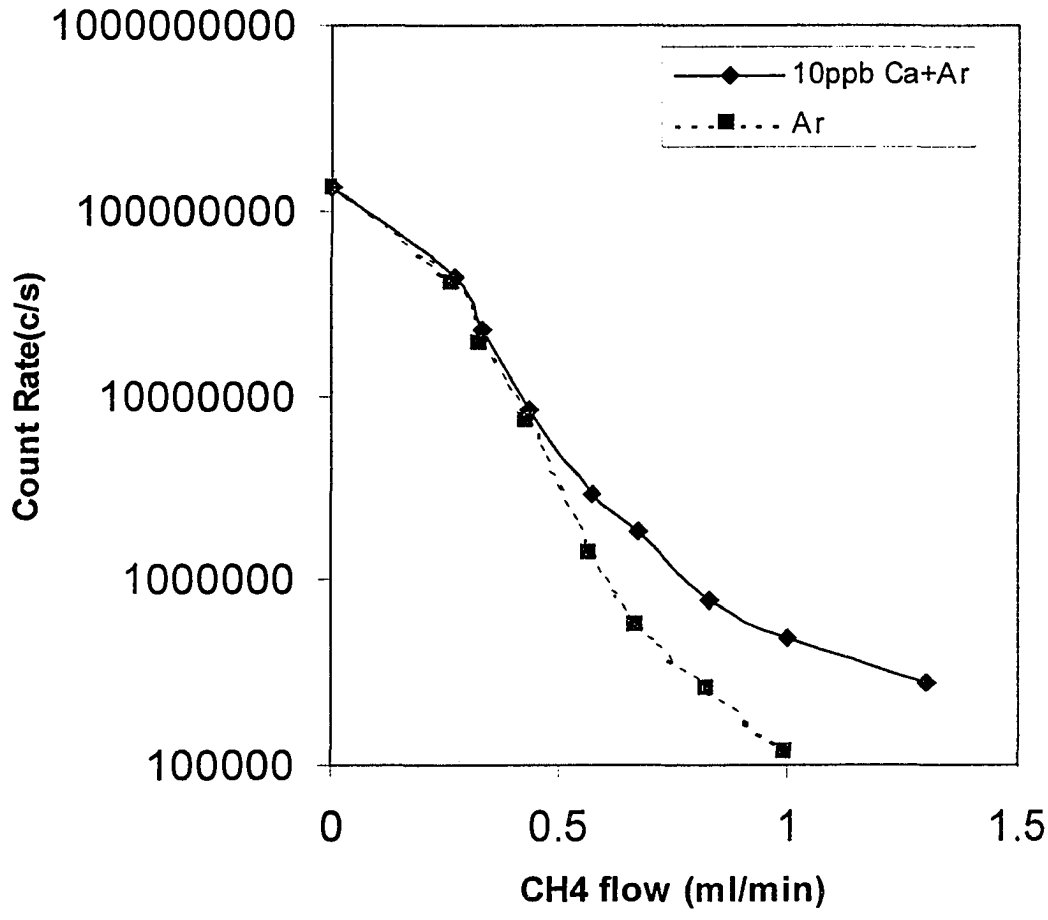

Fig. 13. The effect of methane in the collision cell on the signal at m/z = 40 from a deionized water solution(dash curve) and a 10ppb Ca^+ in 1% HNO_3 solution (solid curve).

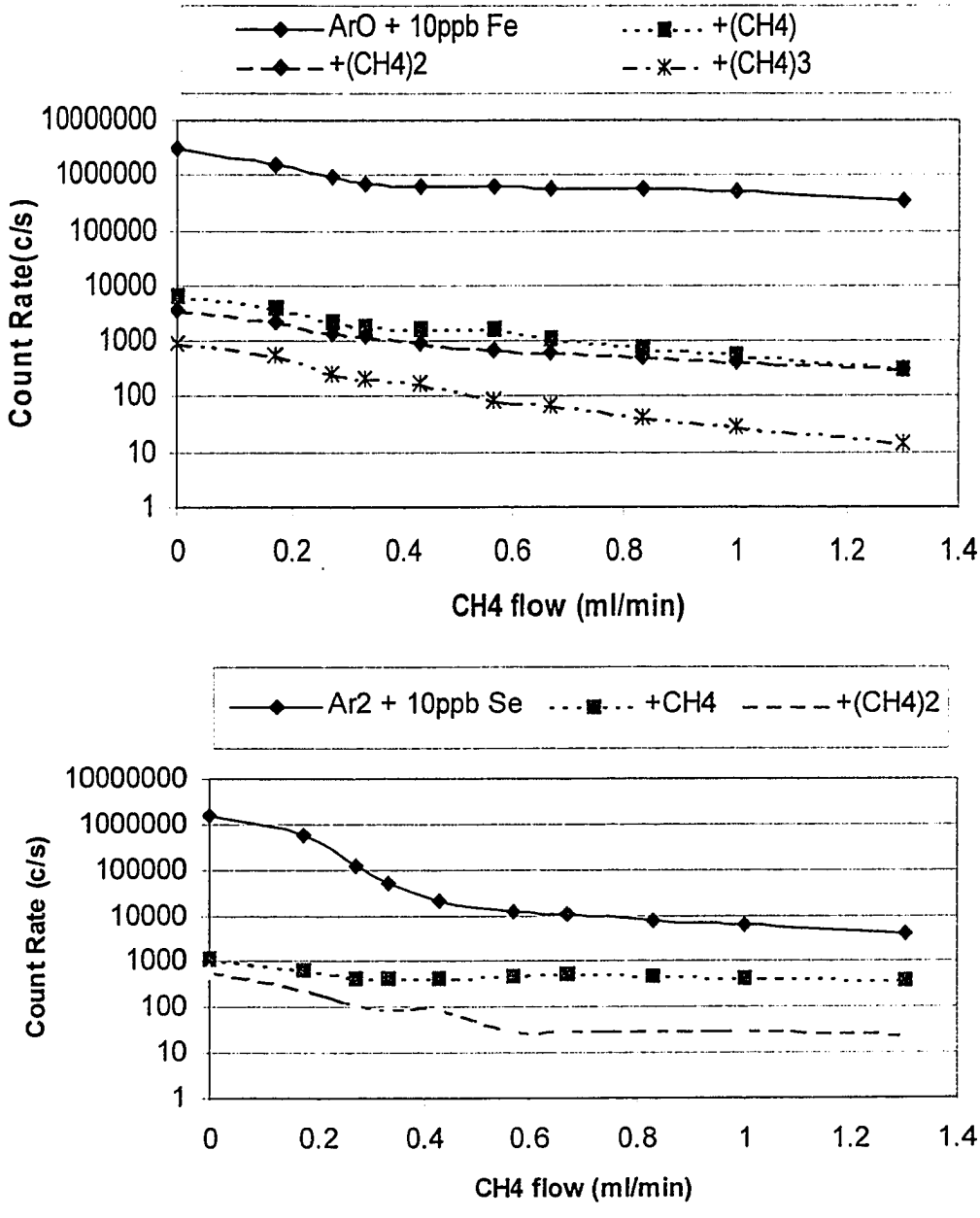

Fig. 14. The effect of methane in the collision cell on the formation of iron methane cluster(upper figure curve) and selinium methane clusters.

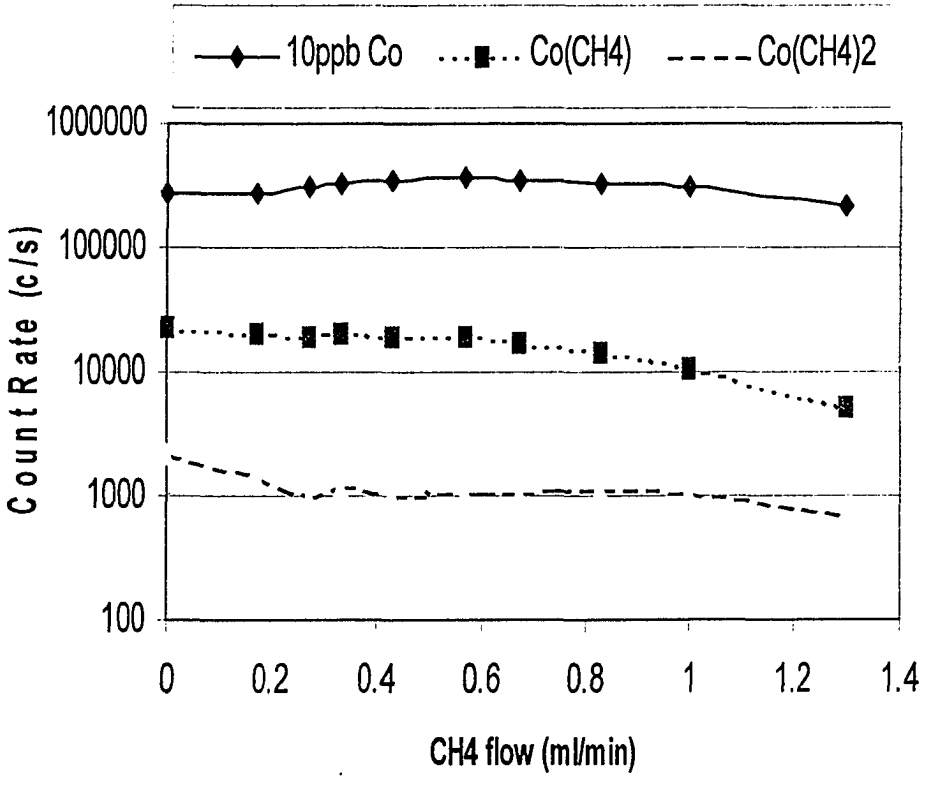

Fig. 15. The effect of methane in the collision cell on the methane cluster with Co^+ for a 10ppb Co^+ in 1% HNO_3 solution.

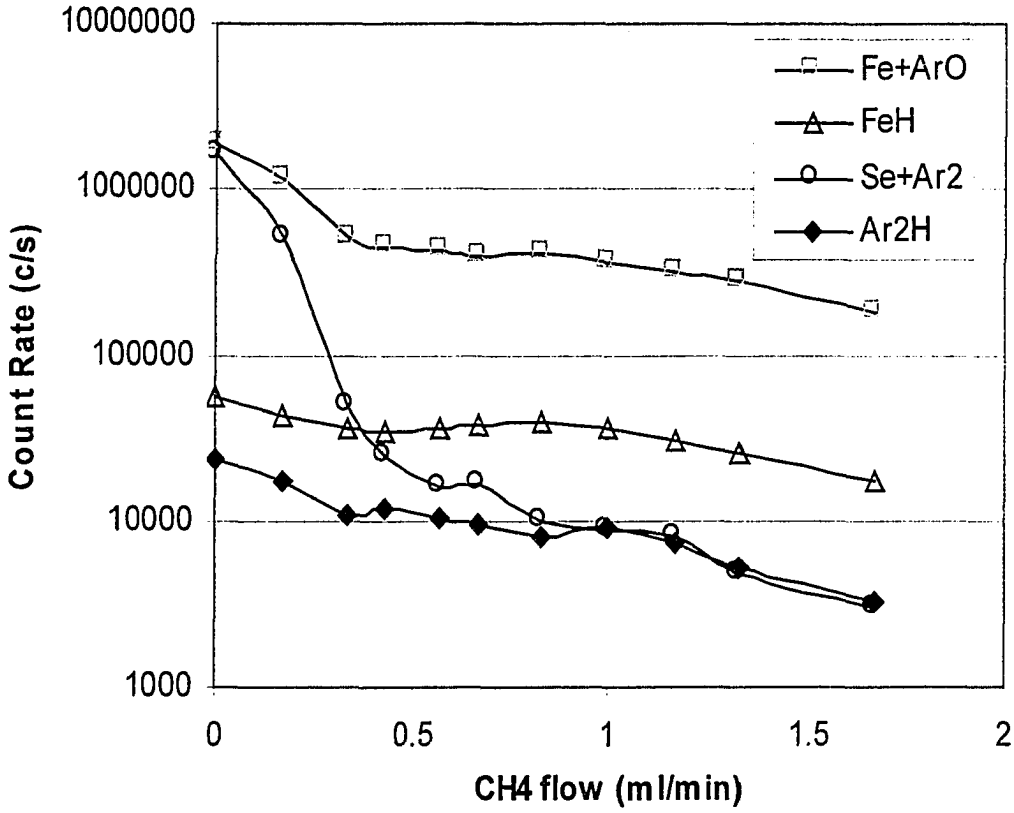

Fig. 16. The effect of methane in the collision cell on the hydride formation from a 10ppb $Fe^{+}$and Se^{+} in 1% HNO_3 solution.

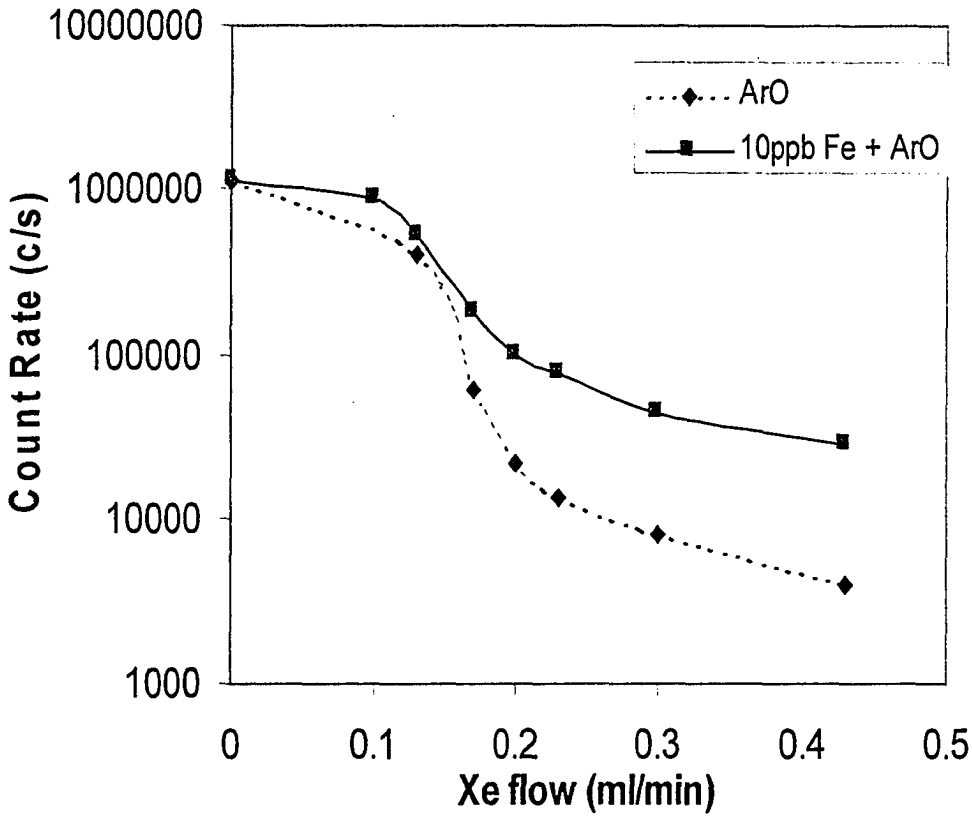

Fig. 17. The effect of xenon in the collision cell on the signal at m/z = 56 from a deionized water solution(dash curve) and a 10ppb Fe^{+} in 1% HNO_3 solution (solid curve).

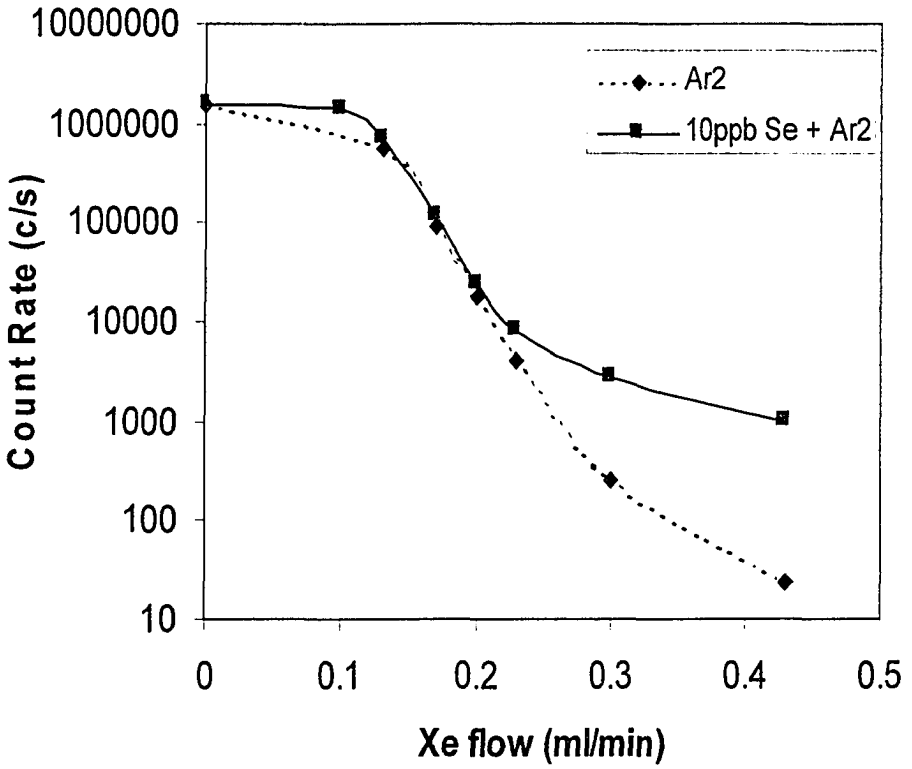

Fig. 18. The effect of xenon in the collision cell on the signal at m/z = 80 from a deionized water solution(dash curve) and a 10ppb Se^{+} in 1% HNO_3 solution (solid curve).

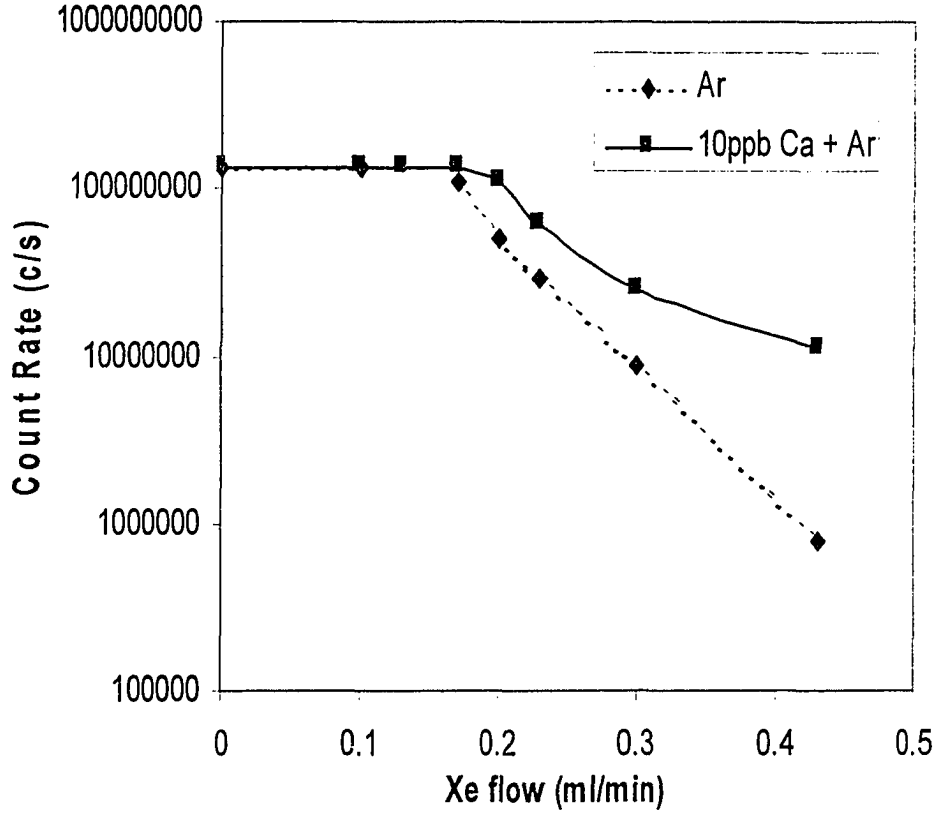

Fig. 19. The effect of xenon in the collision cell on the signal at m/z = 40 from a deionized water solution(dash curve) and a 10ppb Ca^+ in 1% HNO_3 solution (solid curve).

CHAPTER 6: ELEMENTAL SPECIATION IN HUMAN MILK BY SIZE EXCLUSION CHROMATOGRAPHY WITH DETECTION BY ICP-MS WITH A HEXAPOLE COLLISION CELL

A paper is to be submitted to J. Anal. At. Spectrom.

Jin Wang and R. S. Houk*

Abstract

In this chapter some applications of ICP-MS with a collision cell coupled with liquid chromatography in the measurement of metal ions in human milk are described. A microconcentric nebulizer (MCN) with a modified spray chamber and conventional desolvation was used to interface with ICP-MS with a hexapole collision cell (ICP-hQMS). A small amount of hydrogen was introduced into the collision cell to remove interferences from Ar_2^+, $ArCl^+$, ArC^+, Ar^+ etc. Helium in the collision cell is used to improve the ion transmission. Metal binding properties of two standard proteins were studied with ICP-hQMS. Elemental distribution in proteins in human milk was measured by separating milk with size exclusion chromatography and detecting with ICP-hQMS. The method required minimal sample preparation and allowed routine analysis of milk sample, providing the distribution of some typical elements among biomolecular compounds within 20 min.

Introduction

There are a number of vital regulatory, storage, catalytic and transport functions of metalloproteins in humans. Essential elements like Fe, Cu and Zn bound in various proteins and the oxidation states of these elements are of great concern.[1,2] The adsorption of trace elements can be affected by minerals/trace elements, for examples, calcium has a direct inhibitory effect on iron adsorption, addition of calcium to human milk had a marked negative effect on iron adsorption. Also the absorption of trace elements can be affected by dietary protein, for example, a protein component of meat, the so-called meat factor, enhances the adsorption of non-heme iron.

* Corresponding author

Milk is an important biological system.[3] The basic components of milk are water, fatty and nonfat fractions. The water part contains caseins, α-lactalbumin, immunoglobins, serum albumin and low molecular weight substances. Milk should be considered in relation to the colostral, transitional, and mature stages. Milk is comparable to blood in its trace element profiles. As regards early childhood, milk is no doubt the most important food since it is the only source of nutrition during the first months of a baby's life. It is therefore essential that all macronutrients (protein and lipids) in general and all micronutrients (vitamins and elements) in particular are present in milk. It is useful to monitor the supply of trace elements to the baby, especially in the assessment of chromium and manganese.[4] The bioavailability of trace elements for formula-fed and breast-fed children is closely related with its molecular information. The elemental speciation in breast milk can provide important information about elemental bioavailability[5]. The determination of trace elements in milk has stimulated increasing interest and represents an important area in food science and human nutrition.

Many of these elements are difficult to measure by conventional ICP-MS due to the polyatomic ion interferences. A collision cell incorporated in ICP-MS can reduce or eliminate many such interferences. Thus it is possible to measure some difficult elements like Fe, Se, Cr, Ca that suffer from argon related interference with this device. Combined with chromatographic separation technique ICP-hQMS provides a powerful tool in the identification and quantification of species containing metals. Here some applications of collision cell ICP-MS in the study of elemental speciation in human milk were explored. The method can be used to detect the chemical forms of many elements of primary importance, such as Fe, Se, Zn, etc. in human milk.

Experimental Section

Considerations in interfacing HPLC with ICP-MS include: 1) mobile phase: low dissolved solute and low organic content in the mobile phase with isocratic elution is preferred to reduce signal suppression, avoid interface clogging and obtain stable signal; 2) Column: smaller diameter (1- 4.6 mm i.d.) column with appropriate length is chosen, so its flow rate is compatible with nebulizer and ICP-MS; 3) connection: the connecting tubing is

kept small and short to minimize extracolumn volume; this is mainly important for the connection before the nebulizer 4) spray chamber: spray chamber with low volume can reduce washout time and extracolumn dead volume; 5) solvent load into ICP: desolvation can remove solvent and produce dry aerosol.

An Acuflow series III bioclean pump (Fisher Scientific) is used. A Rheodyne PEEK Model 9010 injector with a 5-μl sample injection loop was used. Size exclusion chromatographic separation was performed on a *4.6mm* ID*x 30* cm TSK-GEL Super 2000 (*Tosohaas, PA)* with an exclusion limit of 150 kDa and effective separation range for globular protein between 5 kDa and 120 kDa. The eluent flow rate was 0.35 ml/min. The eluent is *50 m*M aqueous tris/HCl containing 0.05% NaN_3 at pH = 7. In the case of adjusting pH of buffer solution with HCl, the electrode of pH meter should not put into the bulk of buffer solution. when HCl was added each time, one aliquot of buffer solution was transferred to another bottle, and pH was measured, then the aliquot was discarded.

Human milk sample was defatted in a centrifuge at 3000g at 5°C for 30min. The supernatant was filtered through a 0.45μm disposable syringe filter before injection. This was the only sample preparation procedure necessary.

A microconcentric nebulizer (MCN) with a modified spray chamber and conventional desolvation (heater 140°C and condenser 0°C) was used to interface HPLC with a Platform ICP-hQMS (Micromass Ltd.). A small amount of hydrogen was introduced into the hexapole collision cell to remove interferences from $ArAr^+$, $ArCl^+$, ArC^+, Ar^+ etc. Helium in the collision cell is used to improve the ion transmission.[6] Typical operating parameters of ICP-hQMS are listed in Table 1. Other details about the HPLC setup (i.e., tubing connections, inline filter, injection valve, etc.) and MCN desolvation refers to references 7.

Results and Discussions

The ICP-hQMS was first tuned with 10ppb metal standard solution delivered by a peristalic pump at the same sample uptake rate as the SEC flow rate. The setting of the hexapole collision gas flow followed normal ICP-MS tuning procedure (adjusting torch position, nebulizer gas, oxide and doubly charged level, à etc.): helium flow rate was set to

TABLE 1 Typical operating parameters of ICP-hQMS

Gases			Analyzer			Torch		
Cool	14.00	L/min	Cone	590	V	X posn	0.5	
Interm.	1.00	L/min	Hex Exit	330	V	Y posn	0.27	
Neb1.	0.85	L/min	Hex Bias	-2.5	V	Z posn	0.1	
		L/min	LM Res	20.1	V	Power	1300	W
He	4.33	ml/min	HM Res	20.1	V			
H2	2.0	ml/min	Ion Energy	1	V			
SC Temp	4	°C	Multiplier	502	V			

obtain maximum sensitivity at m/z = 208 for 10 ppb Pb. An improvement in resolution can also be observed. Introducing 10ppb Co in deionized water and adjusting H_2 flow rate to eliminate $^{40}Ar^+$ and $^{41}ArH^+$ and maximize the signal ratio of ^{59}Co/(total ions at m/z =56). The hexapole bias was adjusted to minimize background between m/z 50 to 70. After ICP-hQMS was optimized, the size exclusion column outlet is connected to the MCN, and the chromatograms are collected.

Fig.1 shows Fe^+ and Mn^+ chromatograms from human milk. Most of the interferences from $^{40}Ar^{16}O^+$ and $^{40}Ar^{14}N^1H^+$ are removed by using hydrogen collision gas, thus $^{56}Fe^+$ and $^{55}Mn^+$ can be measured. It can be seen that iron is distributed in several protein fractions. Most iron preferably binds to low molecular weight protein s around 14 kDa. There is a small amount of iron in the high molecular weight fractions. The first peak may be related to caseins, which elute within the column dead volume since they are present in milk in a micellar form.[8] The second peak may represent Fe associated with lacalbumin. Manganese is distributed among low molecular weight proteins (14 kDa) and small molecules with much more Mn in small molecules.

Fig. 2 shows the chromatograms for Se^+ in human milk measured with two selenium isotopes (^{80}Se and ^{82}Se). Since hydrogen can remove most of the $^{40}Ar^{40}Ar^+$ in the collision

cell, ^{80}Se and/or ^{82}Se can be used to monitor the selenium signal There is only one peak eluted quite late in the Se^+ chromatogram from selenium in low molecular weight components. Bromine also elutes at the same retention time (Fig.5); Bromine hydride ($^1H^{81}Br^+$) accounts for almost half of the chromatographic peak at m/z = 82.

Fig.3 shows the chromatograms of Ni^+, Cu^+ and Zn^+ in human milk. The chromatograms measured with two isotopes of nickel show that Ni is bound to the proteins with a molecular weight of 14 kDa, although iron has a minor isotope at m/z = 58, the $^{60}Ni^+$ chromatogram show a peak with the same retention time with ^{58}Ni chromatogram and the ratio of ^{58}Ni peak to ^{60}Ni peak is close to the natural abundance ratio. Thus this peak mainly comes from nickel. Zinc is found in several protein fractions with the molecular weight around 150 kDa and small molecular weight protein. Most of the copper is found in larger proteins with a molecular weight around 150 kDa, only a small amount of copper exists in small protein fraction.

Fig. 4 shows chromatograms for Ca and Mg in human milk. Two minor isotopes were used in the measurement of calcium, since there is still substantial background at m/z = 40. The chromatograms show that calcium not only exists in small molecules but also in low molecular weight protein (39 kDa). In contrast, magnesium does not bind to this Ca-binding protein at 39 kDa but is present in ionic form or in small molecules in milk.

Fig. 5 shows chromatograms for the nonmetals S, P and Br in human milk. Measurement of nonmetallic element is also important to help identify the metal binding sites in proteins. The chromatograms show that sulfur is in the high molecular weight protein (>150 kDa) and lower molecular weight protein (36 kDa). Phosphorus is mainly in low molecular weight fraction 8 kDa. Bromine is found only in the low molecular weight fractions (6 kDa)

Fig. 6 shows the chromatograms of Cr and Mo in human milk. Polyatomic interferences $^{40}Ar^{12}C^+$ was reduced by using collision gas H_2, thus major Cr isotope ($^{52}Cr^+$) can be used. There is chromium in the high molecular weight protein (>150 kDa) and lower molecular weight protein (14 kDa). Molybdenum is also found in the high molecular weight protein (150 kDa) and low molecular weight protein (8 kDa).

Fig. 7 shows the chromatograms of U and Th spiked into human milk. Most of the

thorium binds to high molecular weight proteins (presumably caseins), only a small amount binds to low molecular weight substances (these may include small proteins, peptides, amino acids, lactose, citrates, and mineral salts). In contrast, most of the uranium UO_2^{2+} binds to low molecular weight substances, only a small amount of uranium binds to high molecular weight proteins.

Conclusion

ICP-MS with a hexapole collision cell has been successfully coupled with HPLC for trace elemental detection. A collision cell effectively removes argon interferences; thus some important elements like selenium and iron suffering from argon related interferences could be measured. Size exclusion chromatography – ICP-hQMS is proved to be a very effective tool in the study of trace elemental distribution in protein. The results reveal that a lot of elements are in low molecular weight proteins in human milks.

Acknowledgements

The experiments are supported by the Ames Laboratory, U. S. Department of Energy, Office of Basic Energy Sciences, under Contract W-7405-Eng-82. The authors also thank Micromass inc. for providing the mass spectrometer and Tosohaas for donating the column.

References

1. Sergio Caroli Ed, *Element Speciation in Bioinorganic Chemistry.*, Chemical Analysis Series. Vol 135, John Wiley & Sons, Inc. 1996.
2. M.J. Kendrick, M.T. May, M.J. Plishka and K.D.Robinson. *Metals in Biological Systems.* Ellis Horwood 1992
3. P. Bratter, B.gercken, U.Rosick, and A.Tomiak, in *Trace Elemental Analytical Chemistry in Medicine and Biology*, (P.bratter and P.Schramel, eds) Vol 5, 133. De Gruyter, Berlin and New York, 1988.
4. E. J.Underwood, *Trace Elements in human and animal nutrition* 4th ed. Academic Press, New York 1977.

5. B. L. Odell, *Fed. Proc.Fed.Am.Soc.Exp.Biol.* 1983,42 1714; *Nutr. Rev.* 1984, 42, 301; Ramon M. Barnes, *Fresenius J Anal Chem.,* 1996, **355**, 433.

6. P. J. Turner, R.C. Haines, and J. Speakman, *5th International Conference on Plasma Source Mass Spectrometry*, University of Durham, UK, 1996, **September;** N. Lynaugh, P.J. Turner, ; J. Speakman, R.C. Haines, and K.R. Compson, *ICP Information Newsletter,* 1997 **23**, 319

7. J. Wang ; R.S. Houk, D.R. Dreessen, D. Wiederin, *Journal of the American Chemical Society.* 1998, Volume 120, No. 23 5793-5799.

8. A.T. Andrews, M.D.Taylor and A.J. Owen, *J. of Chromatography*, 1985, **348**, 177.

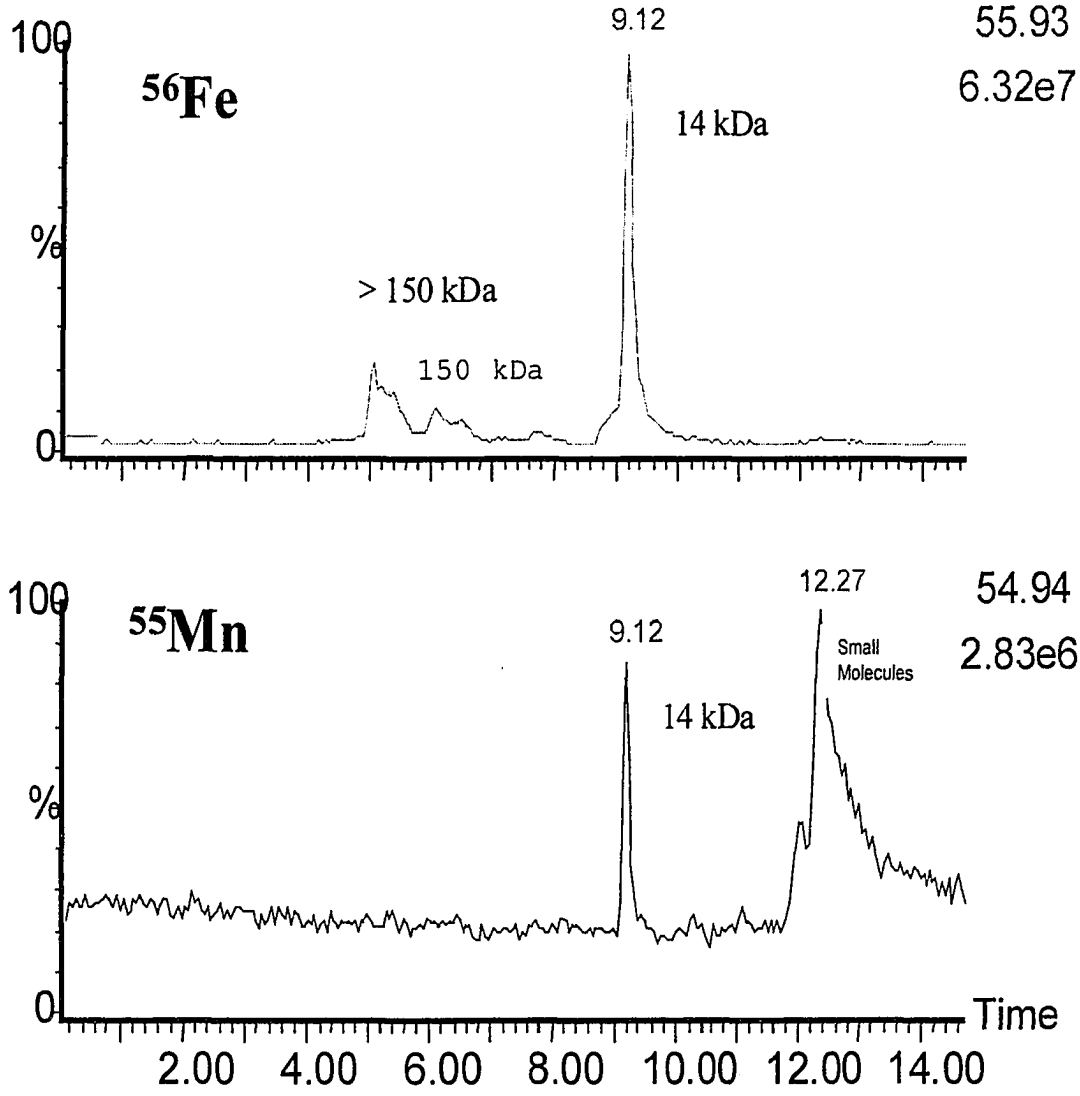

Fig. 1. Chromatograms of Mn and Fe in human milk with the detection by ICP-hQMS.

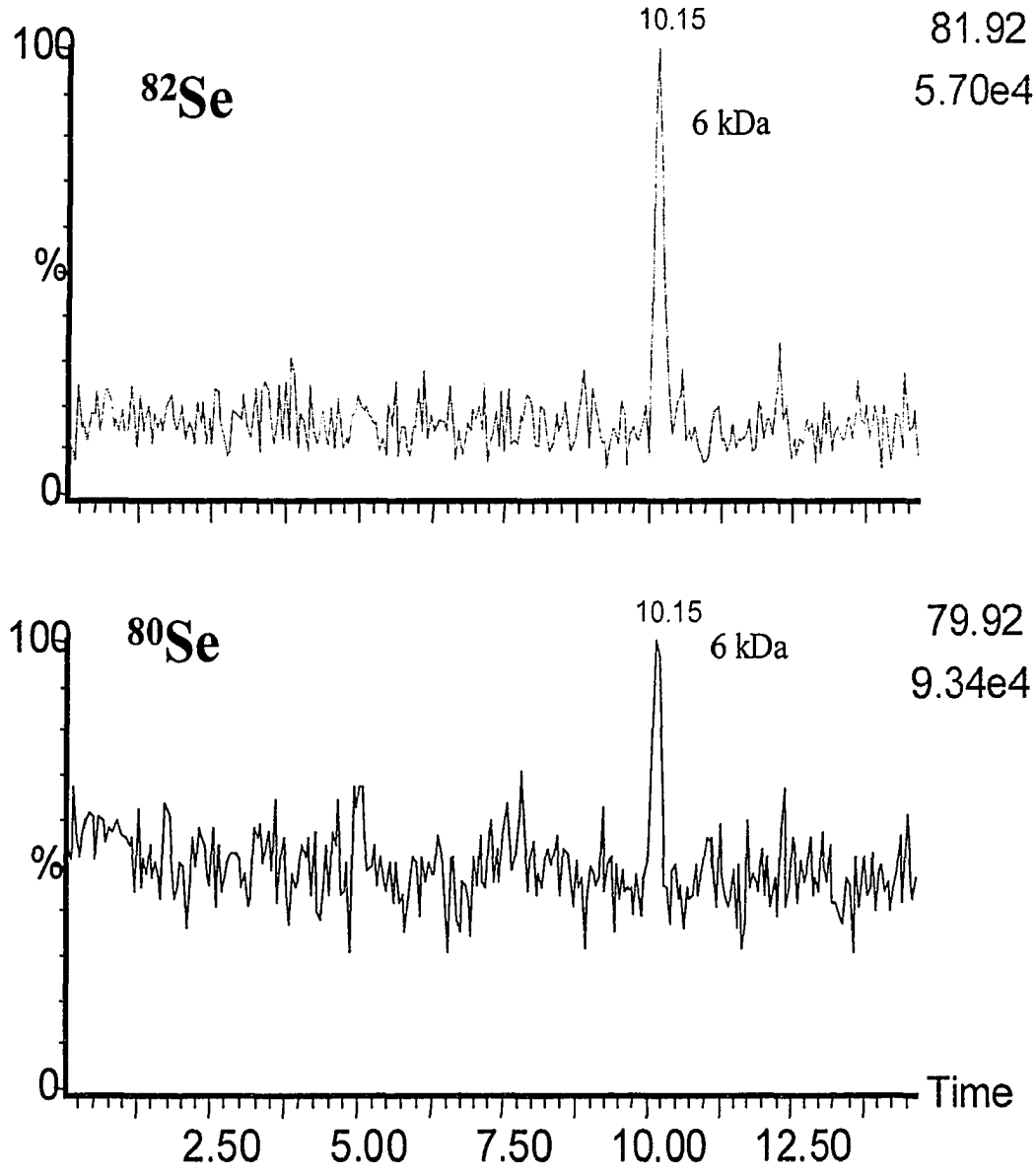

Fig. 2. Chromatograms of Se in human milk with the detection by ICP-hQMS.

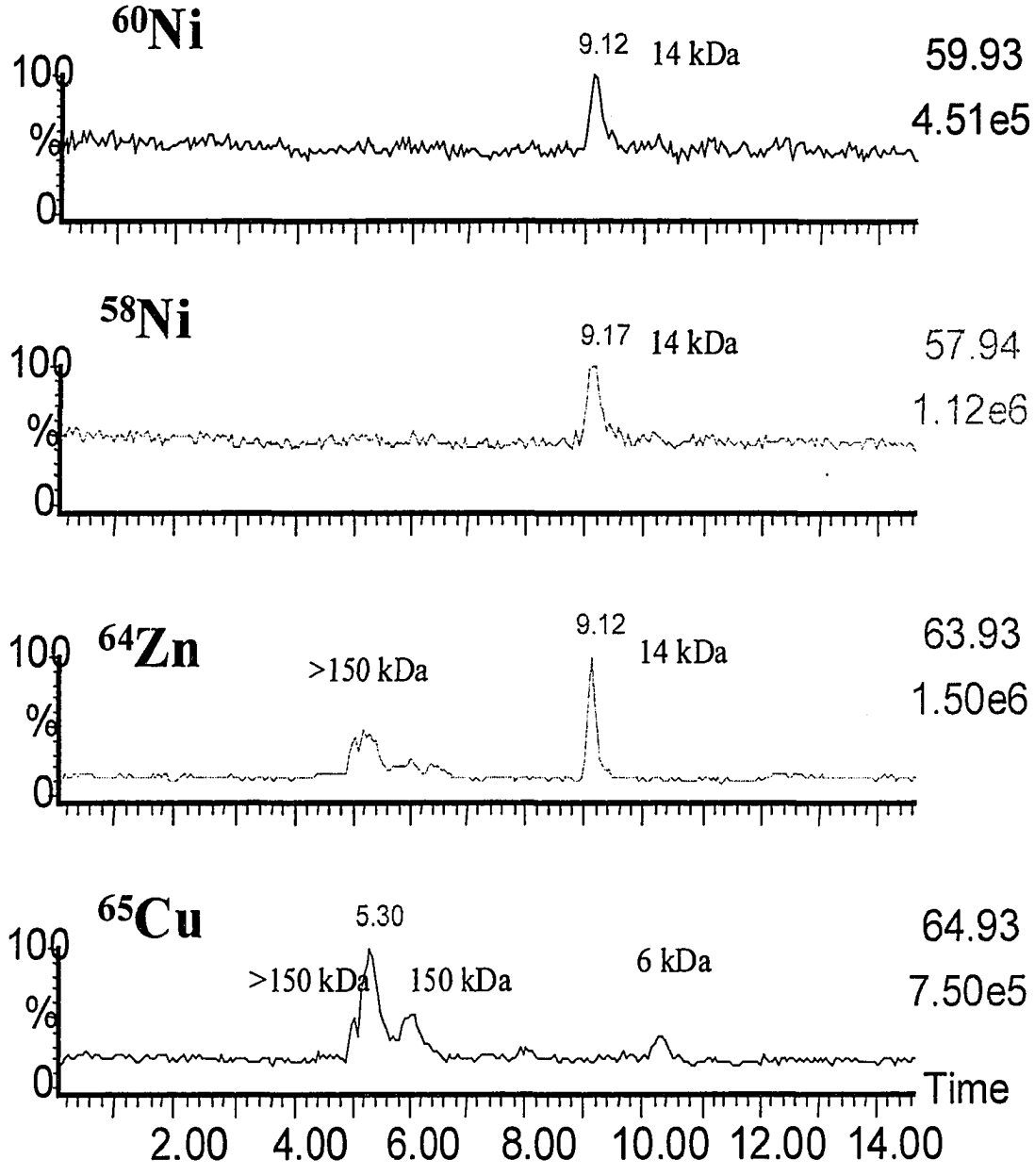

Fig. 3. Chromatograms of Ni, Zn and Cu in human milk with the detection by ICP-hQMS.

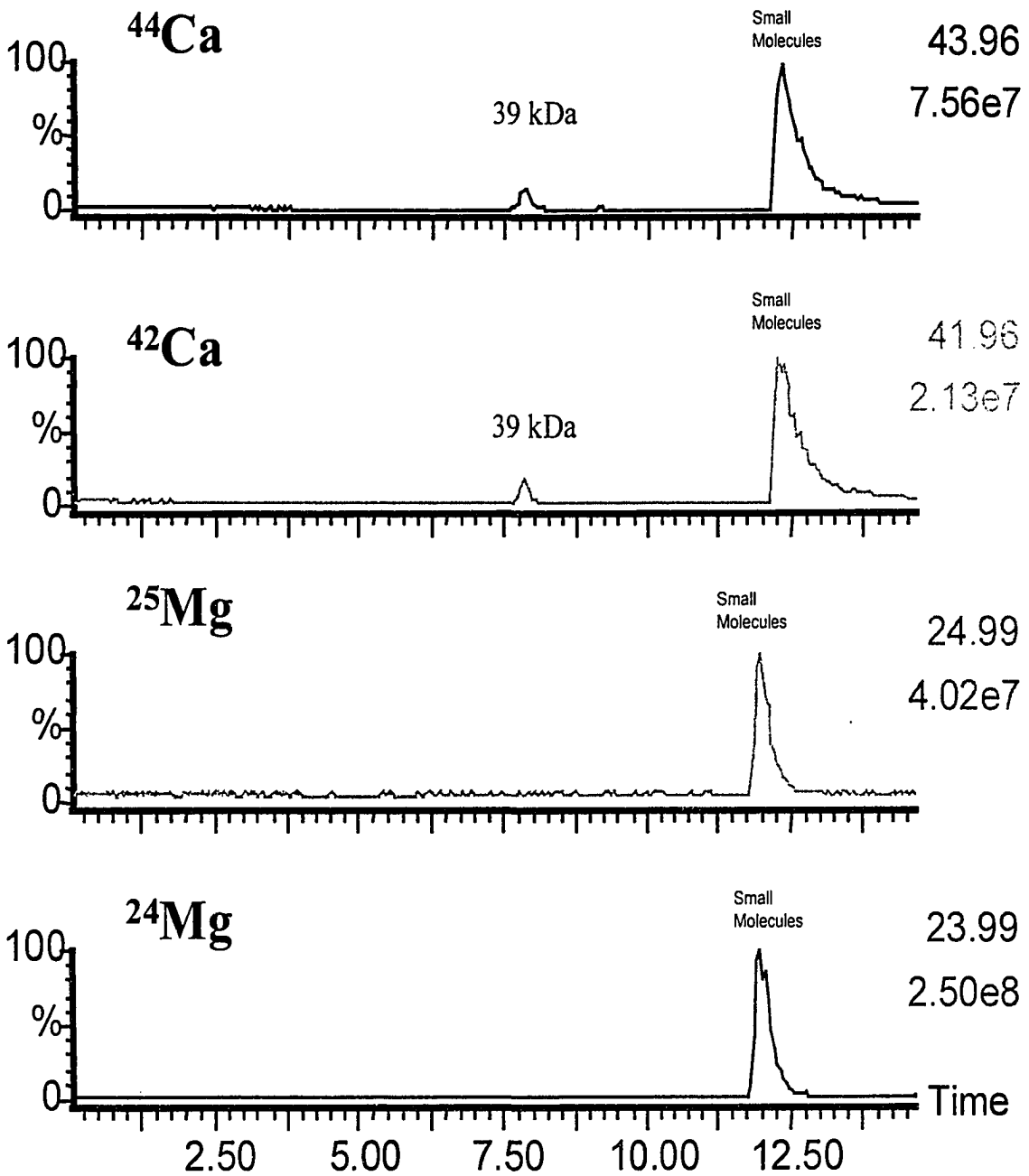

Fig. 4. Chromatograms of Ca and Mg in human milk with the detection by ICP-hQMS.

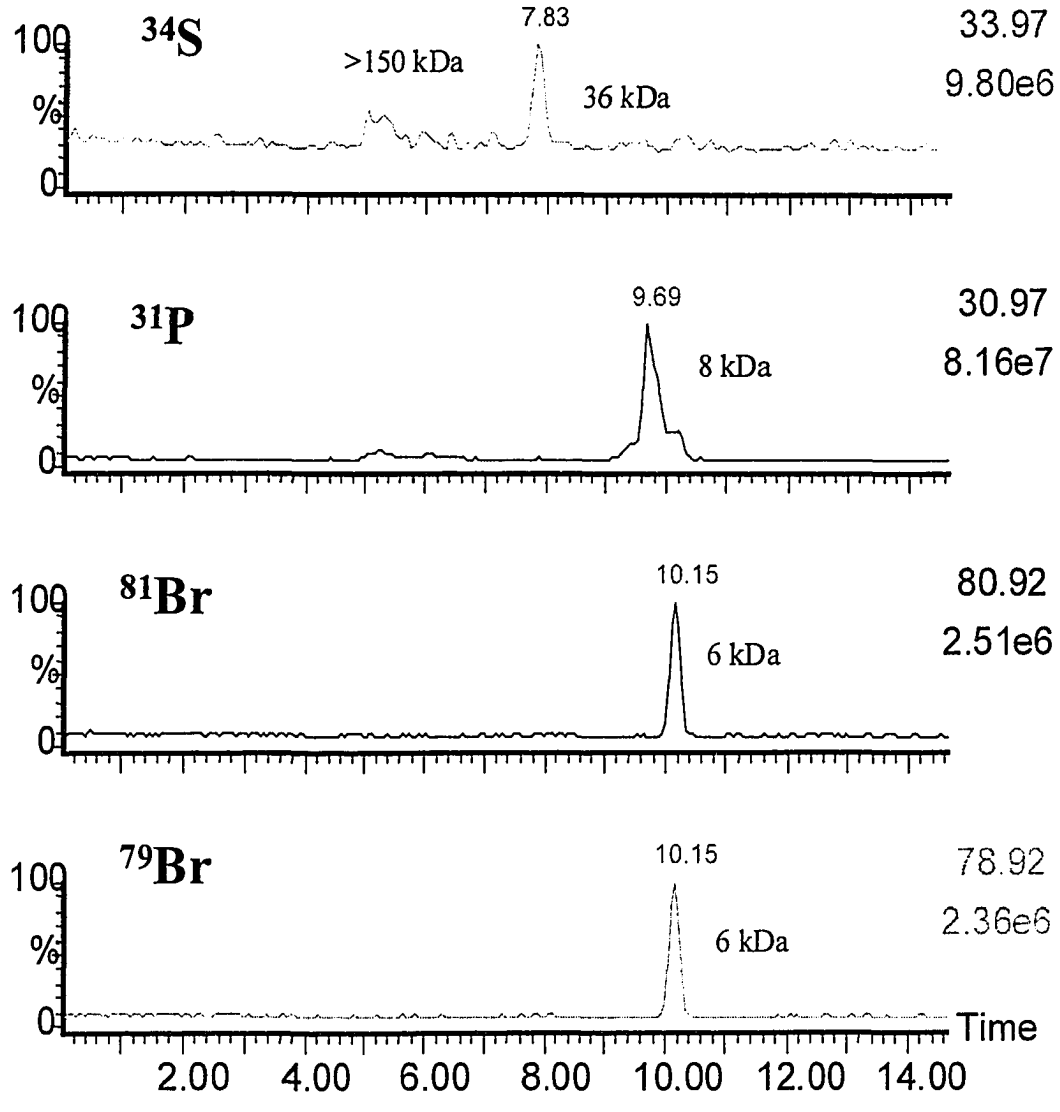

Fig. 5. Chromatograms of S, P and Br in human milk with the detection by ICP-hQMS.

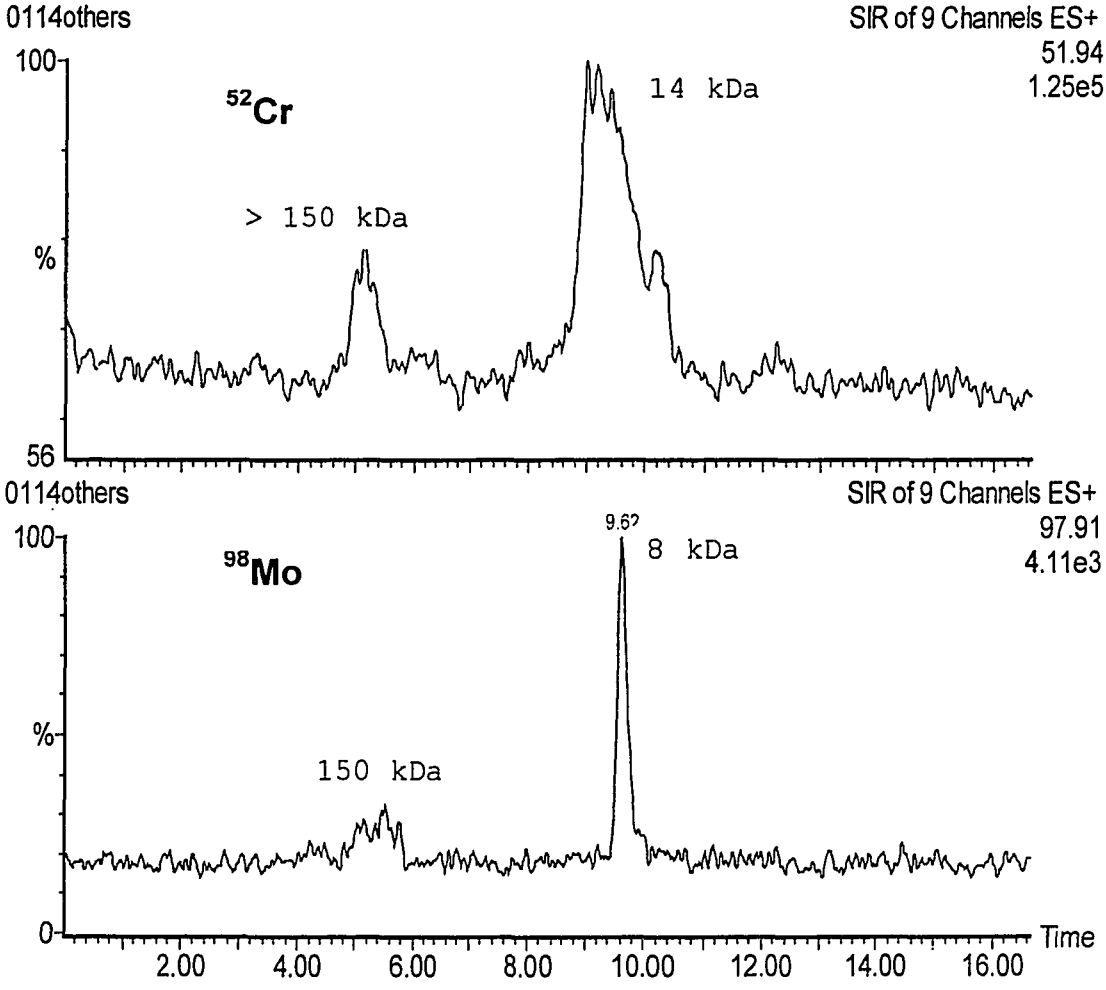

Fig. 6. Chromatograms of Cr and Mo in human milk with the detection by ICP-hQMS.

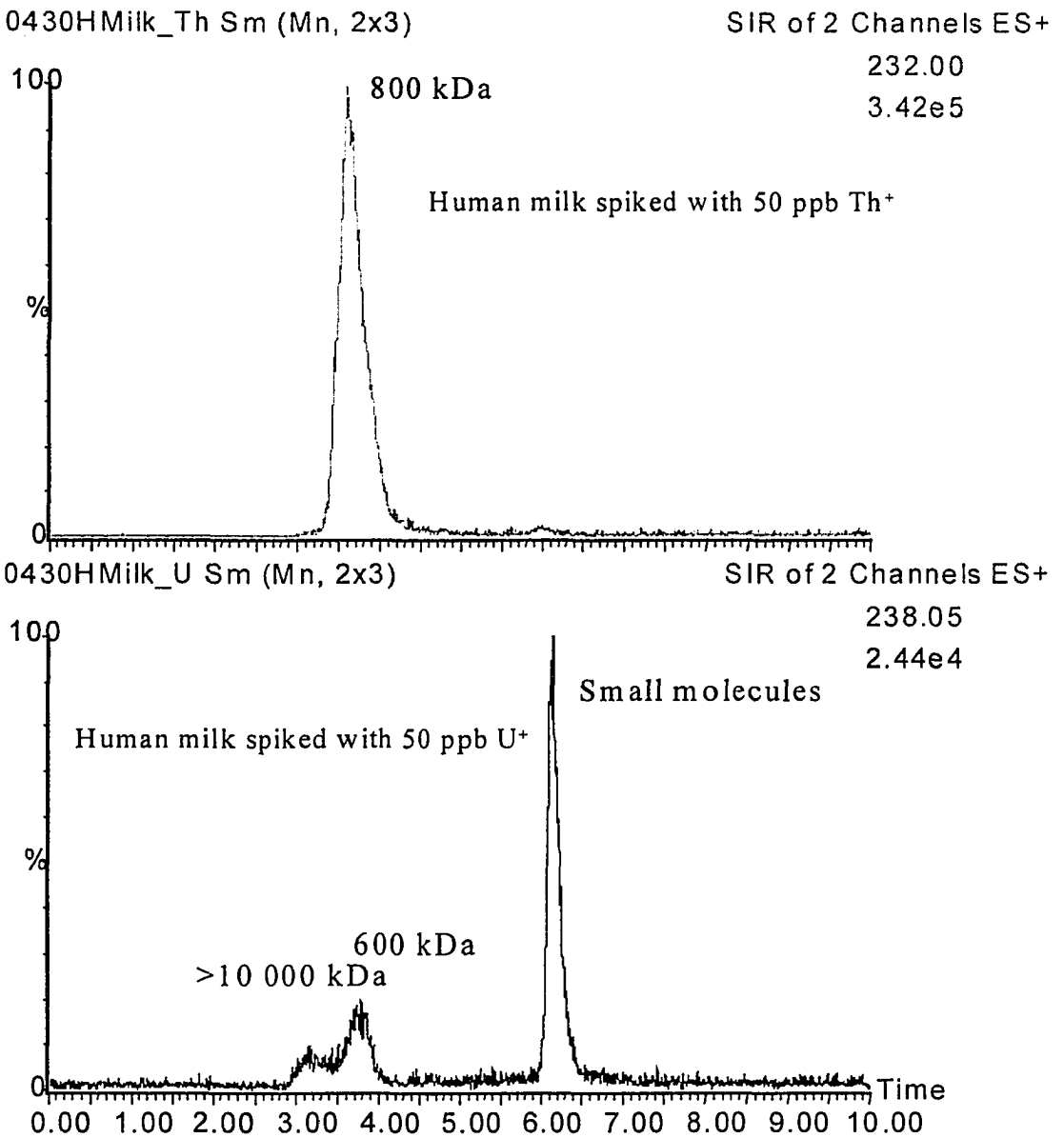

Fig. 7. Chromatograms of human milk spiked with Th and U with the detection by ICP-hQMS.

CHAPTER 7: SUMMARY

A methodology that can monitor and identifying inorganic elements in biological and environmental system was developed. Size exclusion chromatography (SEC) separates biomolecules, which are then nebulized by a microconcentric nebulizer. The resulting aerosol is desolved and introduced into either a high resolution ICP-MS device or a quadrupole device with a collision cell. A double focusing mass spectrometer provides very high sensitivity and low background. The compounds of interest are separated by liquid chromatography. The column effluent is introduced on-line into the ICP-MS device, which monitors the unique element(s) of interest. Because of the high sensitivity and spectral resolution and high sample introduction efficiency, many unusual or difficult elements, such as Cr, Se, Cd and U, can be observed at ambient levels bound to proteins in human serum. These measurements are made in only a few minutes without preliminary isolation and preconcentration steps. Serum samples can be titrated with spikes of various elements to determine which proteins bind a given metal and oxidation state. It can readily be shown that almost all of the Tl^+ is present as free ions, (i.e., not bound to proteins). This is consistent with the usual explanation for the toxic role of Tl^+, which is supposed to minic the essential alkali metal ions Na^+ and K^+. Experiments concerning the effects of breaking disulfide linkages and denaturation on metal binding in proteins were also investigated. The methodology was successfully used to study the elemental distribution in liver extract.

Binding of metal cations to DNA restriction fragments can be observed by similar procedures both for essential elements like Mn and Fe and toxic ones like Cd and Pb. In particular, trace Pb, Cd and Co are completely bound to DNA fragments. Reactions of metal species with DNA can also be observed by these procedures, such as reduction of chromate and subsequent binding of the cation produced and reaction of the chemotherapeutic reagent cisplatin with DNA.

A collision cell interfaced ICP-MS can remove or reduce argon adduct interferences. The effects of some important parameters have been investigated on the enhancement of ion transmission and reduction of polyatomic interferences using a Platform ICP-hQMS. Several gases have been tested as collision gases. The results show that a suitable flow of helium

(He) introduced into the cell increases the ion transmission of the elements in the middle and high mass range. The focusing effect of collision gases is demonstrated based on the experiments with and without introducing collision gas into the cell. The enhancement of ion transmission is closely related with the collision energy and ion energy. Collision of ions with neutral gases narrows the ion energy spread of ions. By examining the reaction rate of hydrogen, methane and xenon with argon adduct ions and related analyte ions, it is clearly demonstrated that the analyte ion signals such as Fe^+ can be separated from the argon adduct interferences such as ArO^+ with the selective reaction between the argon adduct interferences and collision gases. The results provide some important information for developing the optimal collision conditions for the removal of polyatomic interferences, and also for the further modification and development of this new analytical tool.

The application of ICP-hQMS in elemental speciation was also studied. The applications of ICP-hQMS in the measurement of metal ions in metals bound to proteins in human milk have been studied. A metal free HPLC system was successfully coupled ICP-hQMS with MCN and conventional desolvation. Hydrogen was introduced into collision cell to remove interferences from argon adduct ions. Helium in the collision cell was used to improve the ion transmission. The proteins in human milk can be separated by size exclusion chromatography and elements bound to proteins in human milk can be detected online by ICP-hQMS. The collision cell make it possible to measure some important elements suffering polyatomic interferences like Fe, Se, Ca, etc. were detected. The elemental distribution information in milk proteins is very important in identifying nutritional potential and ensuring toxicological risks.

ACKNOWLEDGEMENTS

First, I would like to thank the boss, Dr. Sam Houk. His guidance, instruction, and patience have been of immeasurable value to me in my time here. I derive a particular amount of pride having worked for the one who invented this technique. His ability to motivate and demand inspires me daily to be a better scientist.

I would like to thank my committee members Dr. C. Ng, Dr. J. Fritz, Dr. M. Porter and Dr.R. Serfass for reviewing my thesis.

I would like to thank you all the current and former Houk group members with whom it has been a pleasure to work. I wish each and every one of you the best and hope to keep in contact with you in the years to come.

I would like to thank my entire family.

Most of all, I wish to thank my wife, Yuexia. Her love, support, understanding, and encouragement have been the ultimate blessing during my school. I feel very fortunate to have been able to share my time in graduate school with her.

This work was performed at Ames Laboratory under Contract No. W-7405-Eng-82 with the U.S. Department of Energy. The United States government has assigned the DOE Report number IS-T 1868 to this thesis.